A.N.F.
PLASMA INDUIT PAR LASER POUR L'ANALYSE DE LA MATIÈRE
15-17 novembre 2021, Orléans

# Analyse LIBS sans étalonnage

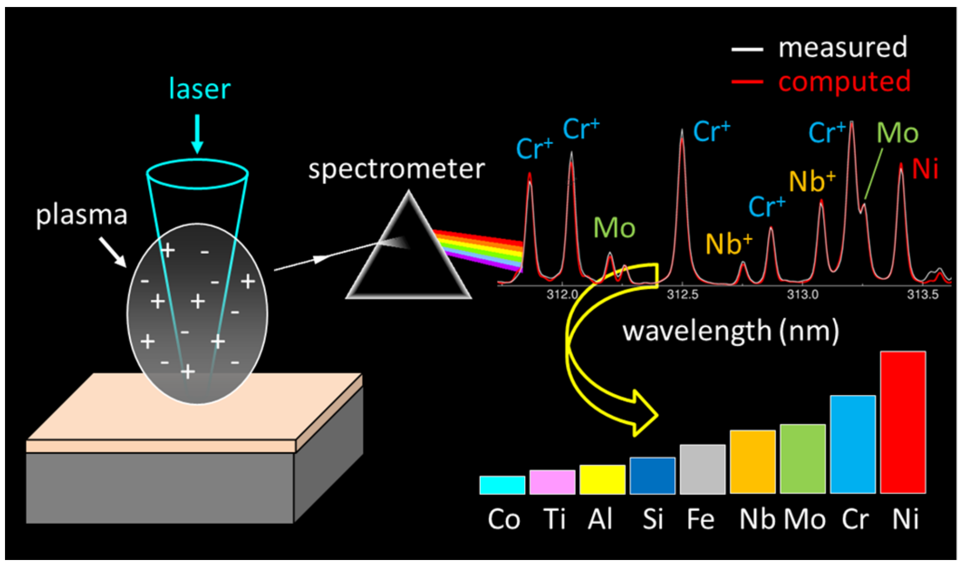


Jörg Hermann

LP3, CNRS, Aix-Marseille Université, 13009 Marseille

# Calibration-free LIBS

## Introduction

- **Principle and historical background**

## Validity conditions of physical model

## Methods of calibration-free measurements

## Critical review of analytical performance

## Recommendations

## Practical advice

# Principle of calibration-free LIBS

☞ **modeling of plasma emission spectrum**

☞ **comparison to measured spectrum**

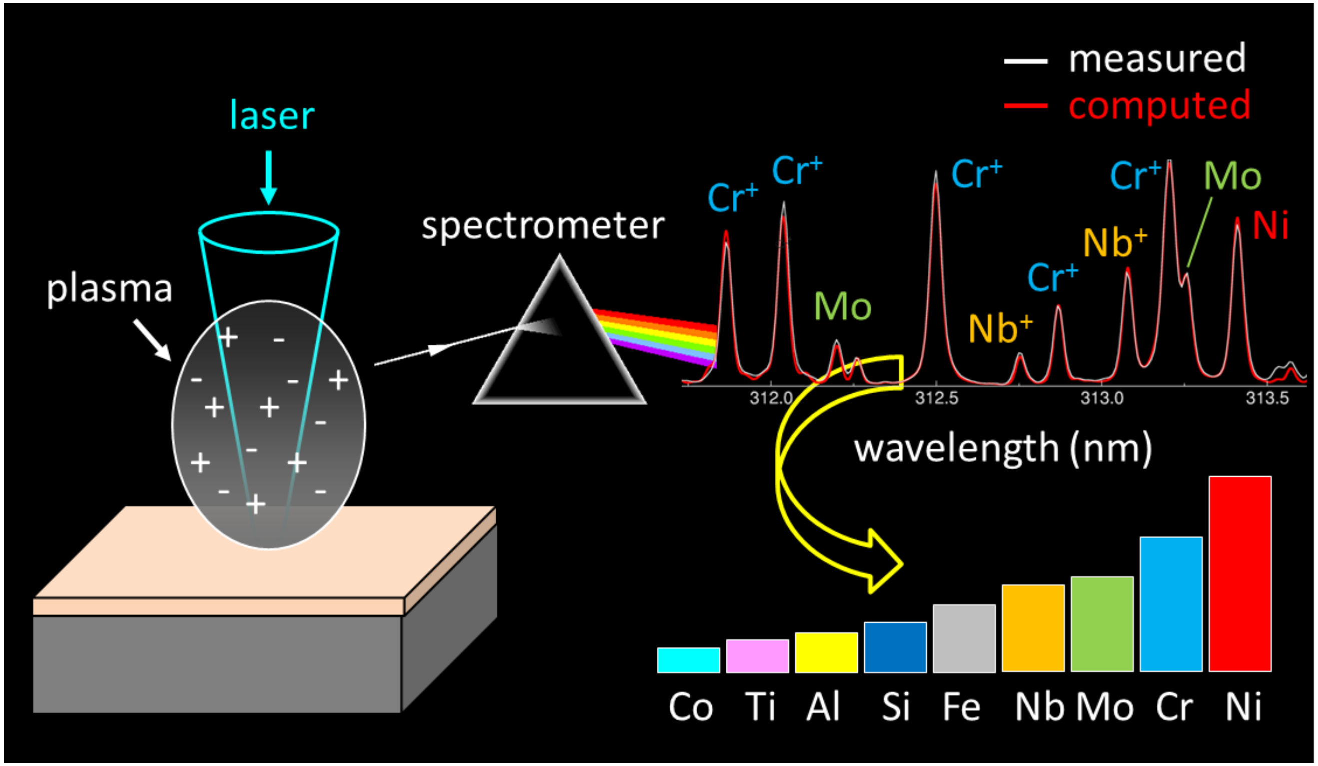

# Principle of calibration-free LIBS

☞ **calibration curve generated by calculation**

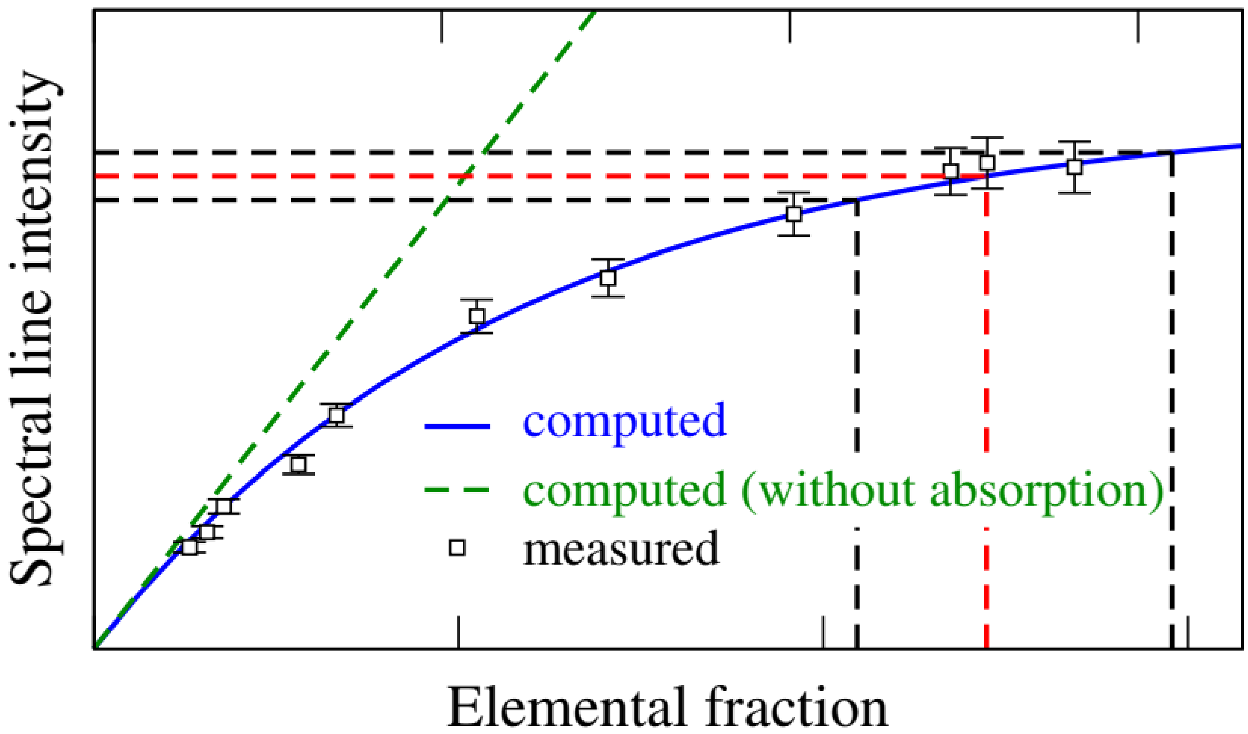

# Principle of calibration-free LIBS

☞ **CF-LIBS requires model for spectrum calculation**

multielemental plasma ☞ unique model enables this calculation

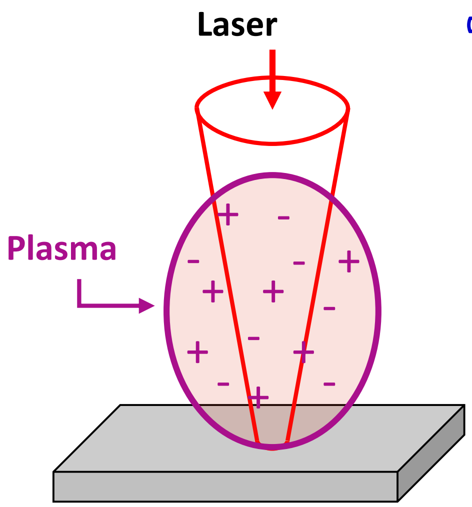


☞ **Local thermodynamic equilibrium (LTE)**

**Is the laser-induced plasma in LTE ?**

**Plasma produced by laser ablation**

**+ large initial density**

**- fast expansion dynamics**

⇨ **conclusion about LTE is not straightforward**

# Historical background

- 1978 : validity of LTE in laser-produced plasma, *Eliezer et al. J. Phys D*

**A generalised validity condition for local thermodynamic equilibrium in a laser-produced plasma**

Shalom Eliezer, Aaron D Krumbein and David Salzmann
Department of Plasma Physics, Soreq Nuclear Research Centre, Yavne, Israel

Received 9 January 1978

☞ **theoretical investigation**

☞ **experimental validation difficult**

- low plasma reproducibility
- limited experimental means for time-resolved broadband spectra recording

# Historical background

- 1978 : validity of LTE in laser-produced plasma, *Eliezer et al. J. Phys D*

- 1993 : first Boltzmann-plot for laser plasma, *Hermann et al. J. Appl. Phys*

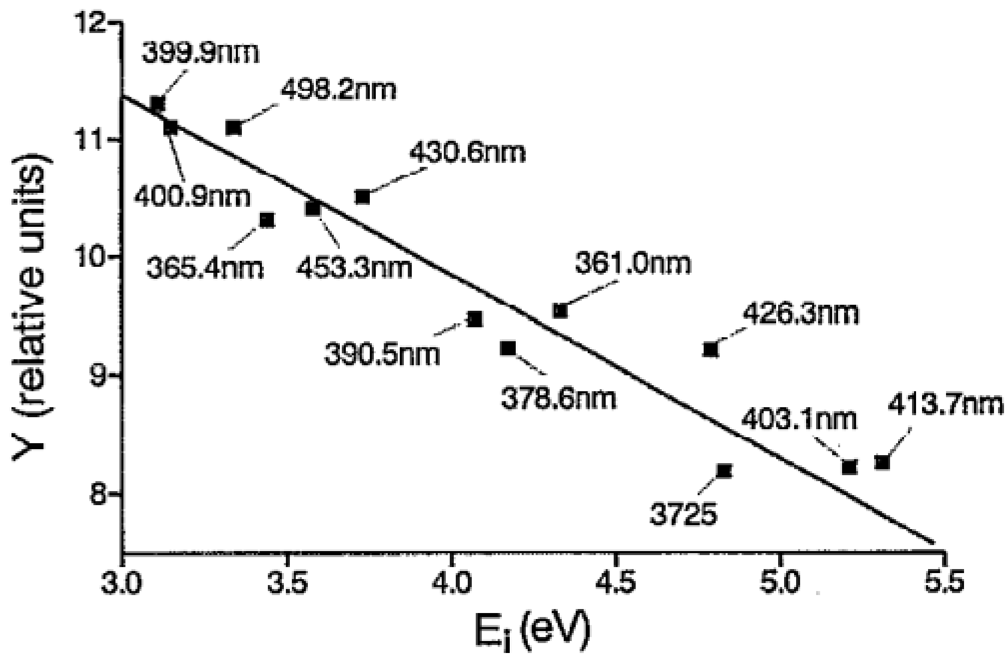


FIG. 7. Boltzmann diagram of Ti I. Delay with respect to the laser pulse: $t=1$ $\mu$s, $E_{las}=53$ mJ (short laser pulse), $p_0=400$ Torr, $d=1.0$ mm.

# Historical background

- 1978 : validity of LTE in laser-produced plasma, *Eliezer et al. J. Phys D*

- 1993 : first Boltzmann-plot for laser plasma, *Hermann et al. J. Appl. Phys*

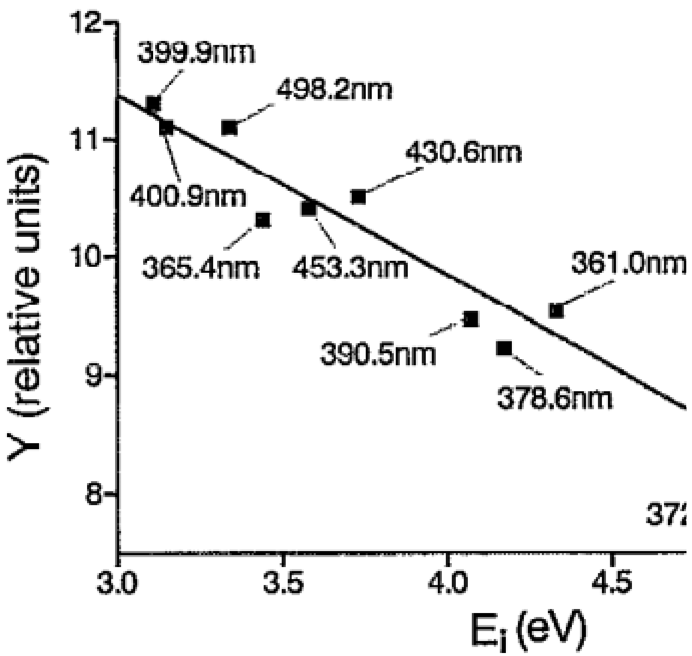


⇨ **temperature evaluation**

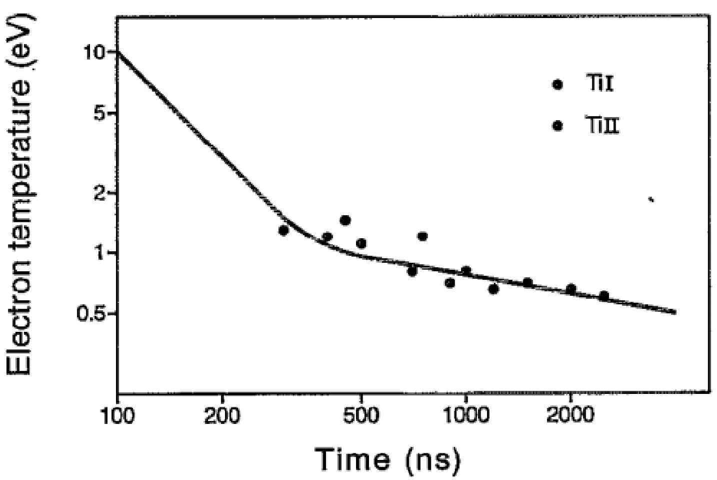


FIG. 8. Temporal evolution of electron temperature deduced from Ti I and Ti II Boltzmann diagrams. $E_{las}=53$ mJ short laser pulse $p_0=400$ Torr, $d=1.0$ mm. The value 10 eV for 100 ns is deduced from LTE calculations.

FIG. 7. Boltzmann diagram of Ti I. Delay with respect to the laser pulse: $t=1$ $\mu$s, $E_{las}=53$ mJ (short laser pulse), $p_0=400$ Torr, $d=1.0$ mm.

# Historical background

- 1978 : validity of LTE in laser-produced plasma, *Eliezer et al. J. Phys D*

- 1993 : first Boltzmann-plot for laser plasma, *Hermann et al. J. Appl. Phys*

- 1995 : comparison of plasma emission to LTE calculation, *Hermann et al. J. Appl. Phys*

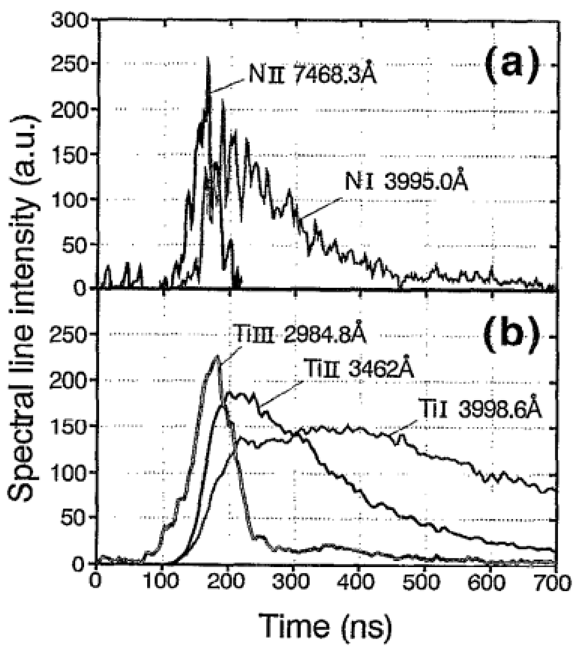


FIG. 9. Spectral line kinetics of neutral atoms and ions of (b) N and (a) Ti. $z=3$ mm, $p=0.5$ mb, $I_{las}=500$ MW cm$^{-2}$.

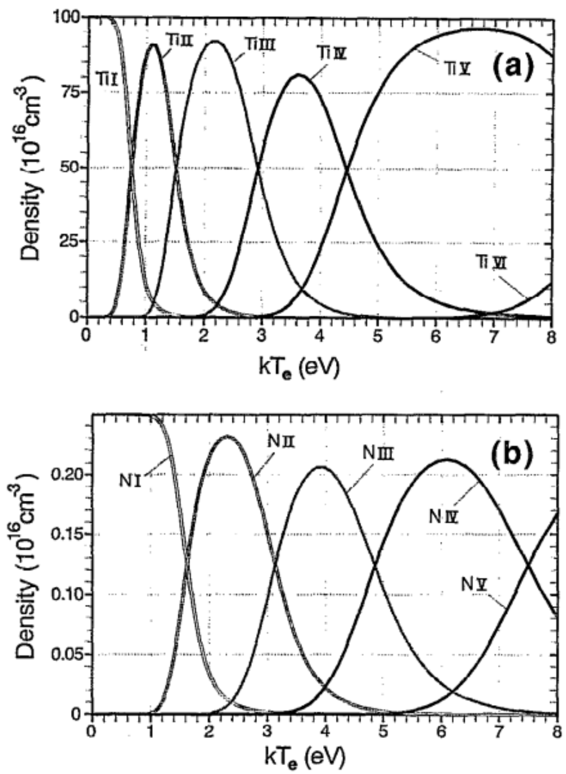


FIG. 8. Computed equilibrium densities of (a) Ti and (b) N species as a function of $kT_e$ for $10^{18}$ cm$^{-3}$ vapor density.

# Historical background

- 1978 : validity of LTE in laser-produced plasma, *Eliezer et al. J. Phys D*
- 1993 : first Boltzmann-plot for laser plasma, *Hermann et al. J. Appl. Phys*
- 1995 : comparison of plasma emission to LTE calculation, *Hermann et al. J. Appl. Phys*
- 1999 : invention of calibration-free LIBS, *Ciucci et al. Appl. Spectrosc.*

☞ **assumption of stoichiometric ablation**

☞ **multielemental Boltzmann plot**

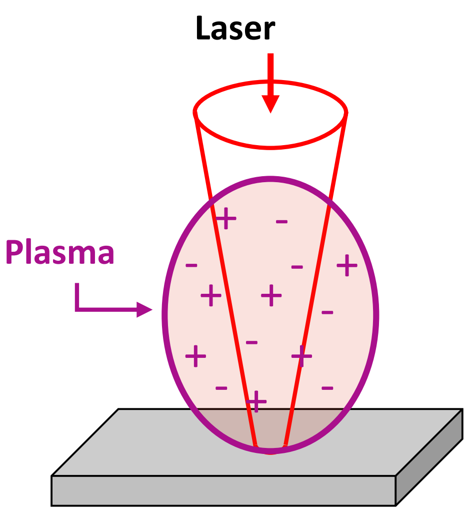


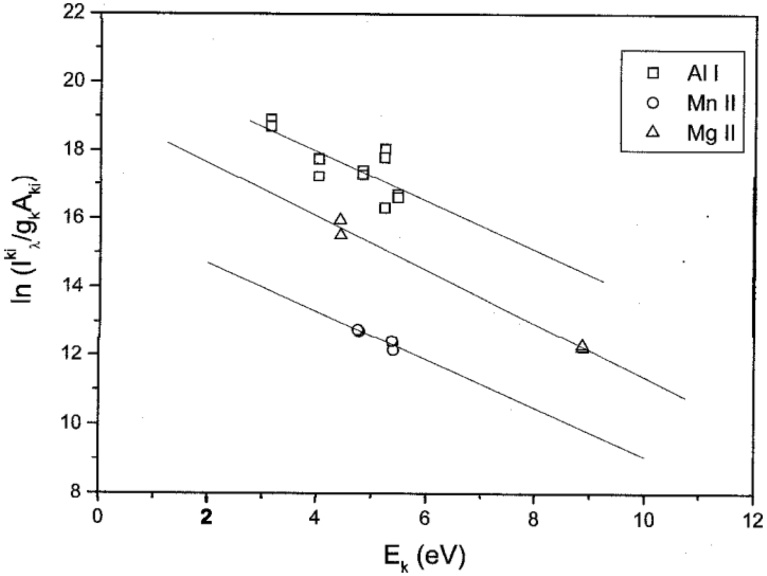


☞ **easy to handle ⇨ large success**

# Historical background

- 1978 : validity of LTE in laser-produced plasma, *Eliezer et al. J. Phys D*
- 1993 : first Boltzmann-plot for laser plasma, *Hermann et al. J. Appl. Phys*
- 1995 : comparison of plasma emission to LTE calculation, *Hermann et al. J. Appl. Phys*
- 1999 : invention of calibration-free LIBS, *Ciucci et al. Appl. Spectrosc.*

☞ **low analytical performance**

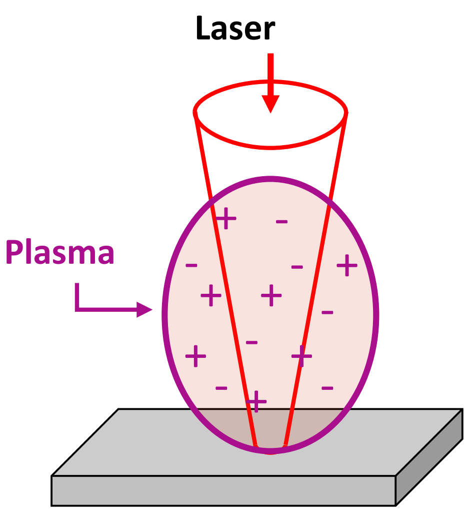


hypotheses :

- **stoichiometric ablation** ✓
- **local thermodynamic equilibrium** ✓
- **plasma uniform** (✓)
- **plasma optically thin** ***no***

# Historical background

- 1978 : validity of LTE in laser-produced plasma, *Eliezer et al. J. Phys D*
- 1993 : first Boltzmann-plot for laser plasma, *Hermann et al. J. Appl. Phys*
- 1995 : comparison of plasma emission to LTE calculation, *Hermann et al. J. Appl. Phys*
- 1999 : invention of calibration-free LIBS, *Ciucci et al. Appl. Spectrosc.*

\> 1999 : amended CF-LIBS approaches, most devoted to correction of self-absorption

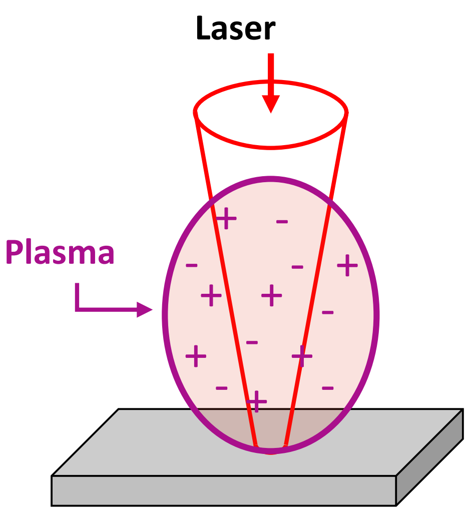


hypotheses :

- **stoichiometric ablation** ✓
- **local thermodynamic equilibrium** ✓
- **plasma uniform** (✓)
- ~~**plasma optically thin**~~

# Historical background

- 1978 : validity of LTE in laser-produced plasma, *Eliezer et al. J. Phys D*
- 1993 : first Boltzmann-plot for laser plasma, *Hermann et al. J. Appl. Phys*
- 1995 : comparison of plasma emission to LTE calculation, *Hermann et al. J. Appl. Phys*
- 1999 : invention of calibration-free LIBS, *Ciucci et al. Appl. Spectrosc.*

> 1999 : amended CF-LIBS approaches, most devoted to correction of self-absorption

≥ 2008 : CF-LIBS based on spectra simulation

☞ **self-absorption intrinsically taken into account**

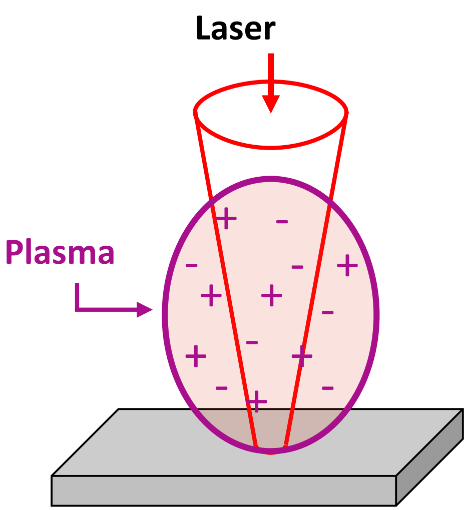


hypotheses :

- **stoichiometric ablation** ✓
- **local thermodynamic equilibrium** ✓
- **plasma uniform** (✓)
- ~~**plasma optically thin**~~

# Validity conditions of physical model

## Mass transfer from solid towards plasma is congruent ?

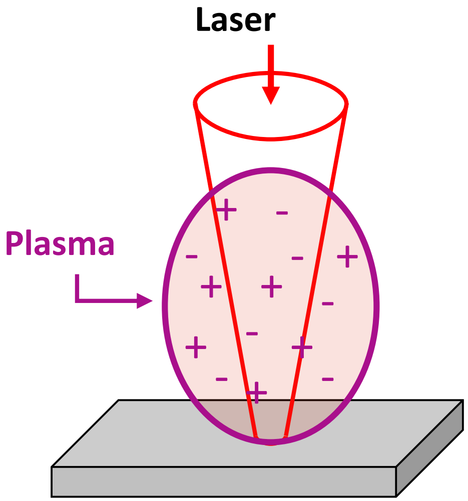


hypotheses :

- **stoichiometric ablation**
- local thermodynamic equilibrium
- plasma uniform
- plasma optically thin

# Validity conditions of physical model

## Mass transfer from solid towards plasma is congruent ?

☞ **question on mechanism of laser ablation**

+ thermal evaporation

☞ element-dependent evaporation pressure (Clausius-Clapeyron equation)

⇨ **non-stoichiometric mass transfer**

+ phase explosion

☞ high laser intensity induces large rate of vaporization ⇨ **no time for segregation**

⇨ **stoichiometric mass transfer**

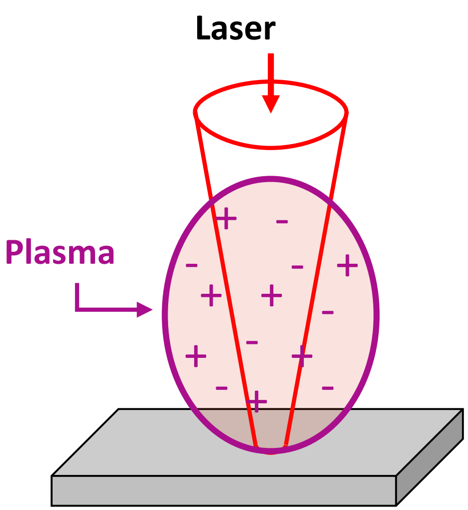


hypotheses :

- **stoichiometric ablation**
- **local thermodynamic equilibrium**
- **plasma uniform**
- **plasma optically thin**

# Validity conditions of physical model

## Mass transfer from solid towards plasma is congruent ?

☞ **question on mechanism of laser ablation**

+ thermal evaporation

☞ element-dependent evaporation pressure (Clausius-Clapeyron equation)

⇨ **non-stoichiometric mass transfer**

+ phase explosion

☞ high laser intensity induces large rate of vaporization ⇨ **no time for segregation**

⇨ **stoichiometric mass transfer**

☞ **stoichiometric ablation depends on laser intensity**

# Validity conditions of physical model

## Mass transfer from solid towards plasma is congruent ?

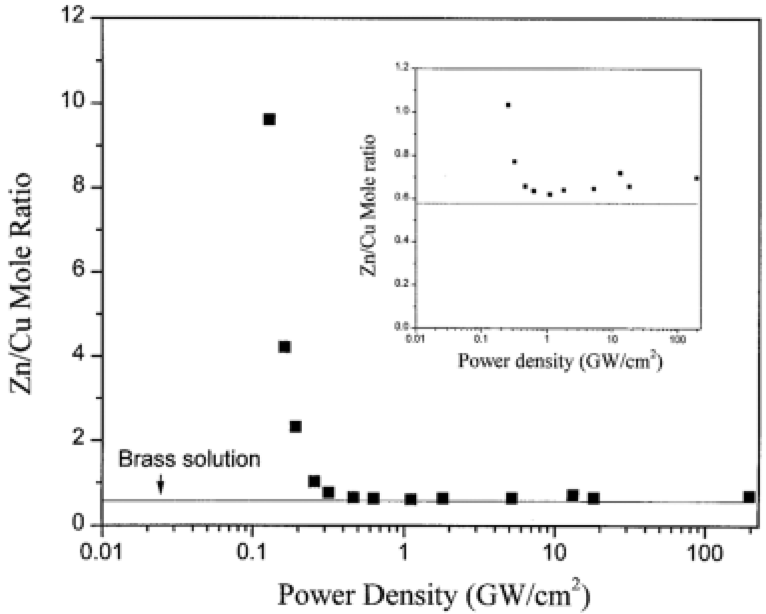


*Mao et al., Appl. Spectrosc. 1998*

Zn/Cu ratio in brass measured via LA-ICP-AES

(Laser ablation inductively coupled plasma atomic emission spectroscopy)

☞ **stoichiometric ablation depends on laser intensity**

in conditions typical for LIBS ($F_{las}$ = 100 Jcm$^{-3}$)

⇨ **mass transfer from solid to plasma stoichiometric**

# Validity conditions of physical model

**Plasma is in local thermodynamic equilibrium (LTE) ?**

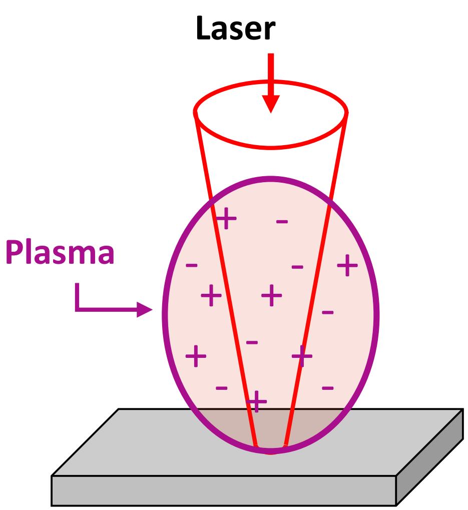


hypotheses :

- stoichiometric ablation
- **local thermodynamic equilibrium**
- plasma uniform
- plasma optically thin

# Validity conditions of physical model

## Plasma is in local thermodynamic equilibrium (LTE) ?

**Elementary processes**

**collisional processes :**

collisional excitation / desexcitation

$$A^l + e^- (E) \Leftrightarrow A^u + e^- (E')$$

electron impact ionization / 3 body recombination

$$A + e^- (E) \Leftrightarrow A^+ + e^- (E') + e^- (E'')$$

**radiative processes :**

spontaneous emission / absorption (bound-bound transitions)

$$A^u \Leftrightarrow A^l + h\nu$$

photoionization / radiative recombination (free-bound transitions)

$$A + h\nu \Leftrightarrow A^+ + e^- (E)$$

bremsstrahlung emission / inverse bremsstrahlung absorption (free-free transitions)

$$A + e^- (E) \Leftrightarrow A + e^- (E')$$

**out of equilibrium ☞ collisional-radiative modeling**

**⇨ requires rates of all processes**

# Validity conditions of physical model

## Plasma is in local thermodynamic equilibrium (LTE) ?

**equilibrium ☞ principle of microscopic reversibility**

⇨ **each process is counterbalanced by its reverse process**

☞ plasma of large size in steady state

laboratory plasmas ☞ size < characteristic length of absorption

⇨ **no microreversibility for radiative processes**

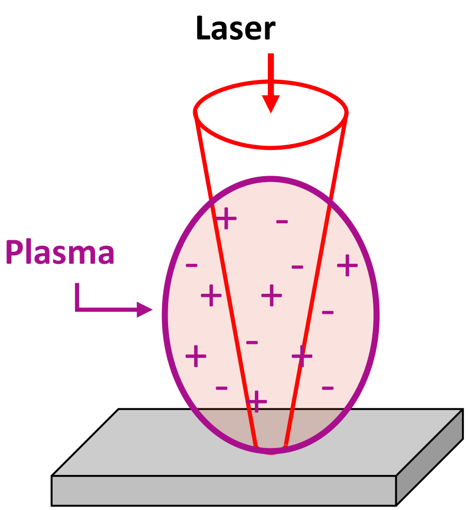


**equilibrium may still exist**

**if collisional processes dominate**

# Validity conditions of physical model

## Plasma is in local thermodynamic equilibrium (LTE) ?

high mobility of electrons (small mass)

⇨ collisional processes dominated by electrons

☞ **validity of LTE depends on electron density**

rates of collisional excitation / desexcitation $\Gamma_{ul}$ , $\Gamma_{lu}$ >> $A_{ul}$

most difficult case ☞ the levels of largest energy gap $\Delta E_{max}$

Hydrogen

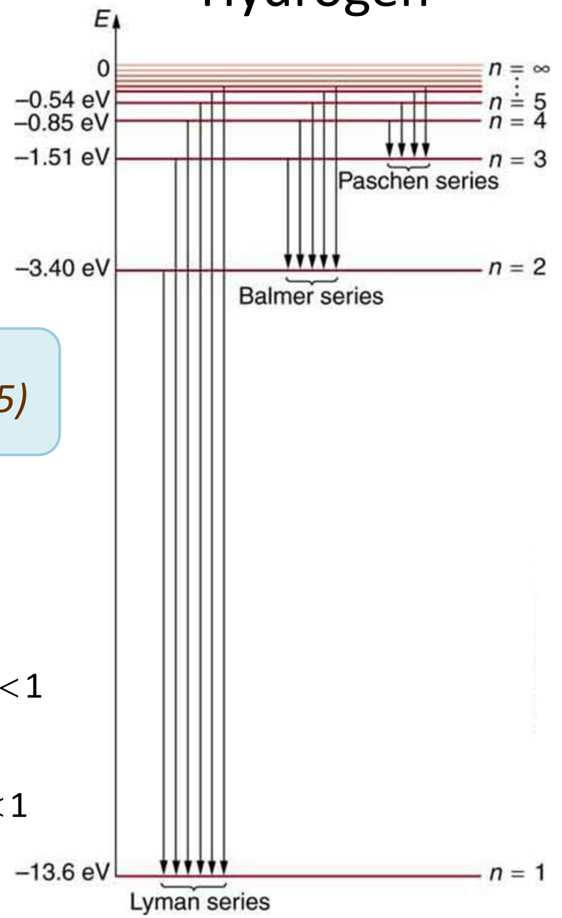


LTE criterion : $n_e > 1.6 \times 10^{12} \sqrt{T} \Delta E_{max}^3$ *(McWhirter, 1965)*

☞ **most elements : $n_e \geq 10^{16}$ cm$^{-3}$**

additional criteria :

☞ **transient plasma** $\frac{T(t+\tau_{rel})-T(t)}{T(t)} << 1$ $\frac{n_e(t+\tau_{rel})-n_e(t)}{n_e(t)} << 1$

☞ **nonuniform plasma** $\frac{T(x)-T(x+\lambda)}{T(x)} << 1$ $\frac{n_e(x)-n_e(x+\lambda)}{n_e(x)} << 1$

$\lambda = \sqrt{D\,\tau_{rel}}$ = diffusion length during relaxation time

# Validity of LTE

## ☞ depends on experimental conditions

**laser :**

plasma density and lifetime depend on laser energy

⇨ sufficiently large $E_{las}$ required

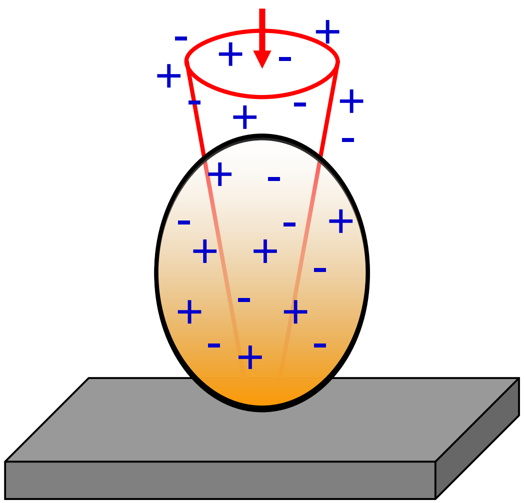


**surrounding atmosphere :**

plasma density and lifetime depend on gas pressure

⇨ plume confinement by gas

**sample material :**

LTE validity depends on atomic structure

☞ atoms such as H, N, O, C have large $\Delta E_{max}$ ⇨ equilibrium hardly achieved

☞ metal have many close lying levels ⇨ equilibrium easily achieved

**In conditions typical for LIBS analysis**

nanosecond laser, $E_{las}$ = a few mJ, at atmospheric pressure

☞ **conditions of LTE achieved**

# Validity of LTE

**Material ablation with a ns-laser**

$E_{las}$ = 10 mJ
$d_{spot}$ = 100 µm
} $F_{las}$ = 100 Jcm$^{-2}$

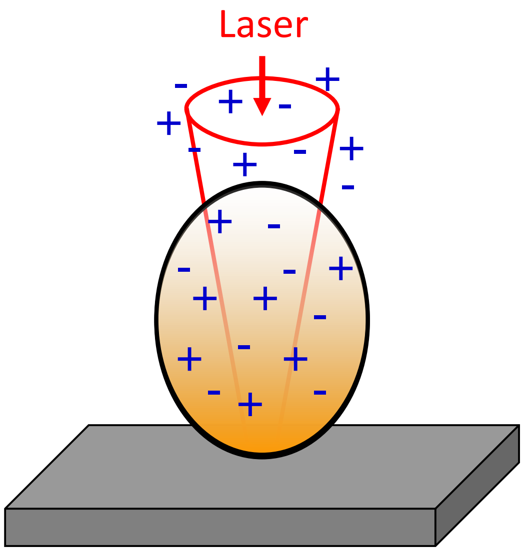


⇨ **$10^{14}$ atomes ( ≅ 10 ng)**

☞ laser heats material to some $10^4$ K

☞ plume expansion $u$ ≅ some $10^3$ m s$^{-1}$

$t$ = 100 ns ⇨ $V$ = 0.1 mm$^3$

⇨ **plasma density ≅ $10^{18}$ cm$^{-3}$** ⇨ **LTE valid**

☞ further plasma evolution depends on surrounding atmosphere

in air, $t$ = 1 µs ⇨ **$n_e$ ≅ $10^{17}$ cm$^{-3}$**

⇨ **plasma in LTE for several µs**

# Validity of LTE

**types of radiation :**

intensity

spontaneous emission

$A^u \Rightarrow A^l + h\nu$ ⇨ **spectral lines** $\propto \quad n_i = n\frac{g_i}{Q(T)}e^{-E_i/kT}$

radiative recombination

$A^+ + e^- \Rightarrow A + h\nu$

bremsstrahlung

$A + e^- (E) \Rightarrow A + e^- (E') + h\nu$

} **continuum** $\propto \; n_e^{\,2}$

plume expansion

⇨ strong decrease of electron density

early expansion stage

☞ continuum dominates spectrum

**setting the detector gate delay**

☞ **compromise LTE / signal-to-noise ratio**

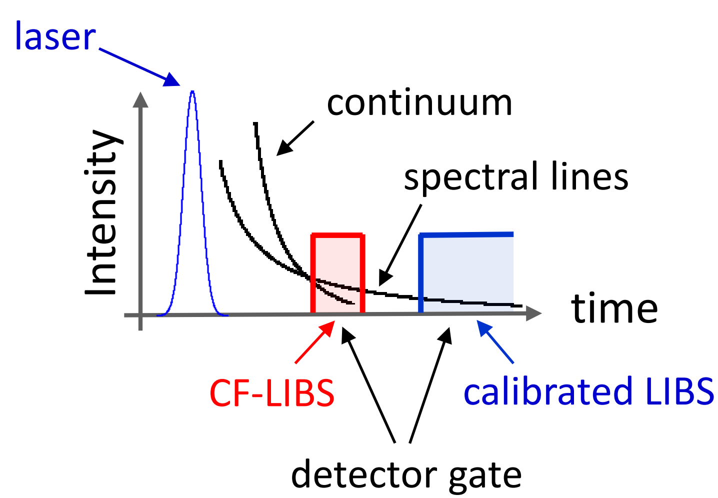

# Validity conditions of physical model

## Plasma is spatially uniform ?

laser ablation under vacuum

⇨ most energetic species in the expanding plume front

laser ablation in ambient gas

⇨ most energetic species at the vapor-gas contact front ($T_{border} > T_{core}$ at early time)

⇨ cooling of plume border by cold gas ($T_{border} < T_{core}$ at late time)

⇨ **time window expected for which the plume has an almost uniform *T*-distribution**

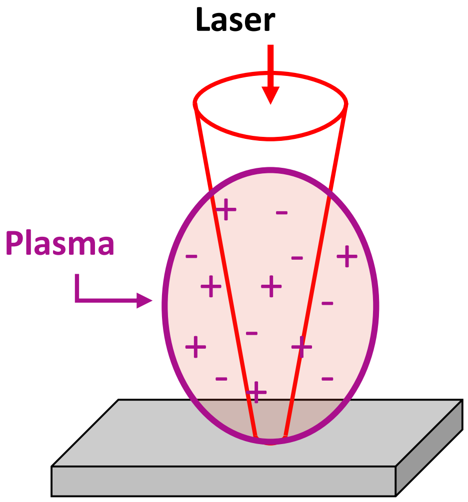


hypotheses :

- stoichiometric ablation
- local thermodynamic equilibrium
- **plasma spatially uniform**
- plasma optically thin

# Validity conditions of physical model

## Plasma is spatially uniform ?

**Spectral shape of strongly Stark-shifted transition**

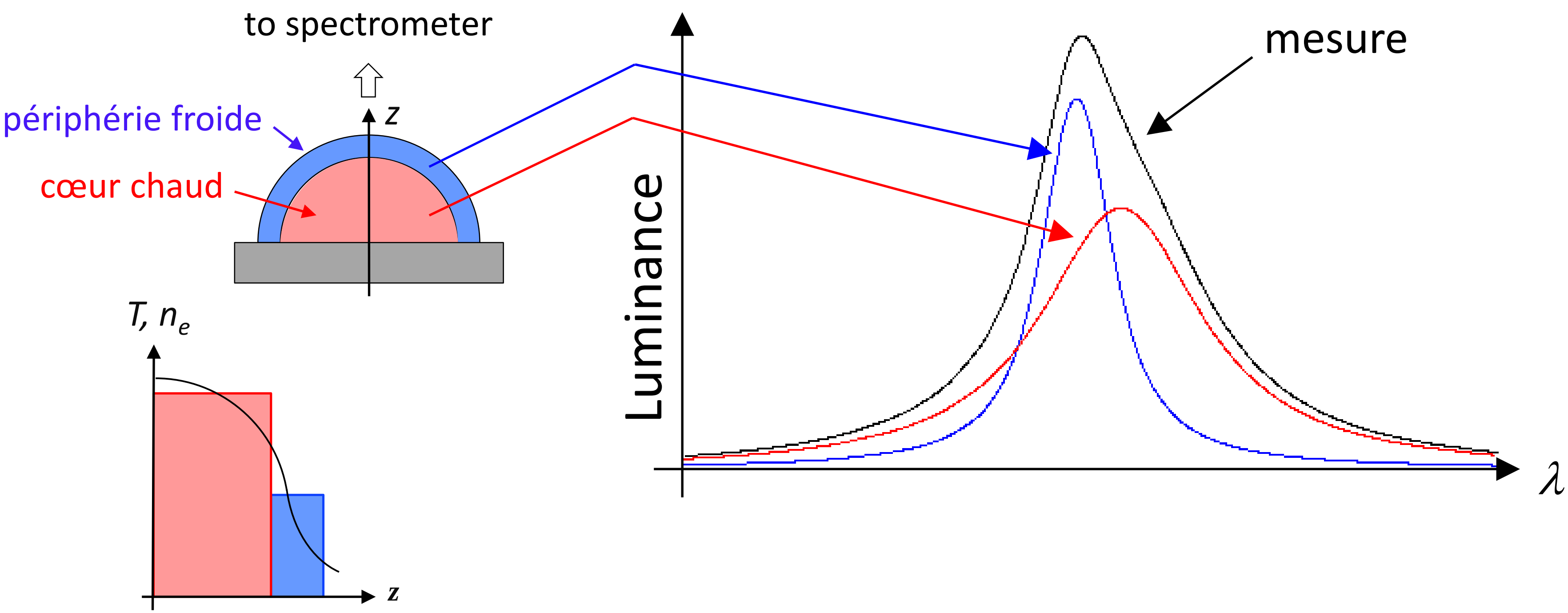


**nonuniform plasma ⇨ asymmetric profile**

# Validity conditions of physical model

## Plasma is spatially uniform ?

### Spectral shape of strongly Stark-shifted transition

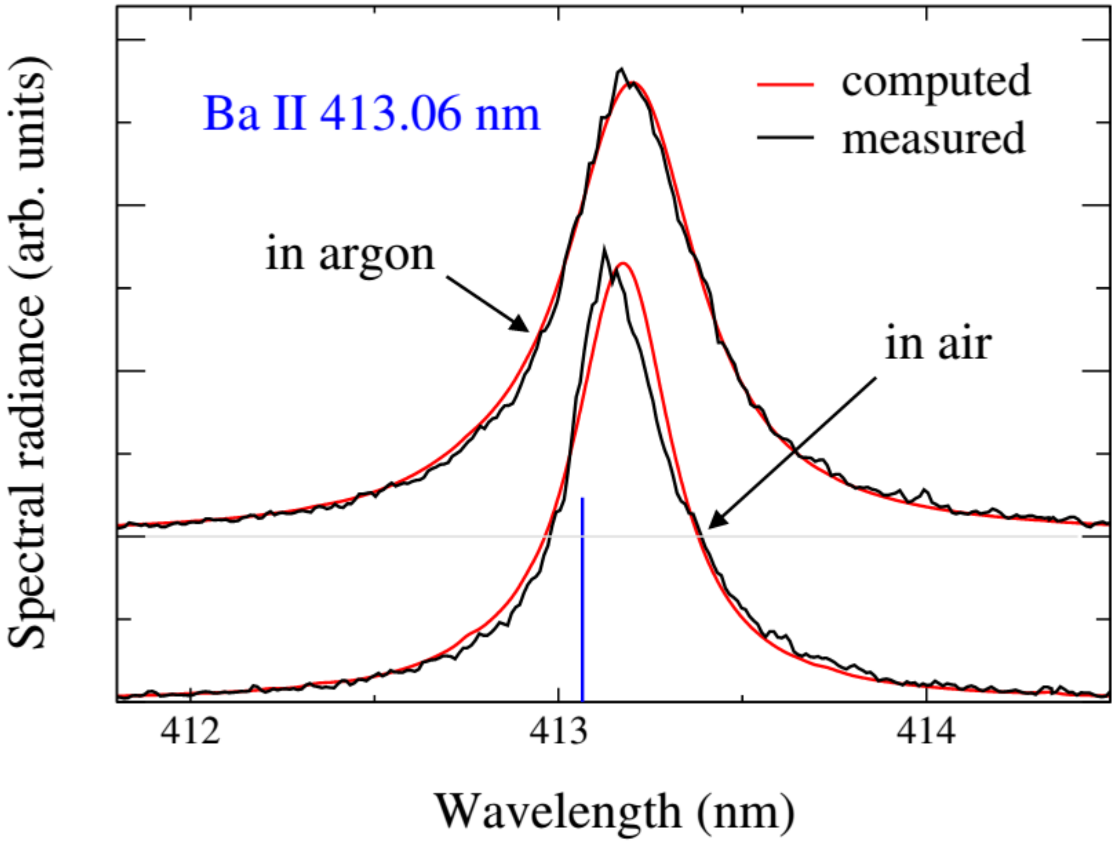


verre N-BaK4

$E_{las}$ = 6 mJ, $\lambda$ = 266 nm, $\tau$ = 5 ns

**sous air**

☞ **plasma non-uniforme**

**sous argon**

☞ **plasma uniforme**

# Validity conditions of physical model

## Plasma is spatially uniform ?

### Spectral shape of strongly self-absorbed resonance line

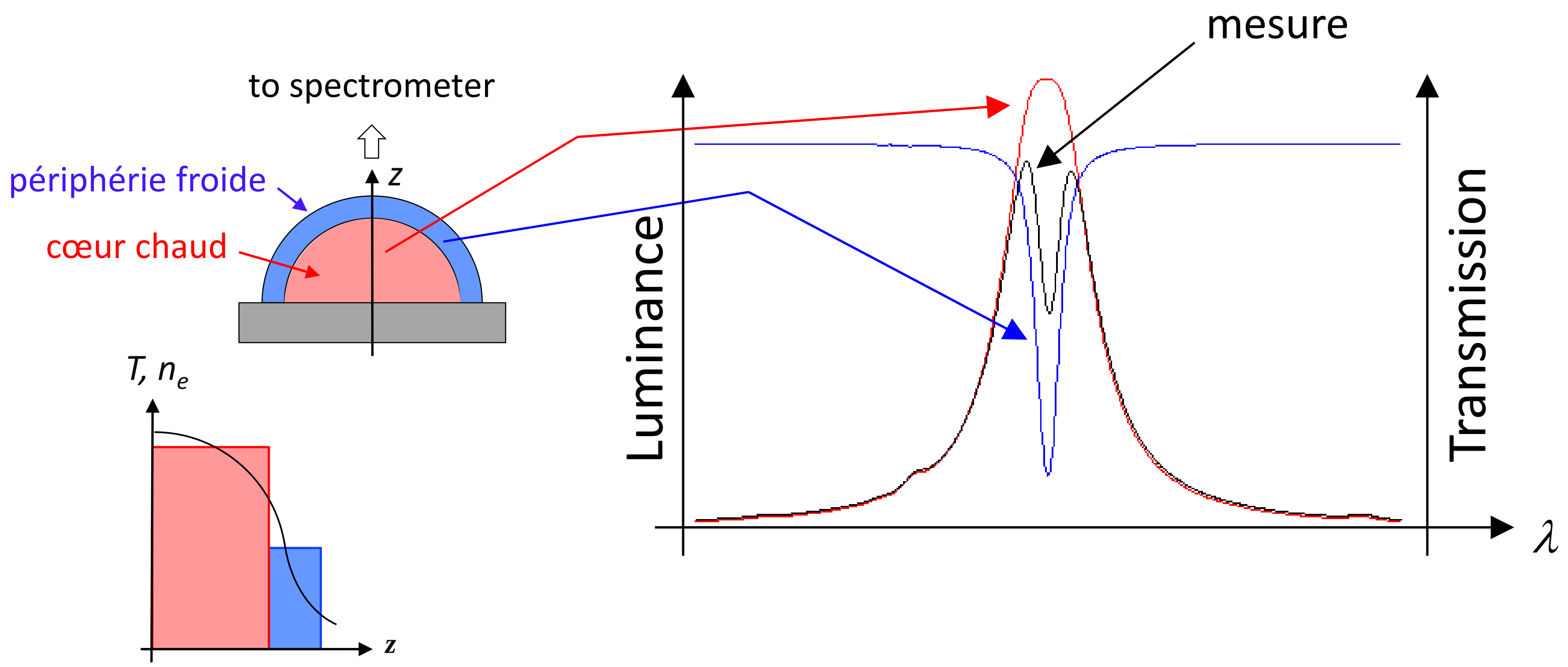


**cold border ⇨ absorption dip**

# Validity conditions of physical model

## Plasma is spatially uniform ?

### Spectral shape of strongly self-absorbed resonance line

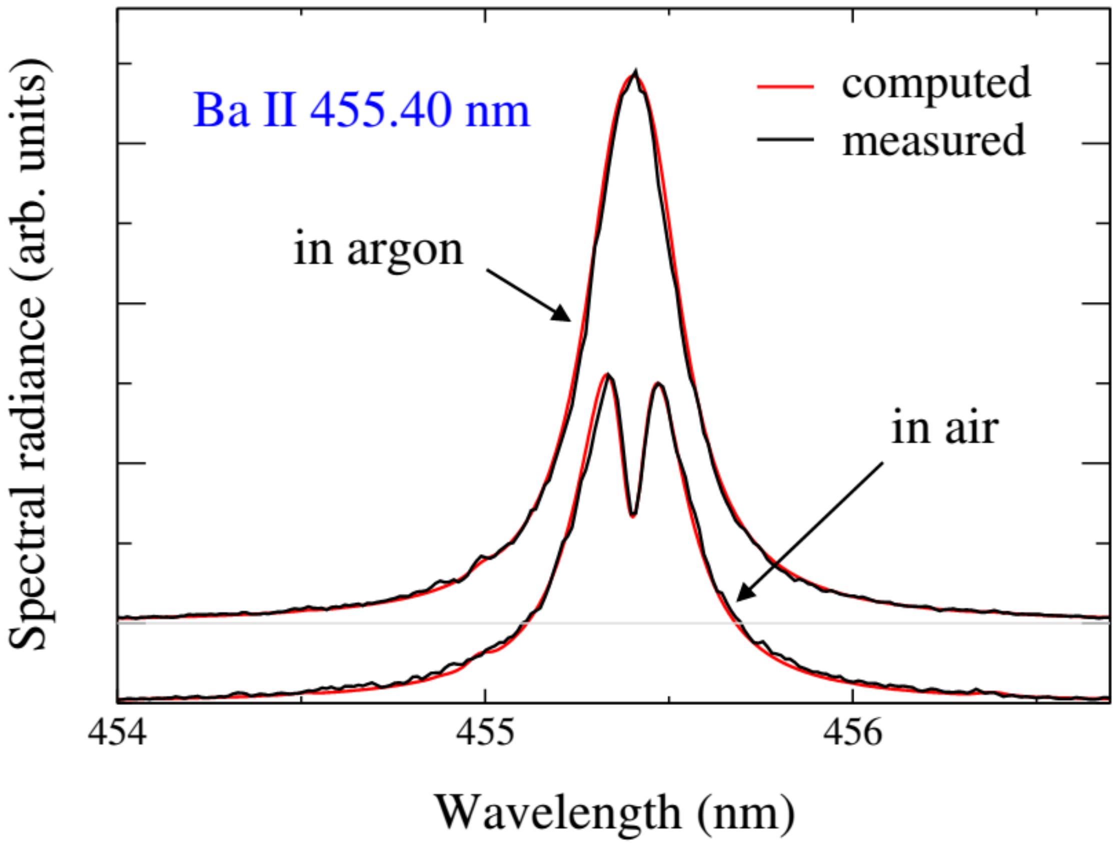


verre N-BaK4

$E_{las}$ = 6 mJ, $\lambda$ = 266 nm, $\tau$ = 5 ns

**sous air**

☞ **plasma non-uniforme**

**sous argon**

☞ **plasma uniforme**

# Validity conditions of physical model

**Self-absorption is negligible ?**

LTE validity requires high density ($n_e \geq 10^{16}$ cm$^{-3}$)

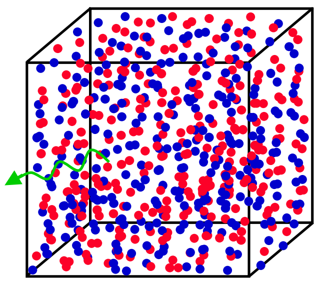

⇨ **self-absorption significant**

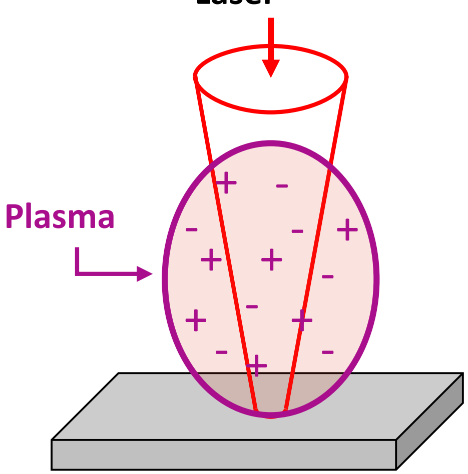


hypotheses :

- **stoichiometric ablation**
- **local thermodynamic equilibrium**
- **plasma spatially uniform**
- **plasma optically thin**

# Methods of calibration-free measurements

## Compositional measurements: the mathematical problem

mass fraction of element A : $C_A = \dfrac{n_A m_A}{\rho_{tot}}$

LTE plasma of $M$ elements ☞ $M + 1$ parameters

⇨ $n_A$ of $M$ elements and $T$

⇔ $C_A$ of $M$-$1$ elements, $n_e$ and $T$

$$n_A = \sum_{z=0}^{z_{max}} n_A^z + 2\sum_{z=0}^{1} n_{A_2}^z + \sum_{B \neq A} \sum_{z=0}^{1} n_{AB}^z.$$

neutrality: $$n_e = \sum_A \sum_{z=1}^{z_{max}} z\, n_A^z.$$

$n_A$ = number density of element A

$m_A$ = atomic mass

$\rho_{tot} = \sum_A n_A m_A$

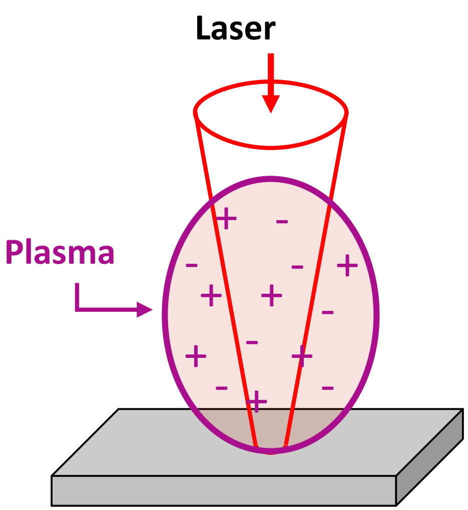

# Methods of calibration-free measurements

## Compositional measurements: the mathematical problem

mass fraction of element A : $C_A = \frac{n_A m_A}{\rho_{tot}}$

$$n_A = \sum_{z=0}^{z_{max}} n_A^z + 2\sum_{z=0}^{1} n_{A_2}^z + \sum_{B\neq A}\sum_{z=0}^{1} n_{AB}^z.$$

LTE plasma of *M* elements ☞ *M* + 1 parameters

⇨ $n_A$ of *M* elements and *T*

⇔ $C_A$ of *M-1* elements, $n_e$ and *T*

neutrality: $n_e = \sum_A \sum_{z=1}^{z_{max}} z\, n_A^z.$

$n_A$ = number density of element A

$m_A$ = atomic mass

$\rho_{tot} = \sum_A n_A m_A$

*Emission coeff.* $\varepsilon_{ul} = A_{ul}\frac{h\nu}{4\pi} n_u$

*Boltzmann* $n_u = n\frac{g_u}{Q(T)} e^{-E_u/kT}$

⇨ **measurement of *M* + 1 lines**

**Boltzmann plot**

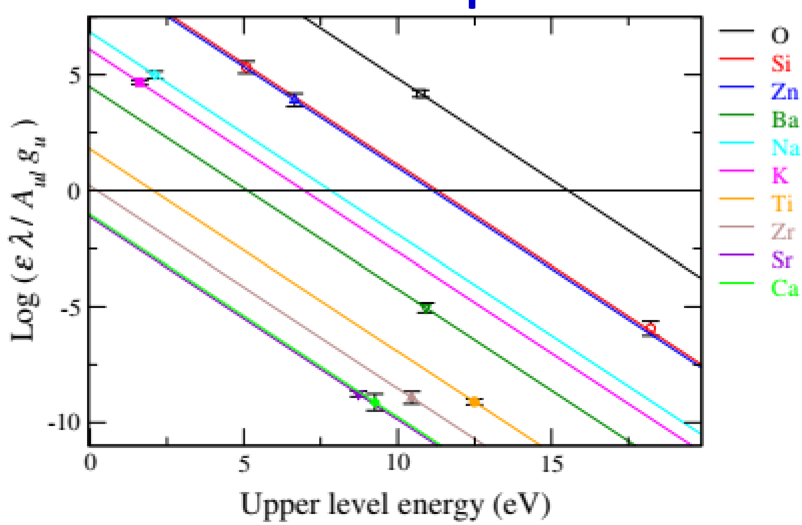

# Methods of calibration-free measurements

**First approach,** *Ciucci et al. Appl. Spectrosc. 1999* ☞ **multielemental Boltzmann plot**

moderate ionization ☞ $n_i << n_n$ ⇨ $n_n \cong n_A := n$

*Emission coeff.* $\varepsilon_{ul} = A_{ul} \dfrac{h\nu}{4\pi} n_u \Rightarrow I_{ul} \propto \varepsilon_{ul}$ **if optically thin**

*Boltzmann* $n_u = n \dfrac{g_u}{Q(T)} e^{-E_u/kT}$ ⇨ $\ln\left(\dfrac{I_{ul}\lambda}{A_{ul} g_u}\right) = -\dfrac{E_u}{kT} + \ln\left(R\dfrac{n}{Q}\right)$

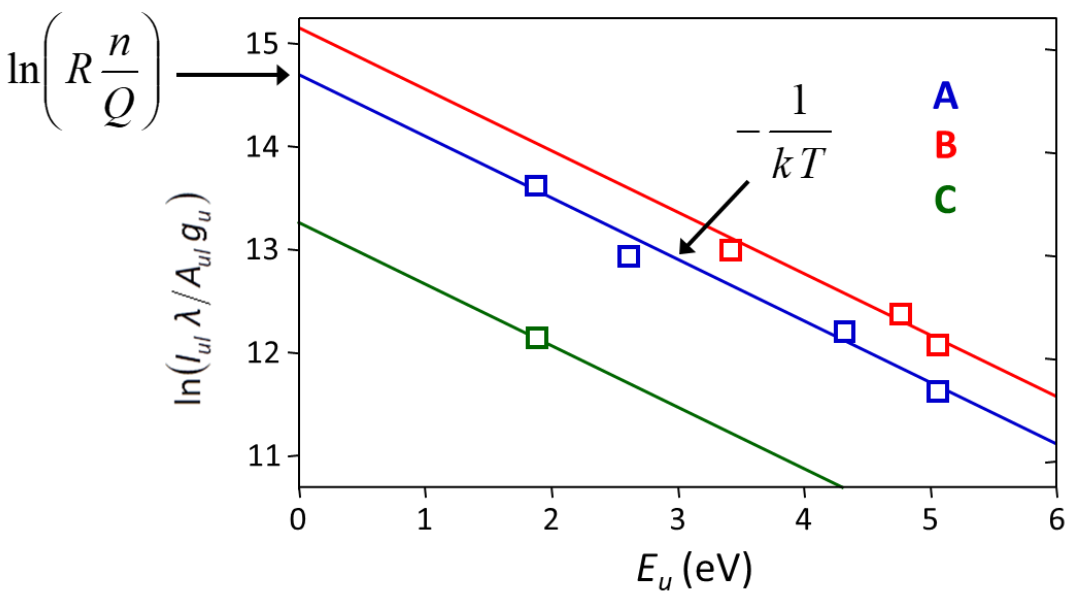


☞ **easy to implement**

⇨ **big success**

☞ **low accuracy**

reduce errors

☞ **use of many lines**

⇨ **error identification difficult**

# Methods of calibration-free measurements

**First approach,** *Ciucci et al. Appl. Spectrosc. 1999* ☞ **multielemental Boltzmann plot**

☞ **low accuracy**

⇨ **amended methods with corrections**

| correction | need | feasibility |
|---|---|---|
| non-stoichiometric ablation | non | limited |
| failure of LTE | non | non |
| plasma non-uniformity | sometimes | limited |
| self-absorption | always | yes |

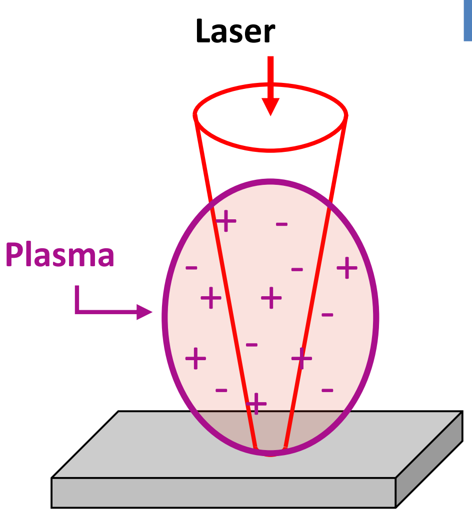


hypotheses :

- **stoichiometric ablation**
- **local thermodynamic equilibrium**
- **plasma spatially uniform**
- **plasma optically thin**

# Methods of calibration-free measurements

## Methods based on spectra simulation

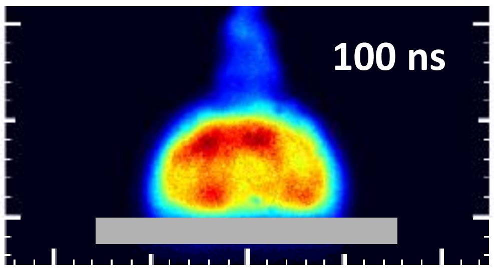


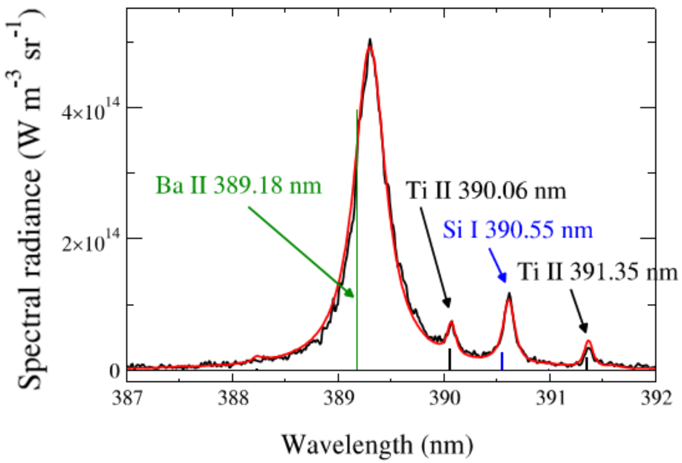


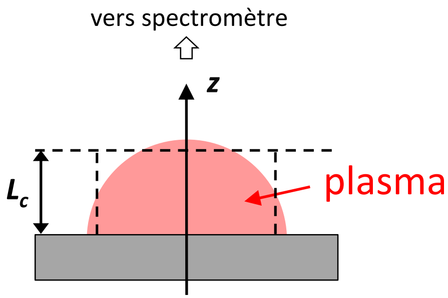


☞ analytical solution of radiation transfer equation

*Hermann et al. J. Appl. Phys 1998*

⇒ Spectral radiance $B_\lambda = U_\lambda\left(1 - e^{-\tau}\right)$

$$\alpha_{line}(\lambda) = \pi r_0 \lambda^2 f_{lu} n_l P(\lambda_0, \lambda)\left(1 - e^{-hc/\lambda kT}\right)$$

**Doppler and Stark broadening**

$U_\lambda$ = blackbody spectral radiance

$\tau$ = optical thickness = $\int \alpha(\lambda, z)dz = \alpha(\lambda)L$

α = absorption coefficient = $\sum_i \alpha_{line}^{(i)} + \alpha_{ion} + \alpha_{IB}$

$L$ = plasma diameter along line of sight

☞ **fast calculation**

# Methods of calibration-free measurements

## Methods based on spectra simulation

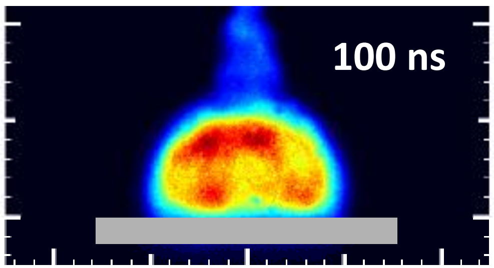


to spectrometer

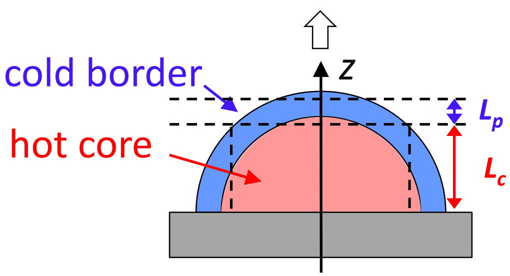


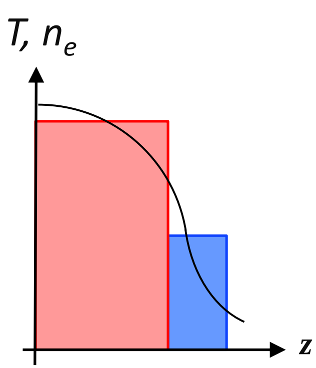


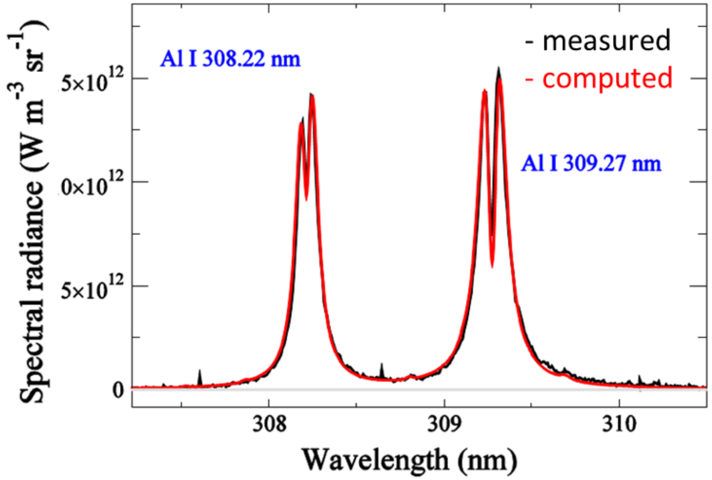


☞ analytical solution of radiation transfer equation
*Hermann et al. J. Appl. Phys 1998*

spectral radiance :

$$B = U_C\left(1-e^{-\alpha_C L_C}\right)e^{-\alpha_P L_P} + U_P\left(1-e^{-\alpha_P L_P}\right)$$

absorption coefficient :

$$\alpha(\lambda,T) = \pi\, r_0\, \lambda^2\, f_{lu}\, n_l\, P(\lambda_0,\lambda)\left(1-e^{-hc/\lambda kT}\right)$$

☞ **fast calculation**



cnrs Aix*Marseille université LP3

# Methods of calibration-free measurements

## Methods based on spectra simulation

### CF-LIBS method developed in LP3

**US patent 8942927 B2 (2015)**

(a)

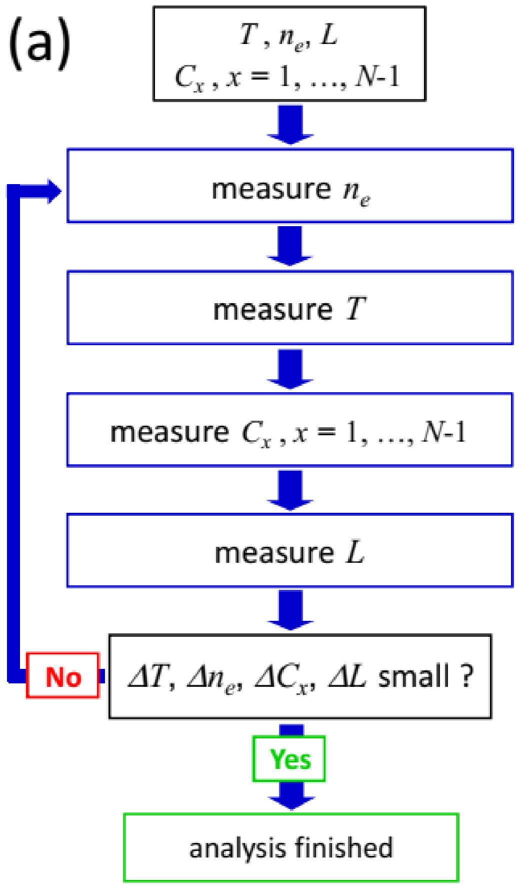


(b)

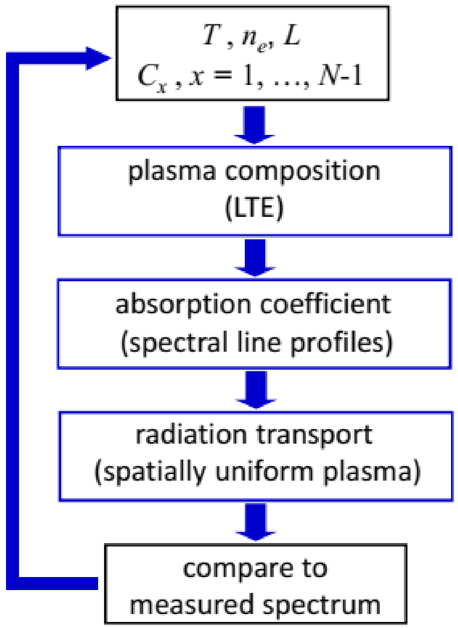

# CF-LIBS method developed in LP3

**US patent 8942927 B2 (2015)**

**example : analysis of fused silica ($SiO_2$)**

LTE plasma of *M* elements ☞ *M* + 1 parameters

⇔ $C_A$ of *M-1* elements, $n_e$ and *T*

*M* = 2 elements ⇨ **measurement of *M* + 1 lines**

- $n_e$ measurement
- *T* measurement
- composition measurement

# analysis of fused silica

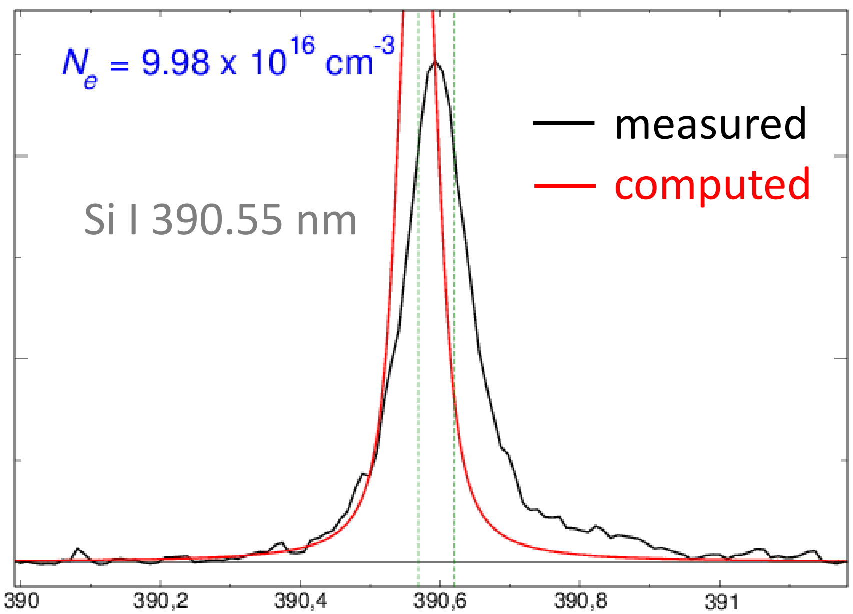


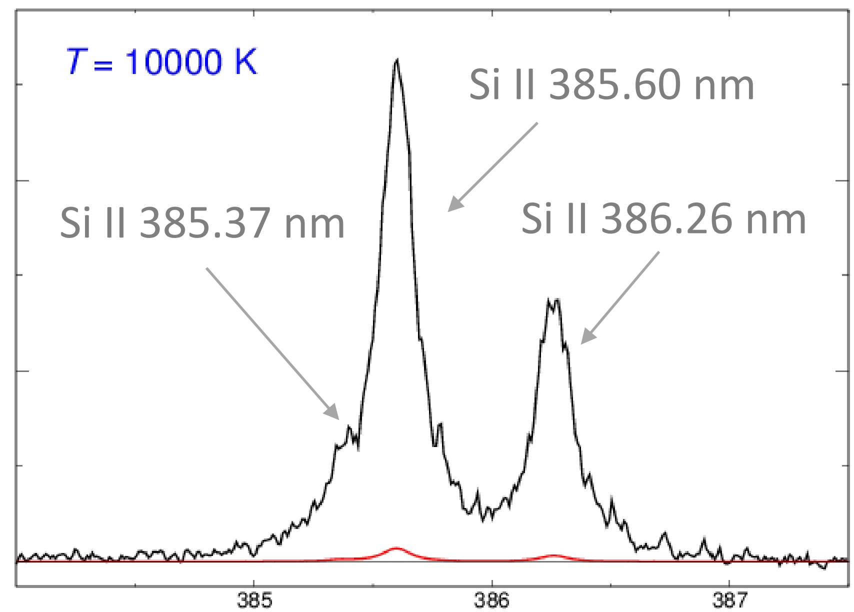


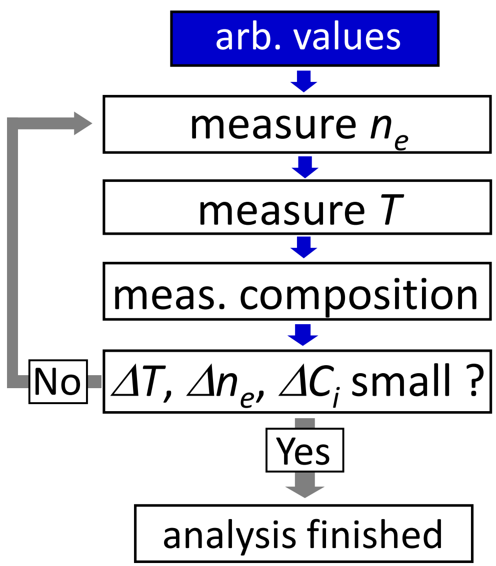


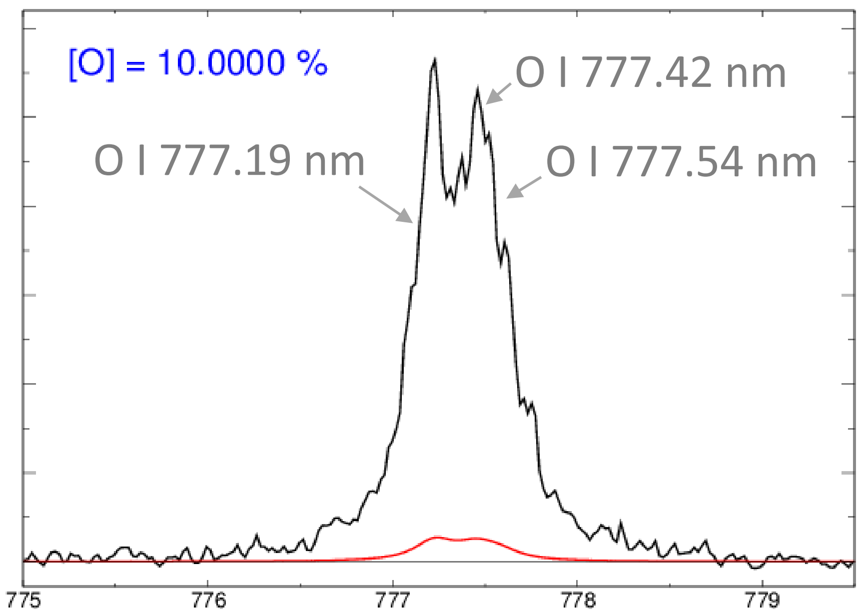


laser: 266 nm, 8 mJ
100 $Jcm^{-2}$
gas: argon, $5 \times 10^4$ Pa
gate: (500 ± 100) ns

NIST data

# analysis of fused silica

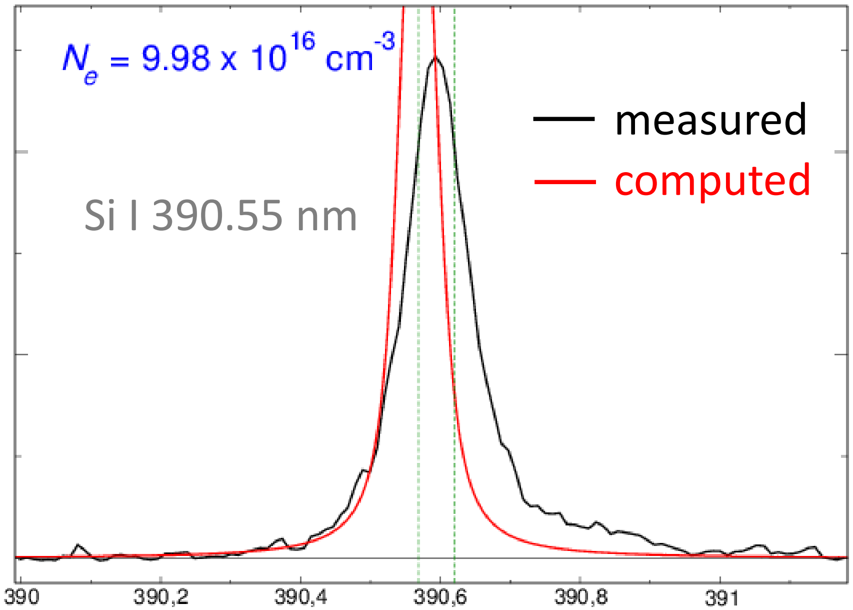


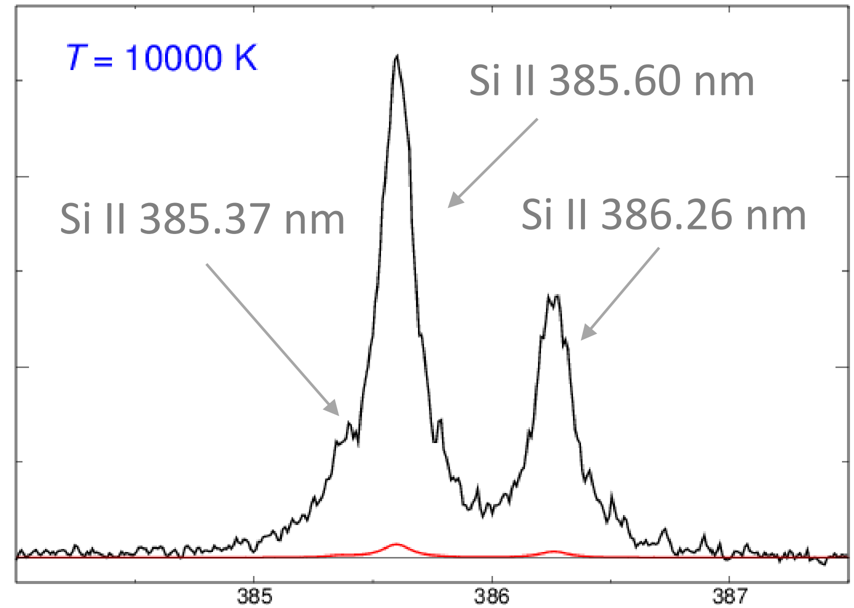


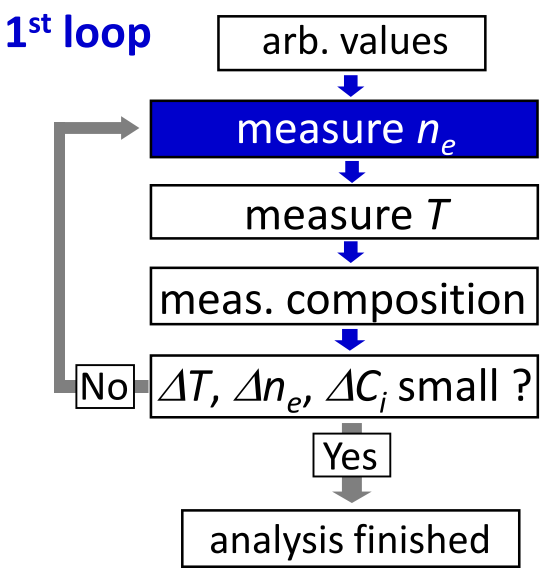


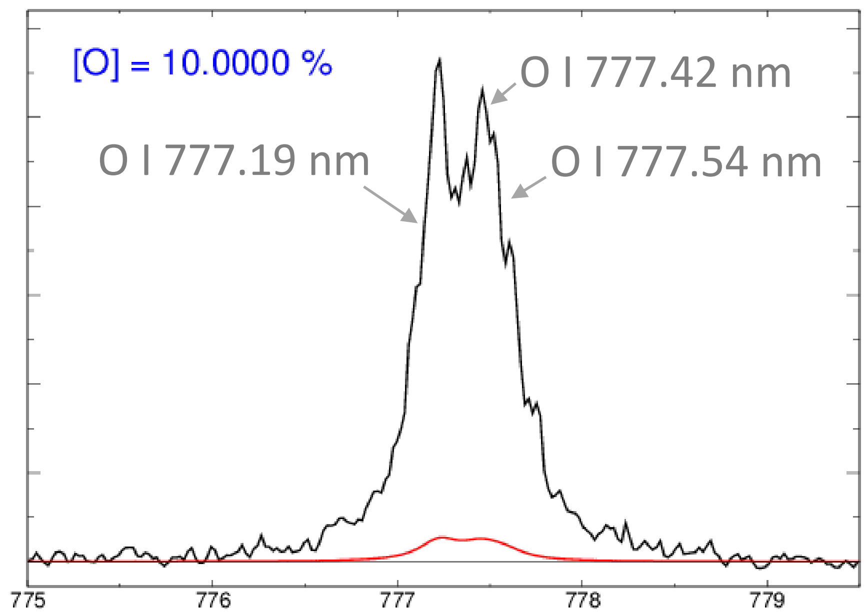


laser: 266 nm, 8 mJ
100 $Jcm^{-2}$
gas: argon, $5\times10^4$ Pa
gate: (500 ± 100) ns

NIST data

# analysis of fused silica

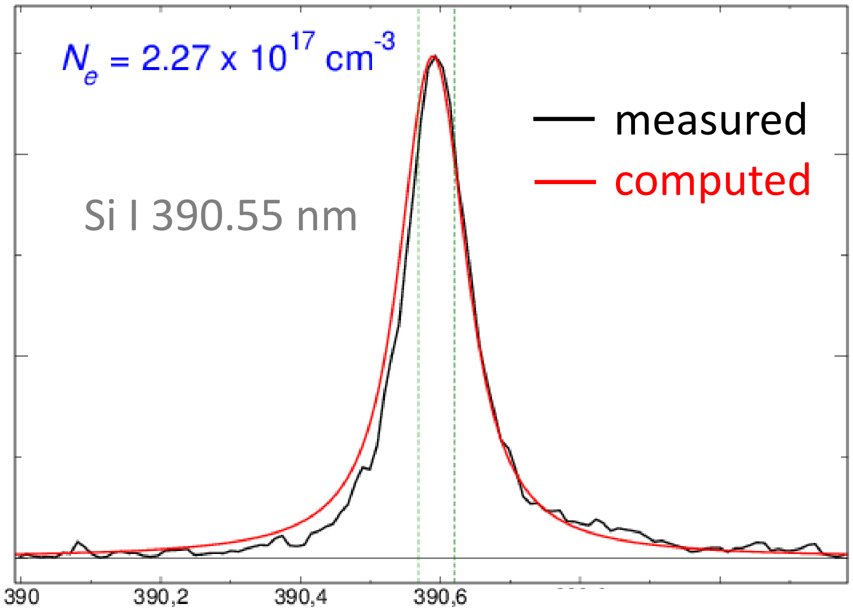


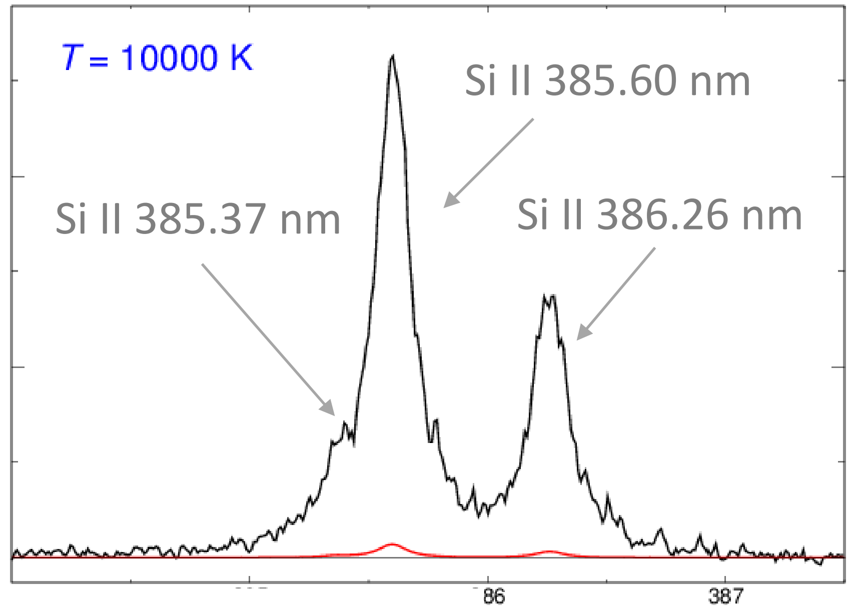


**1st loop**

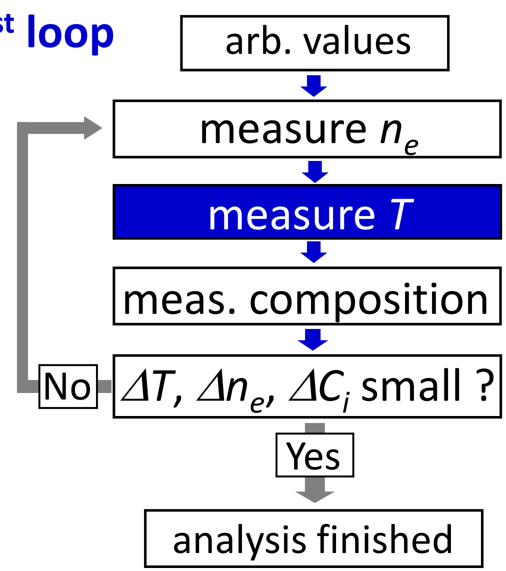


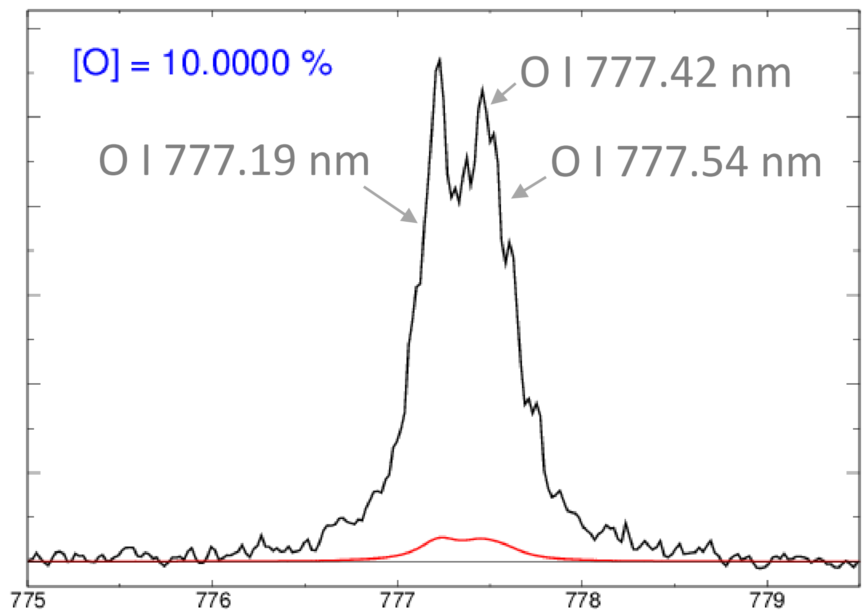


laser: 266 nm, 8 mJ
100 Jcm$^{-2}$
gas: argon, 5×10$^4$ Pa
gate: (500 ± 100) ns

NIST data

# analysis of fused silica

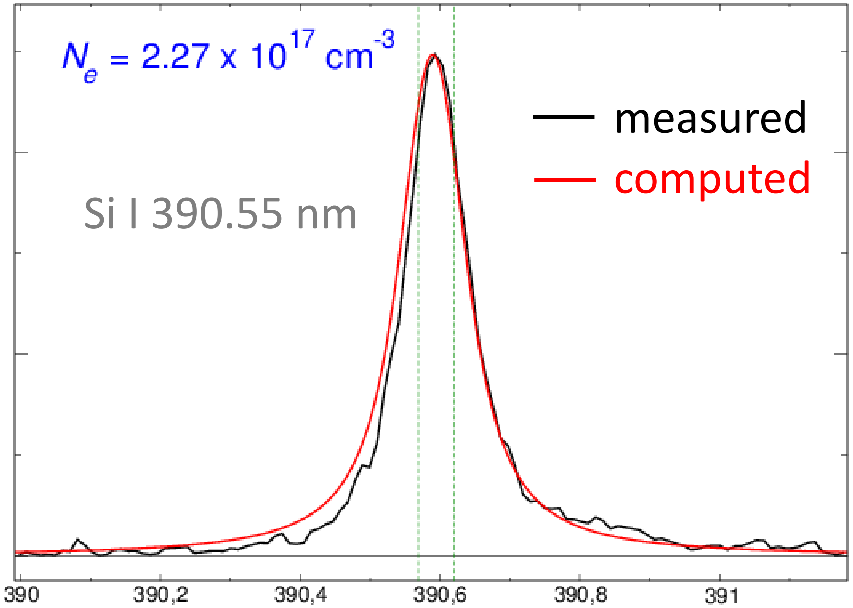


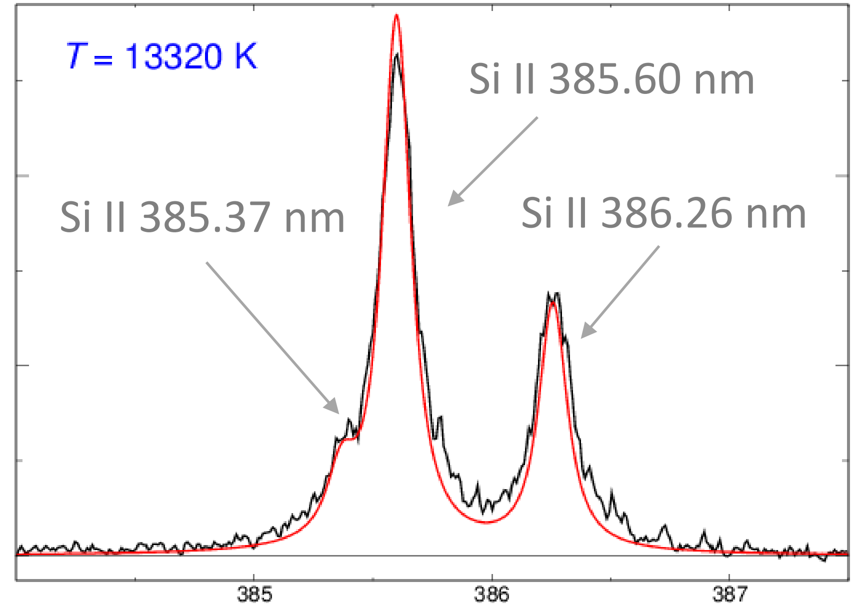


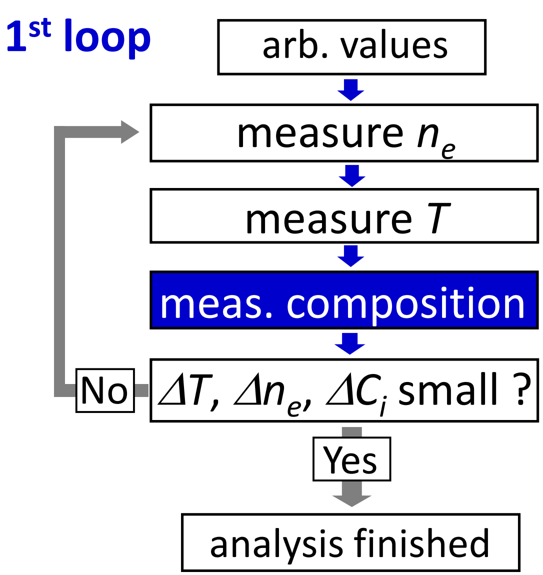


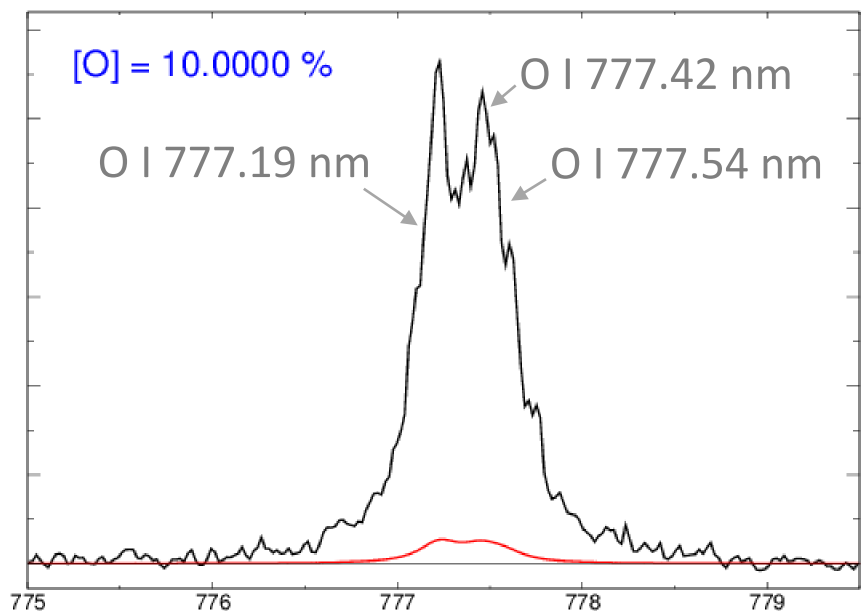


laser: 266 nm, 8 mJ
100 Jcm$^{-2}$
gas: argon, $5\times10^4$ Pa
gate: (500 ± 100) ns

NIST data

# analysis of fused silica

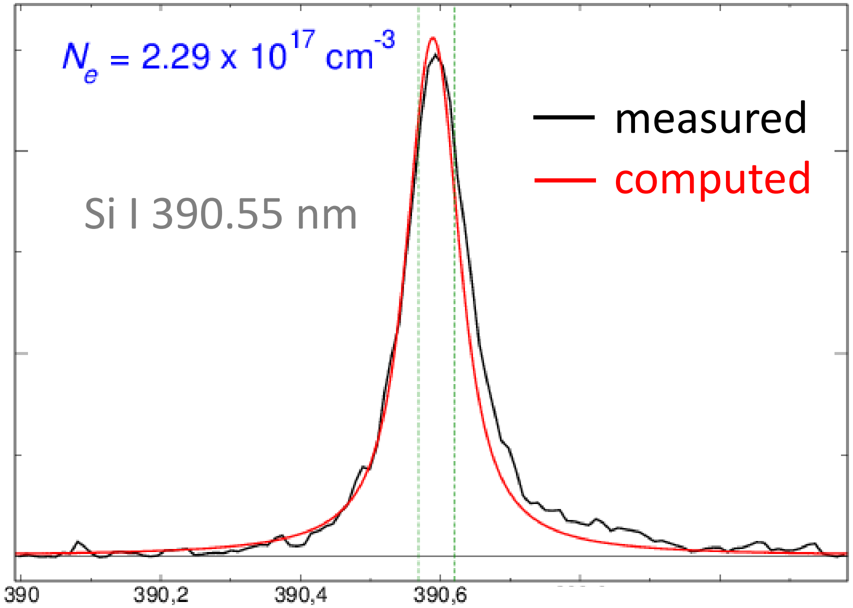


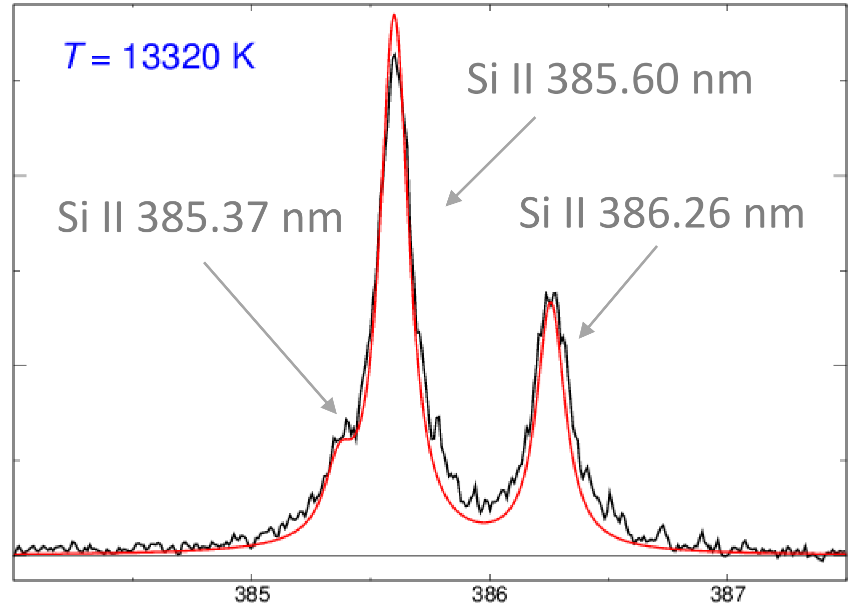


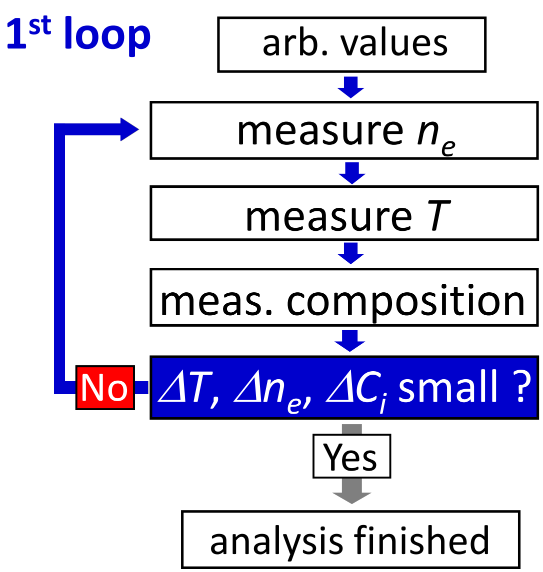


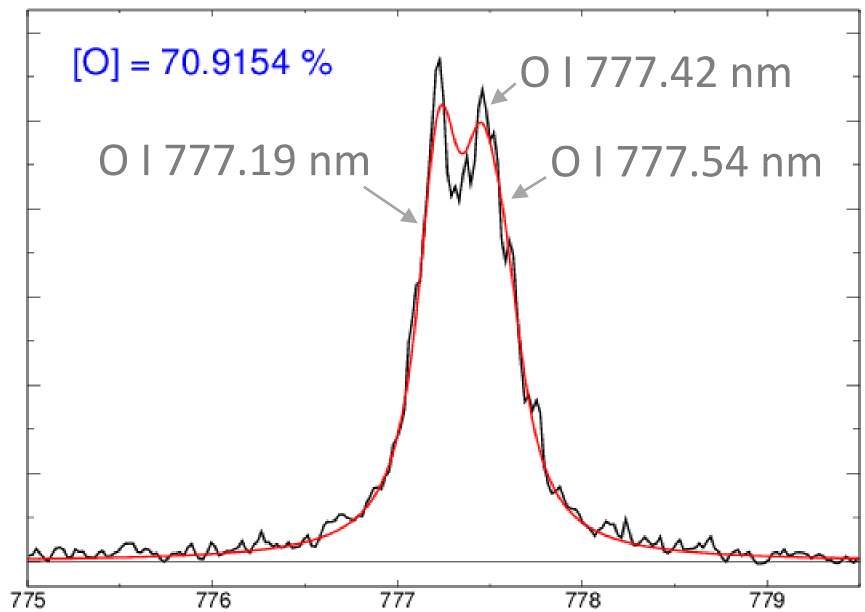


laser: 266 nm, 8 mJ
100 $Jcm^{-2}$
gas: argon, $5\times10^4$ Pa
gate: (500 ± 100) ns

NIST data

# analysis of fused silica

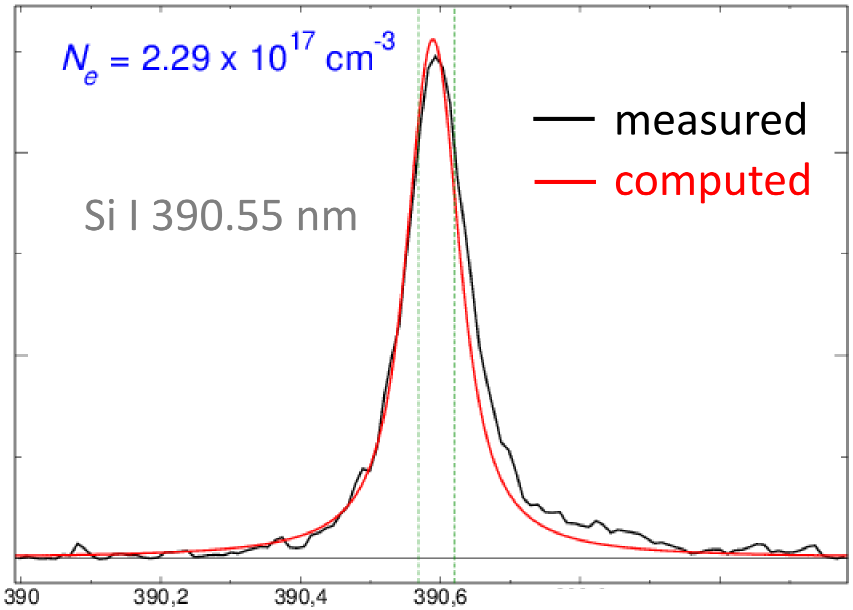


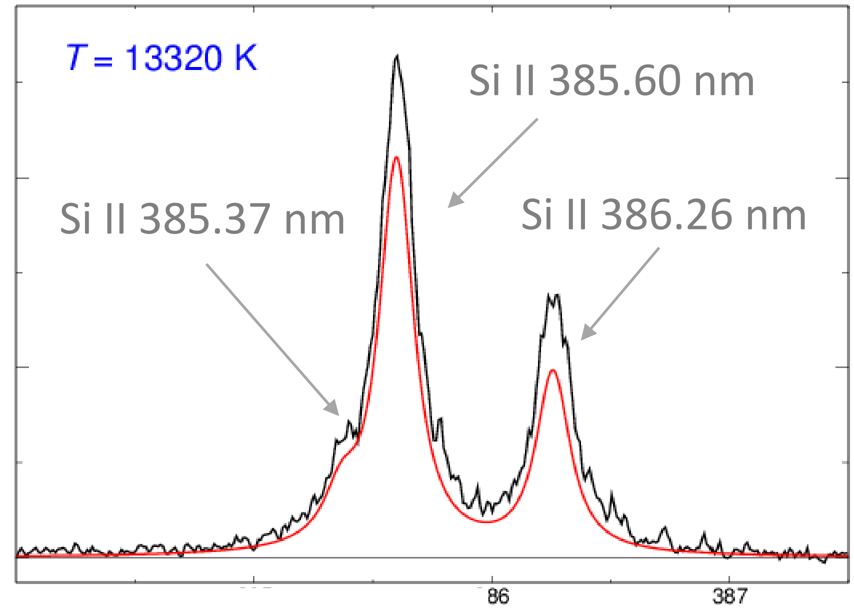


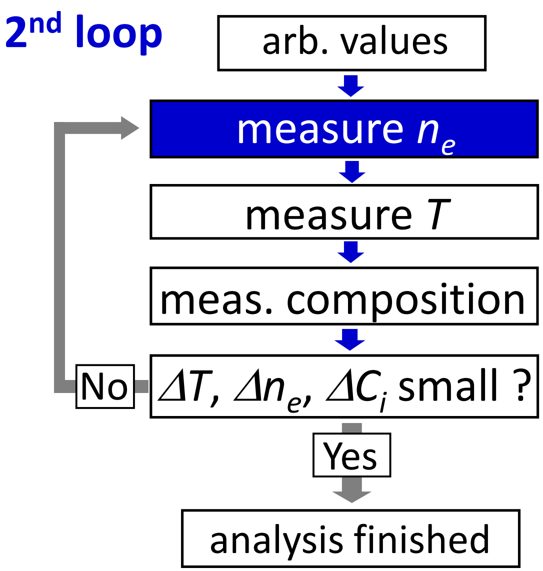


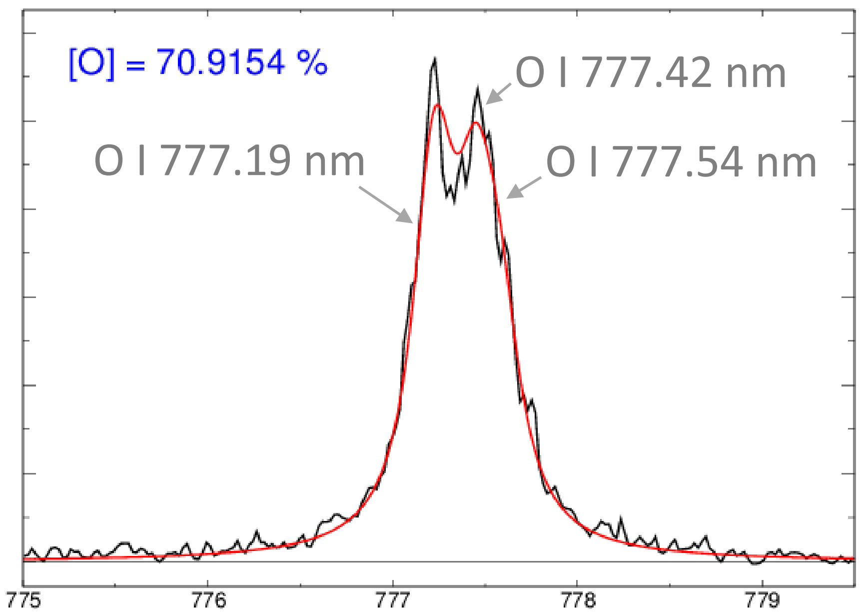


laser: 266 nm, 8 mJ
100 $Jcm^{-2}$
gas: argon, $5\times10^4$ Pa
gate: (500 ± 100) ns

NIST data

# analysis of fused silica

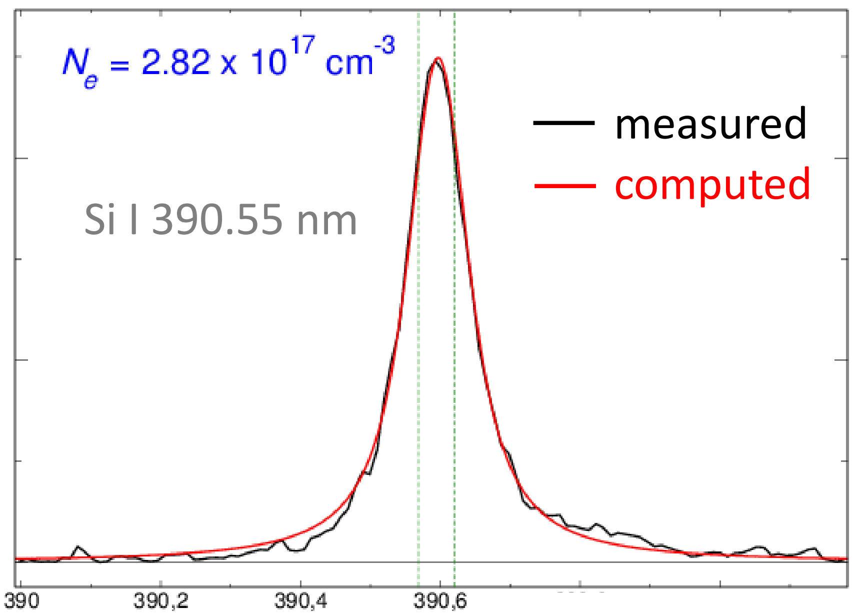


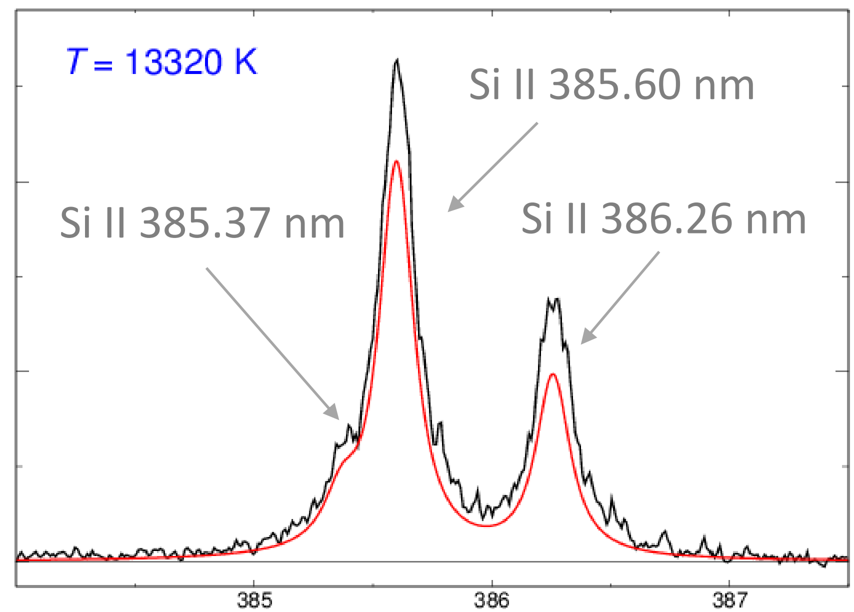


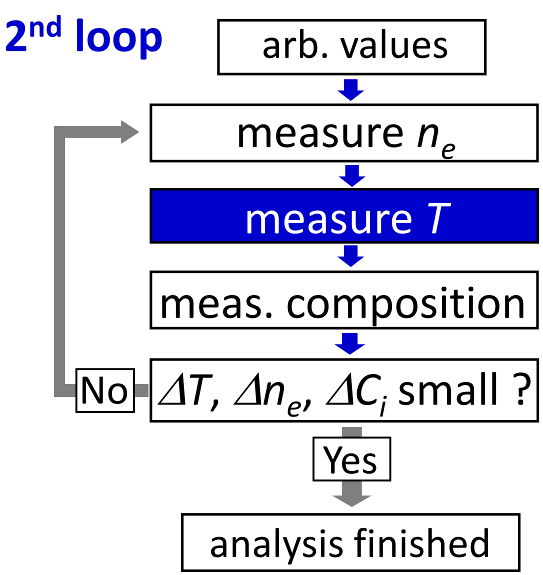


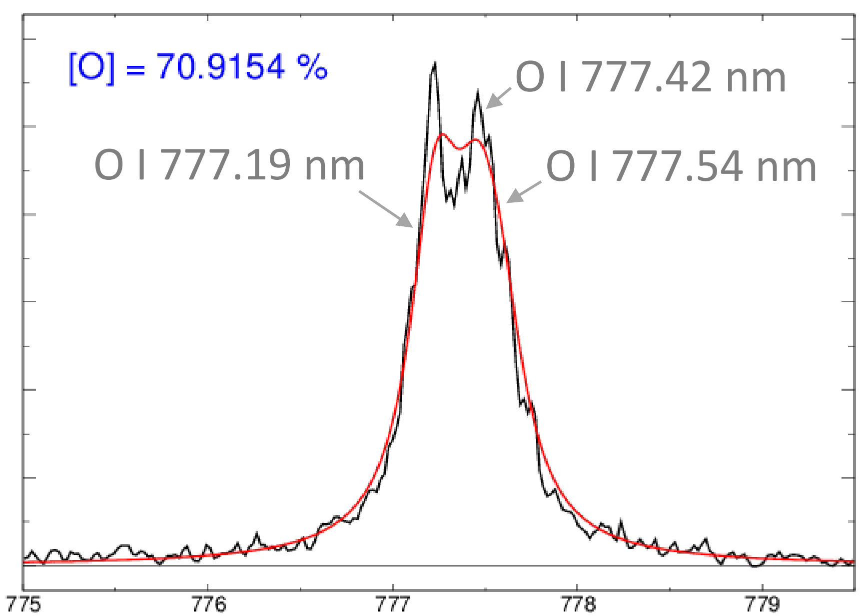


laser: 266 nm, 8 mJ
100 Jcm$^{-2}$
gas: argon, 5×10$^{4}$ Pa
gate: (500 ± 100) ns

NIST data

# analysis of fused silica

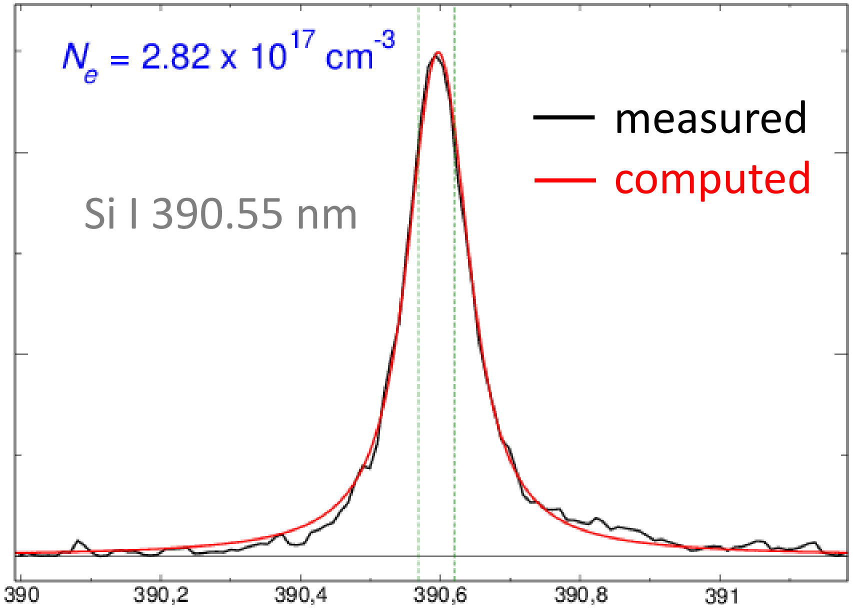


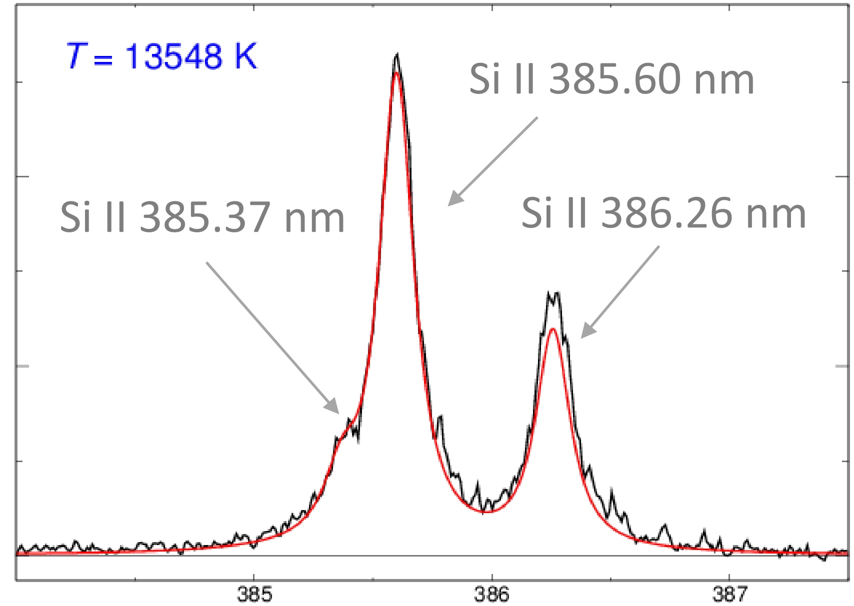


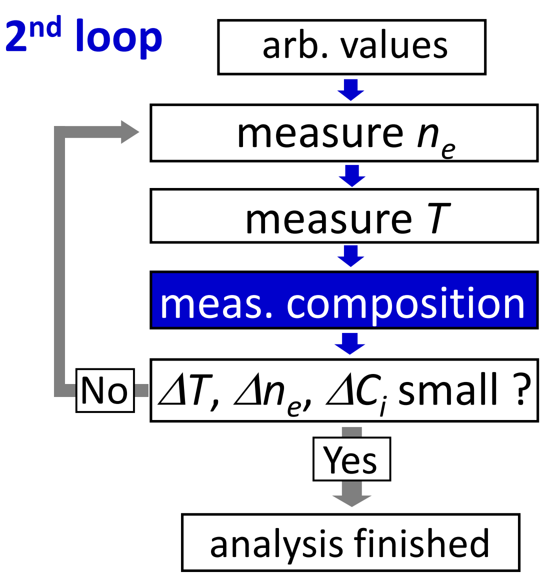


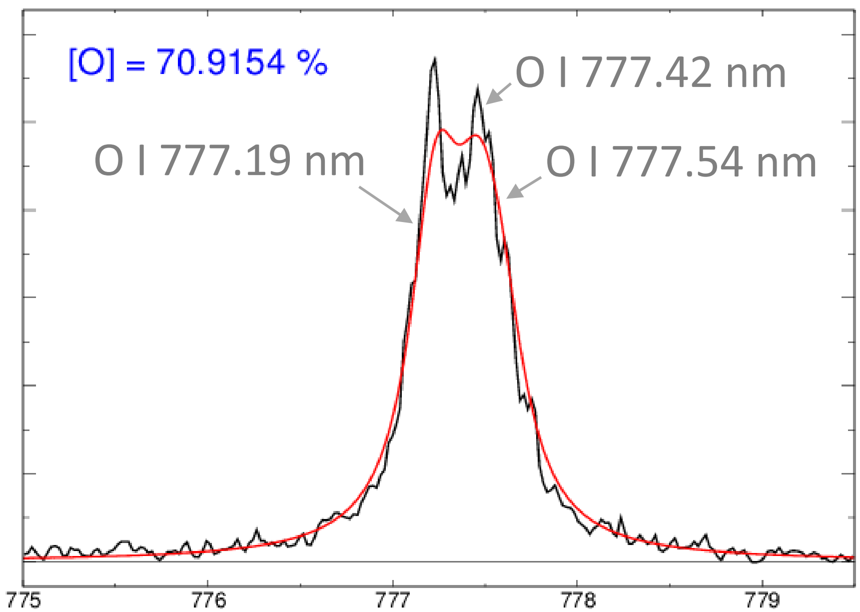


laser: 266 nm, 8 mJ
100 $Jcm^{-2}$
gas: argon, $5\times10^4$ Pa
gate: (500 ± 100) ns

NIST data

# analysis of fused silica

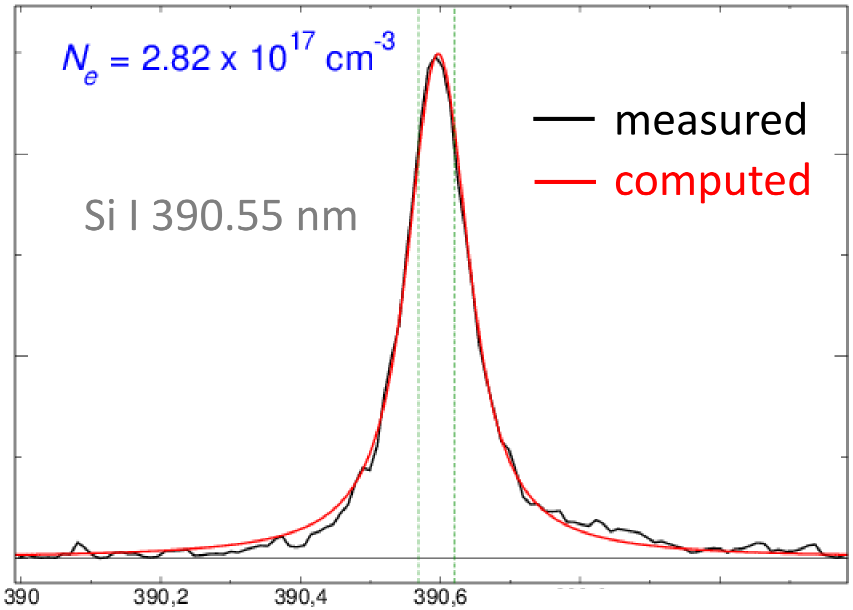


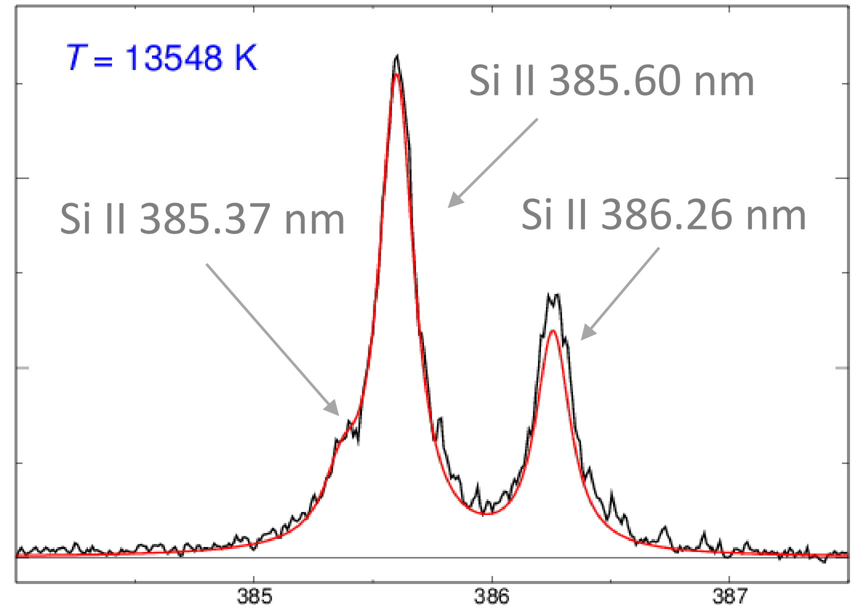


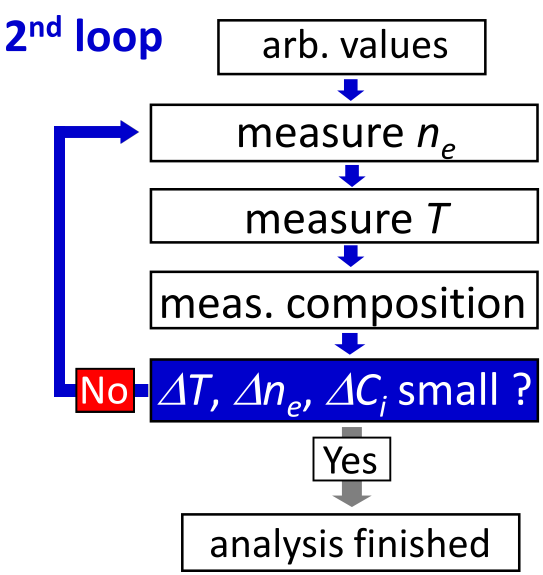


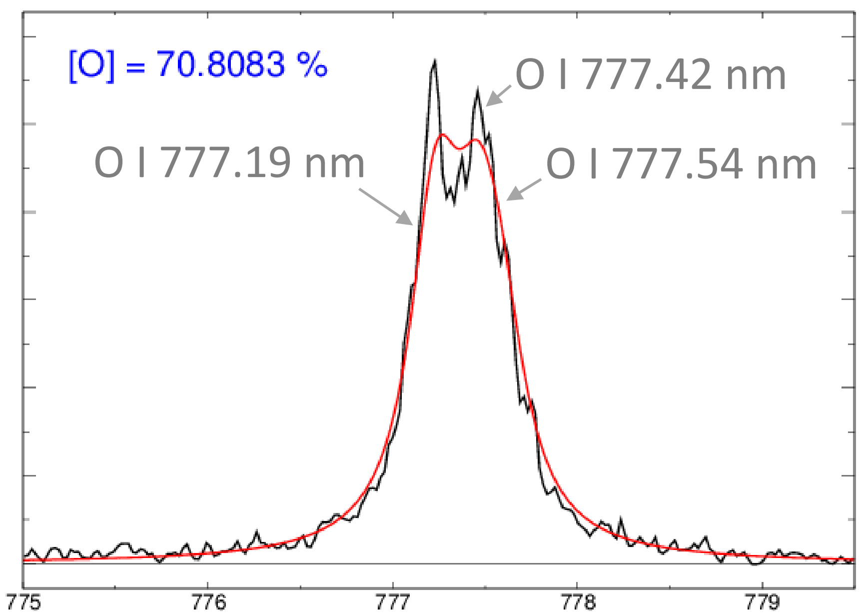


laser: 266 nm, 8 mJ
100 Jcm$^{-2}$
gas: argon, 5×10$^4$ Pa
gate: (500 ± 100) ns

NIST data

# analysis of fused silica

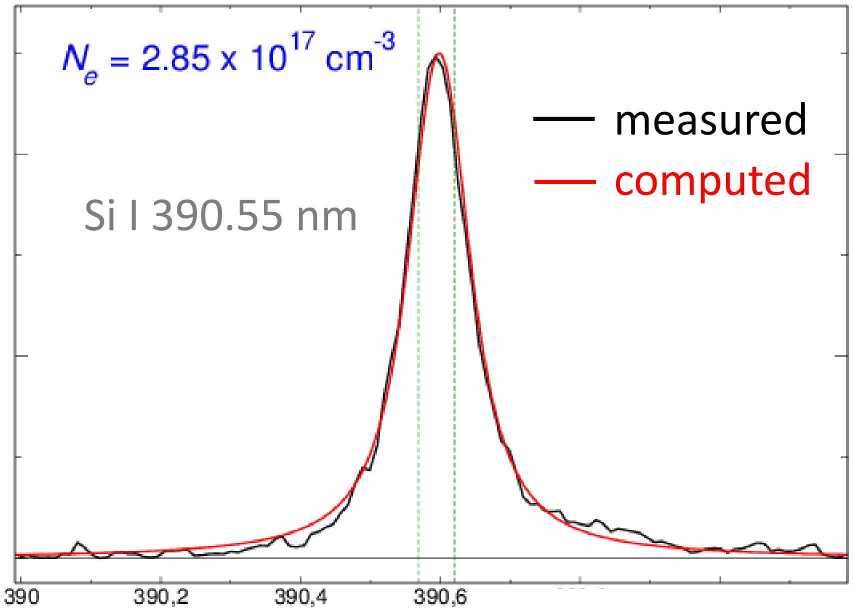


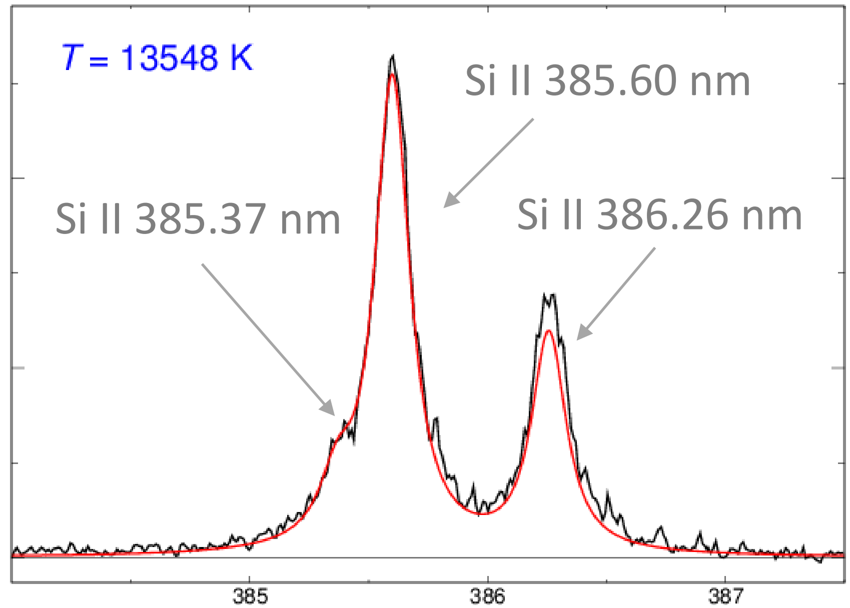


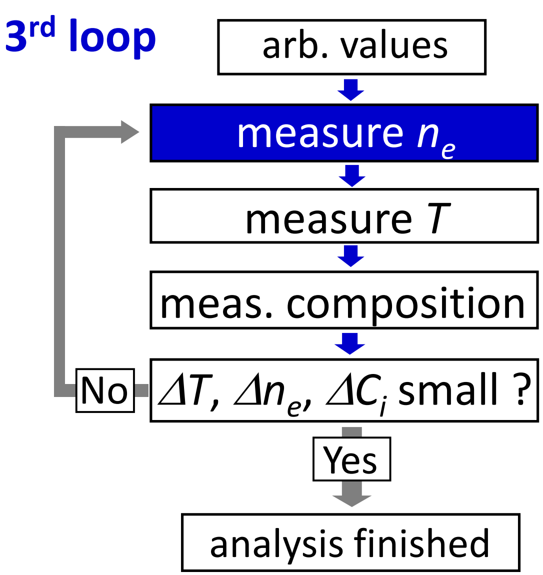


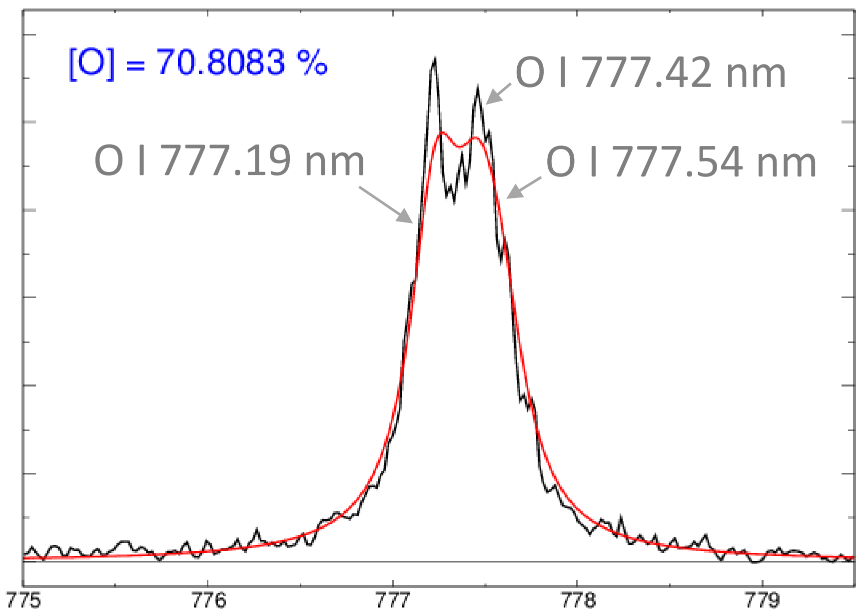


laser: 266 nm, 8 mJ
100 $Jcm^{-2}$
gas: argon, $5\times10^4$ Pa
gate: (500 ± 100) ns

NIST data

# analysis of fused silica

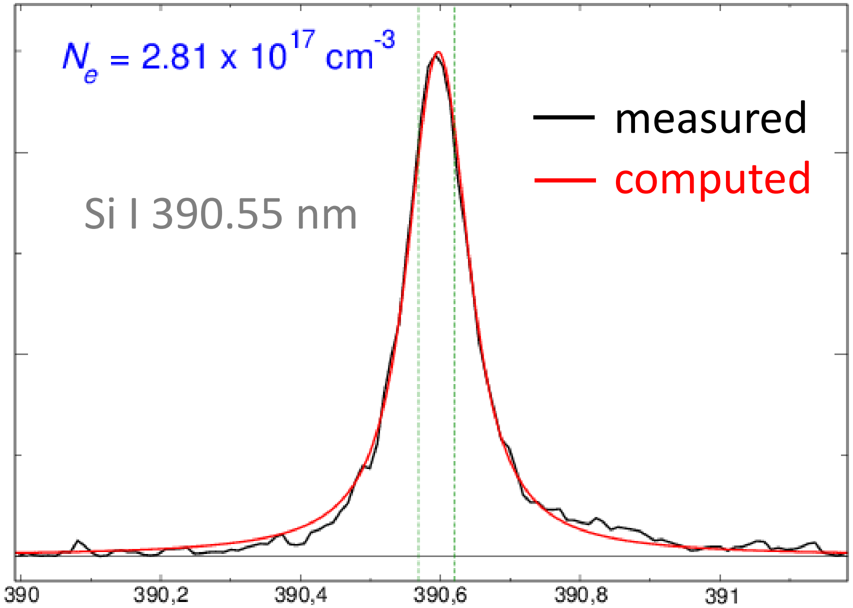


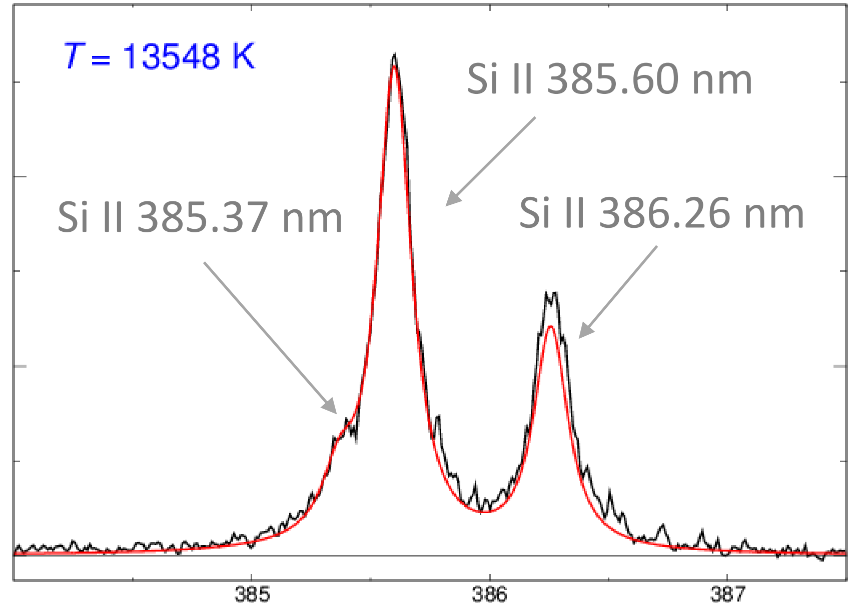


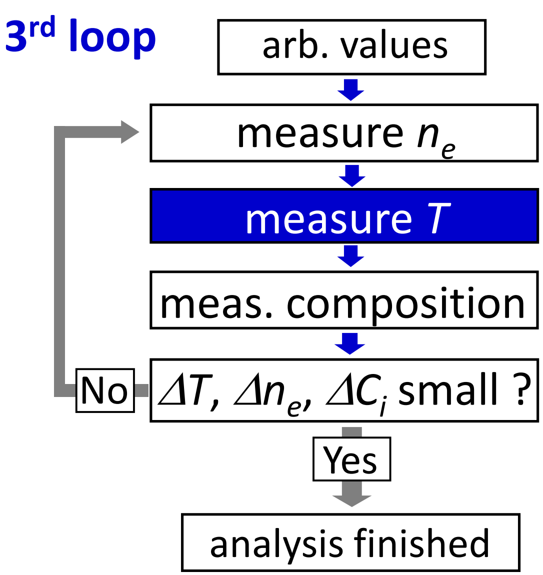


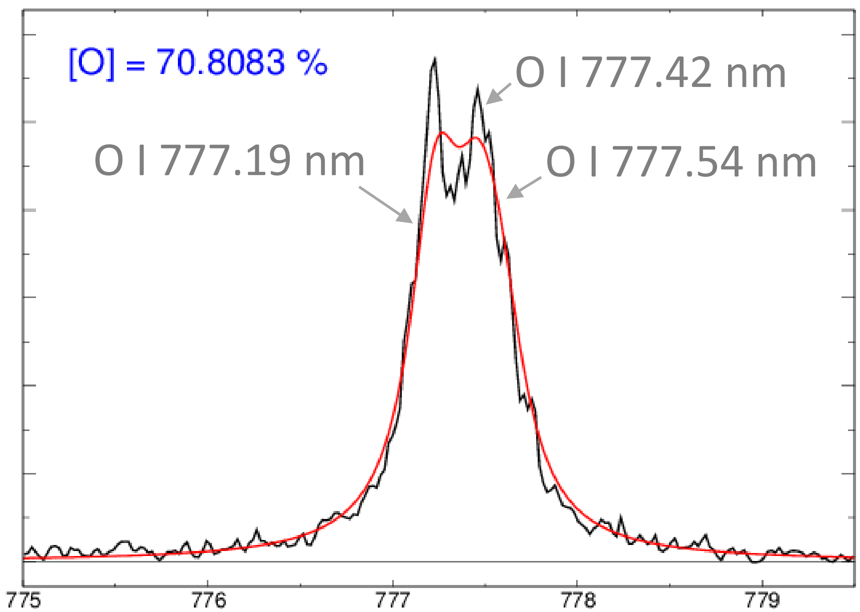


laser: 266 nm, 8 mJ
100 $Jcm^{-2}$
gas: argon, $5\times10^4$ Pa
gate: (500 ± 100) ns

NIST data

# analysis of fused silica

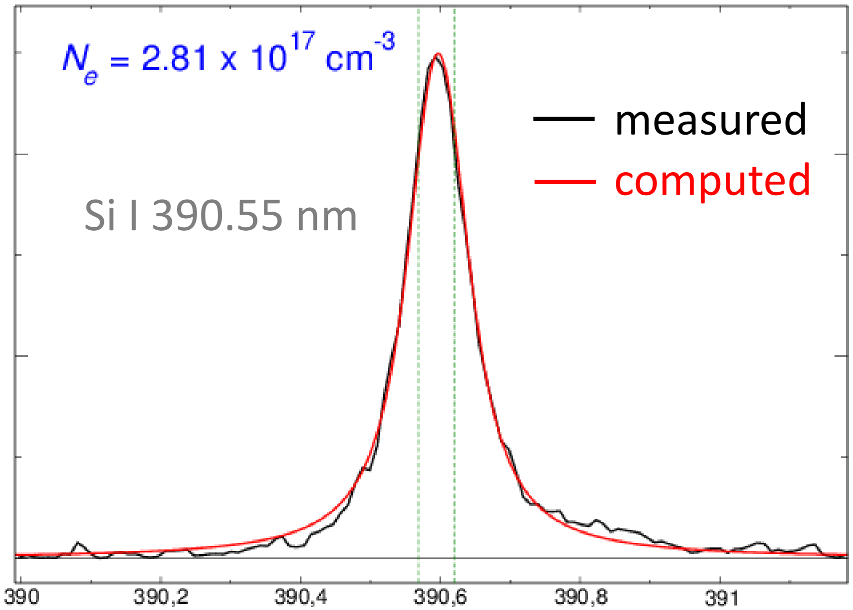


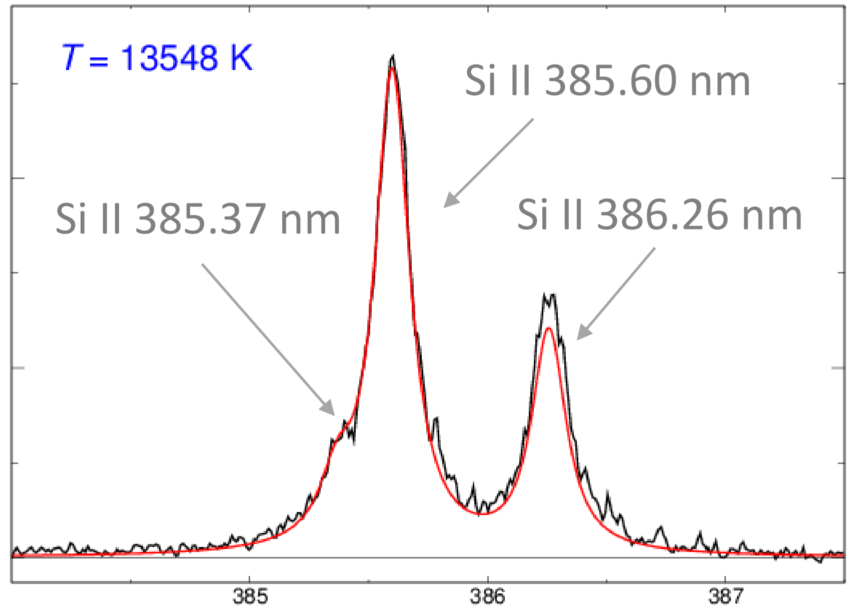


3$^{rd}$ loop

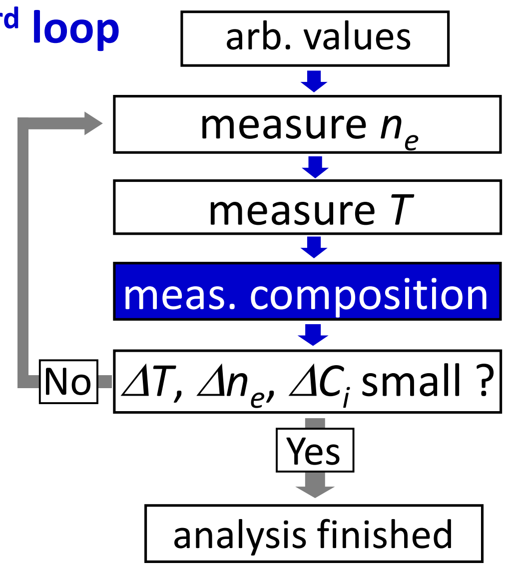


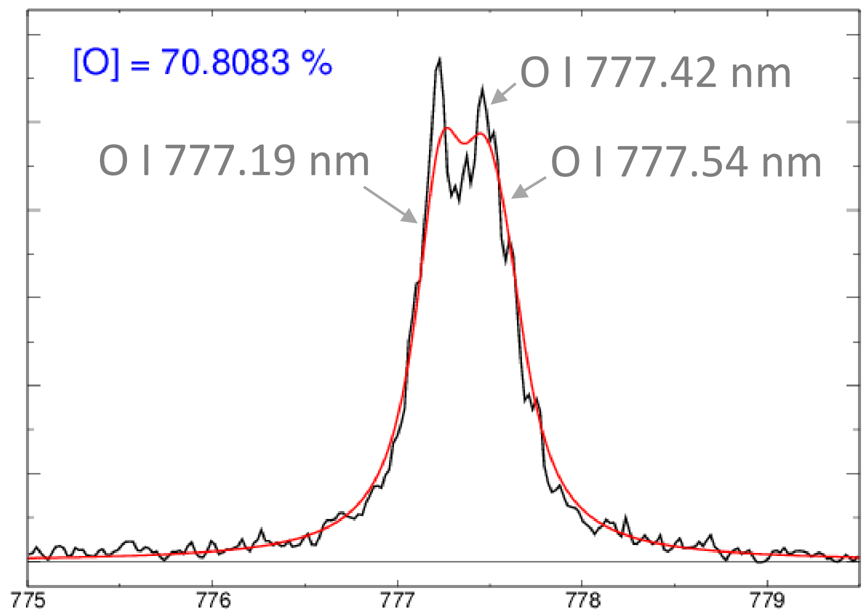


laser: 266 nm, 8 mJ
100 Jcm$^{-2}$
gas: argon, 5×10$^4$ Pa
gate: (500 ± 100) ns

NIST data

# analysis of fused silica

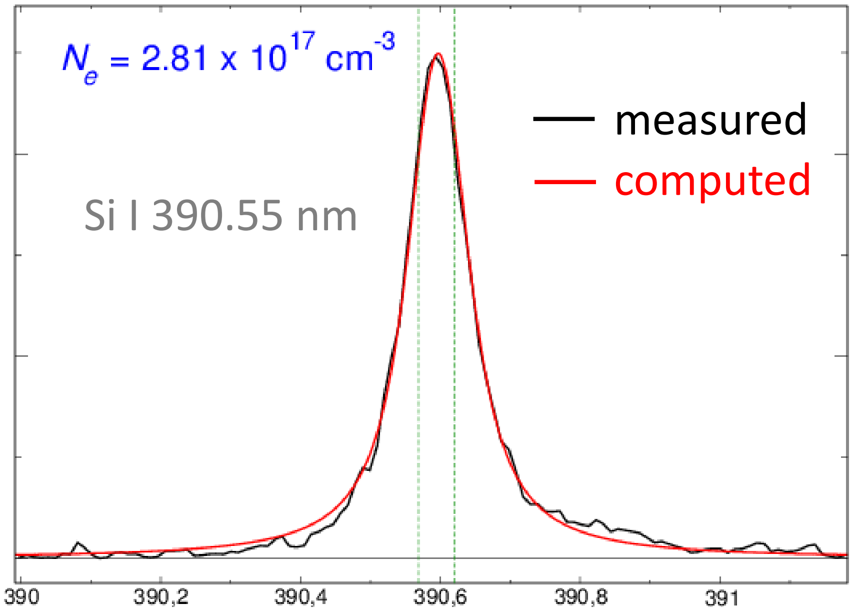


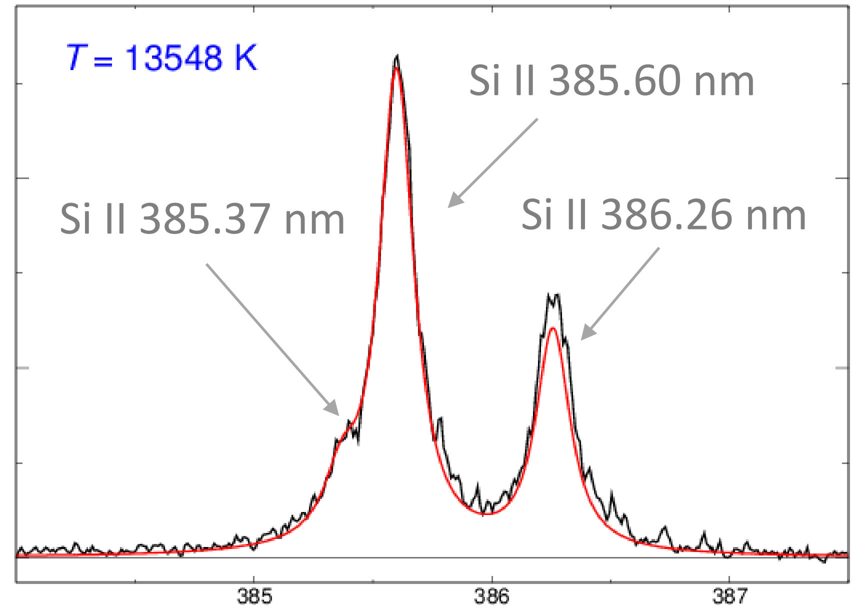


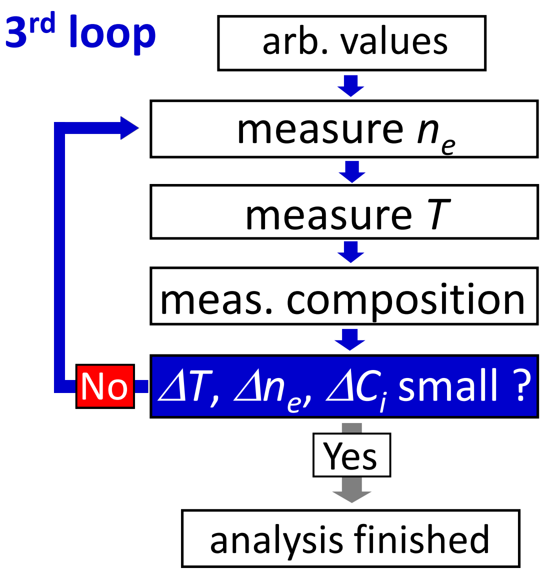


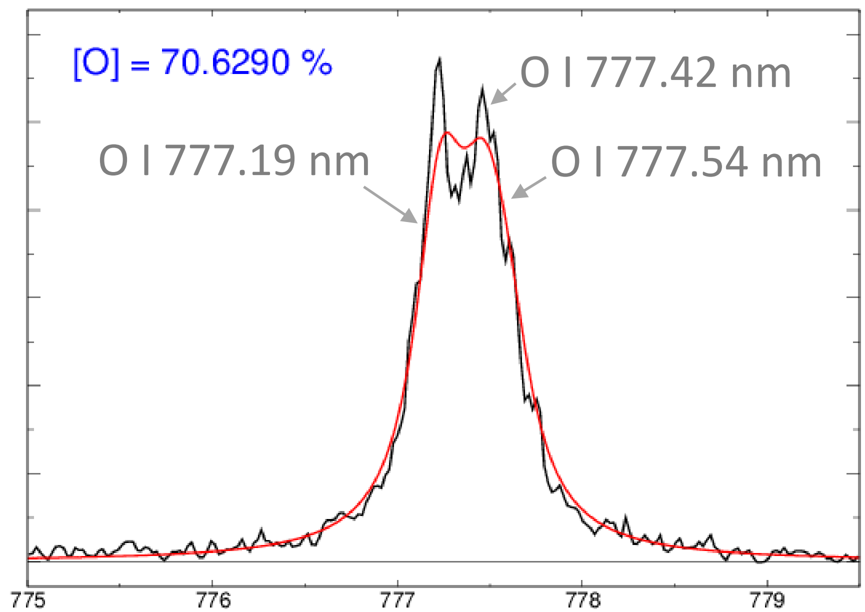


laser: 266 nm, 8 mJ
100 Jcm$^{-2}$
gas: argon, 5×10$^4$ Pa
gate: (500 ± 100) ns

NIST data

# analysis of fused silica

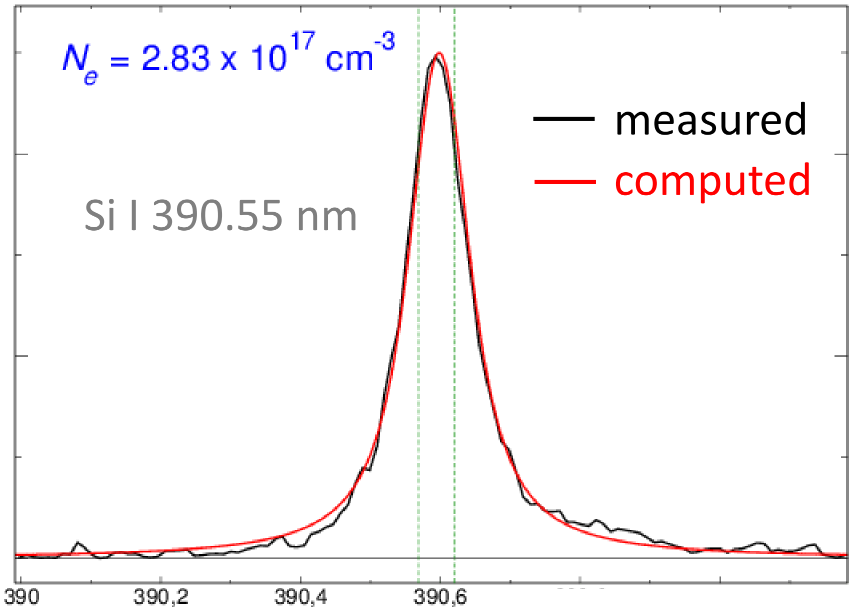


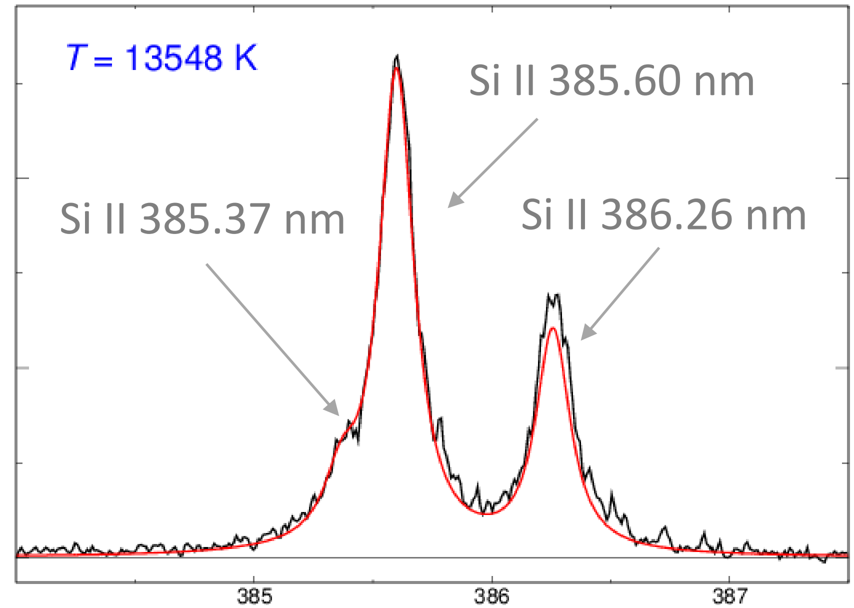


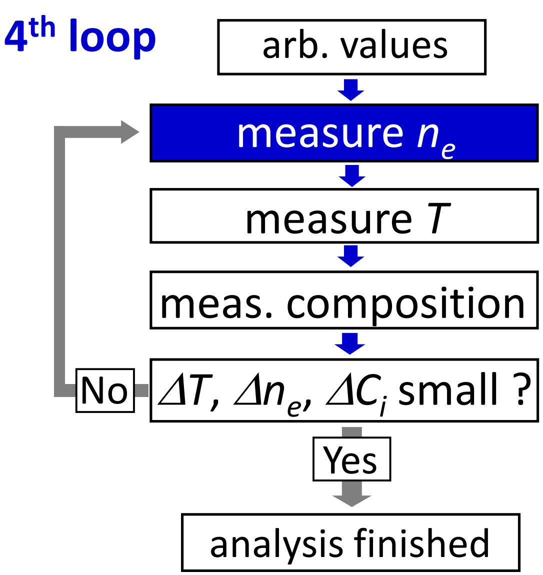


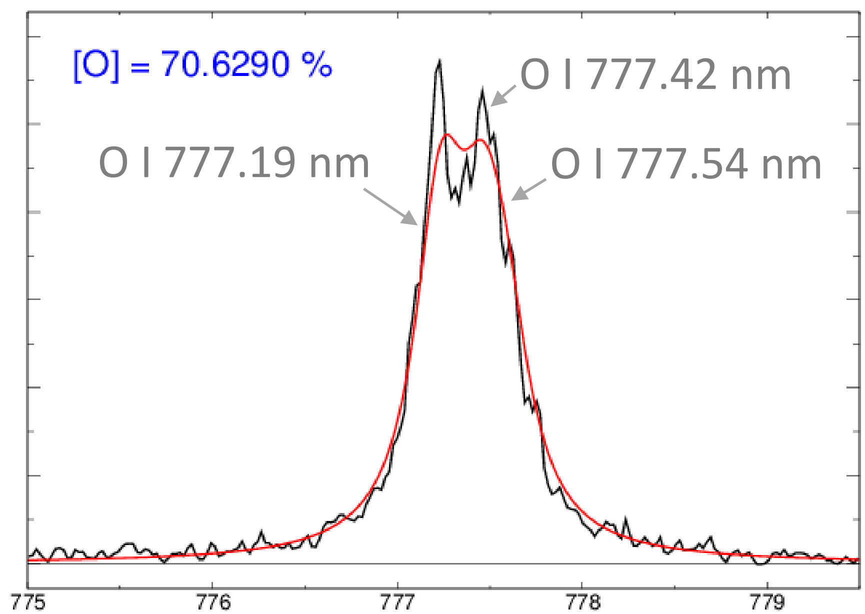


laser: 266 nm, 8 mJ
100 $Jcm^{-2}$
gas: argon, $5\times10^4$ Pa
gate: (500 ± 100) ns

NIST data

# analysis of fused silica

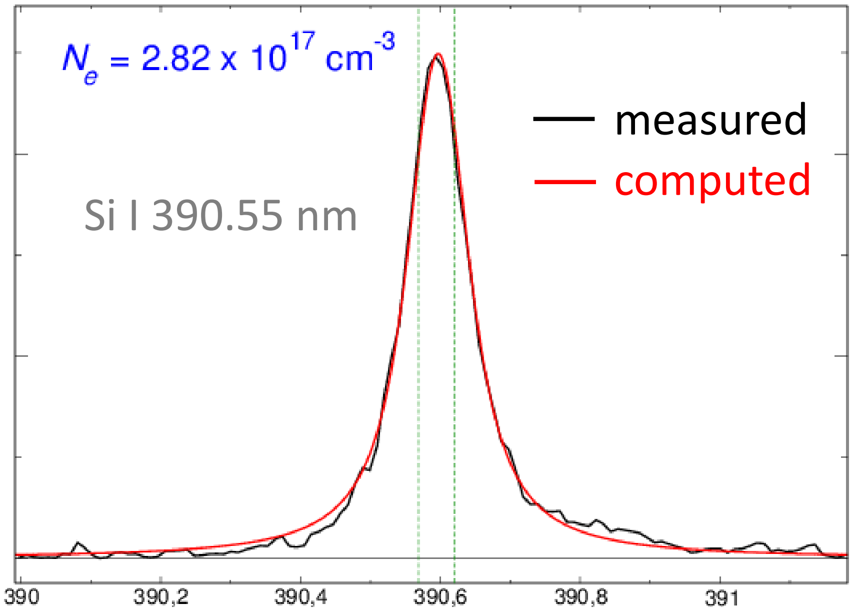


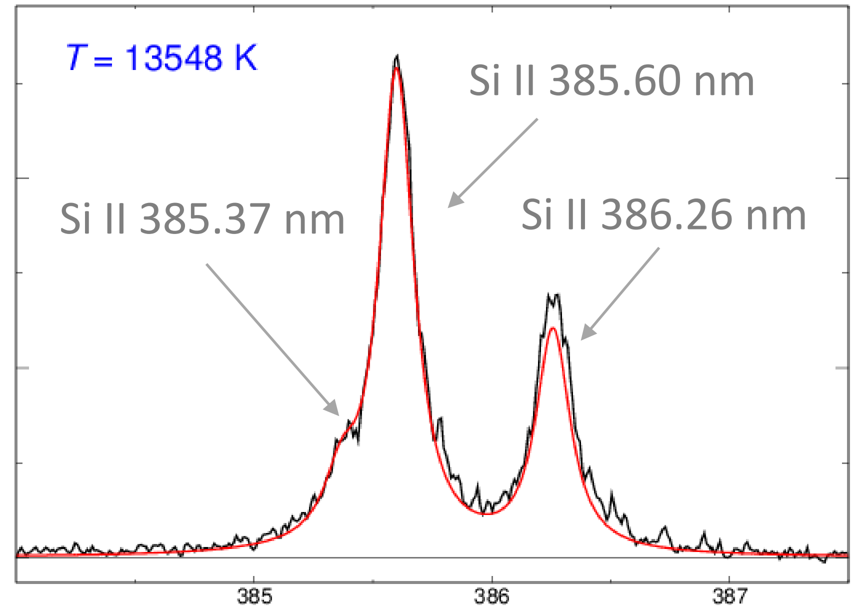


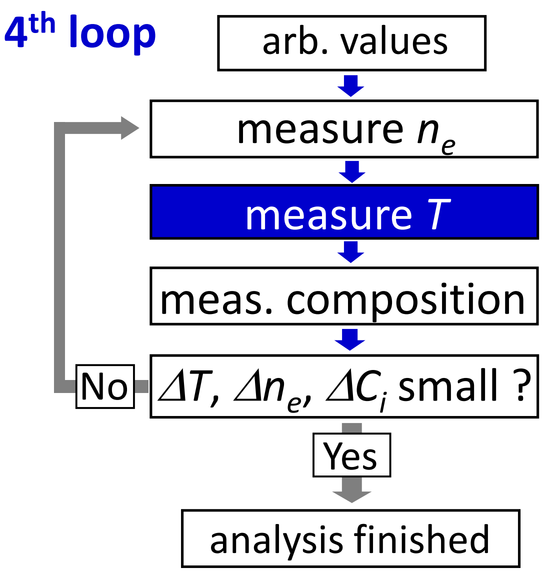


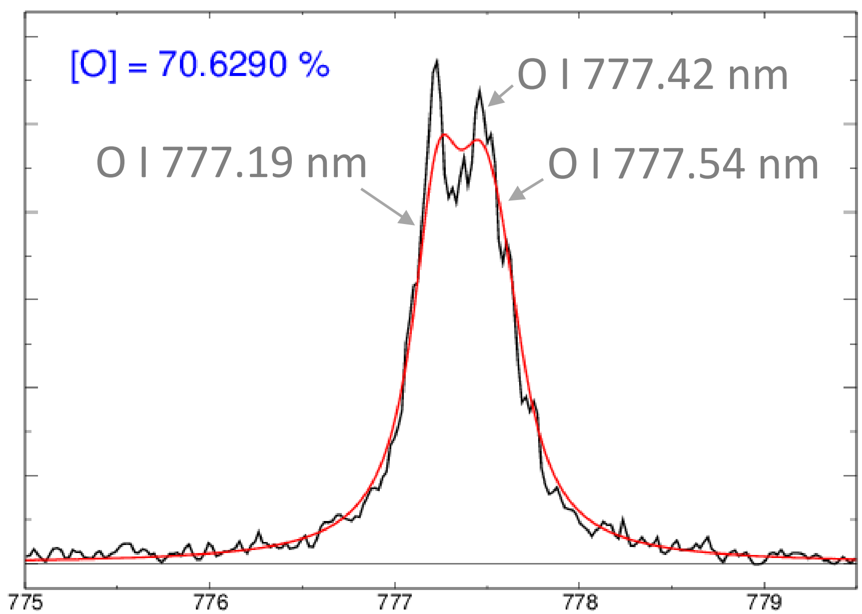


laser: 266 nm, 8 mJ
100 Jcm$^{-2}$

gas: argon, 5×10$^4$ Pa

gate: (500 ± 100) ns

NIST data

# analysis of fused silica

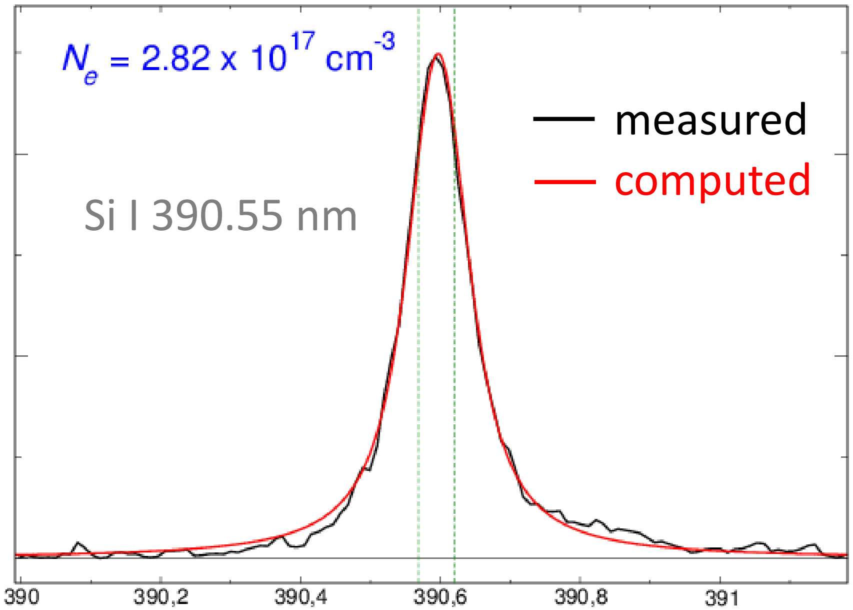


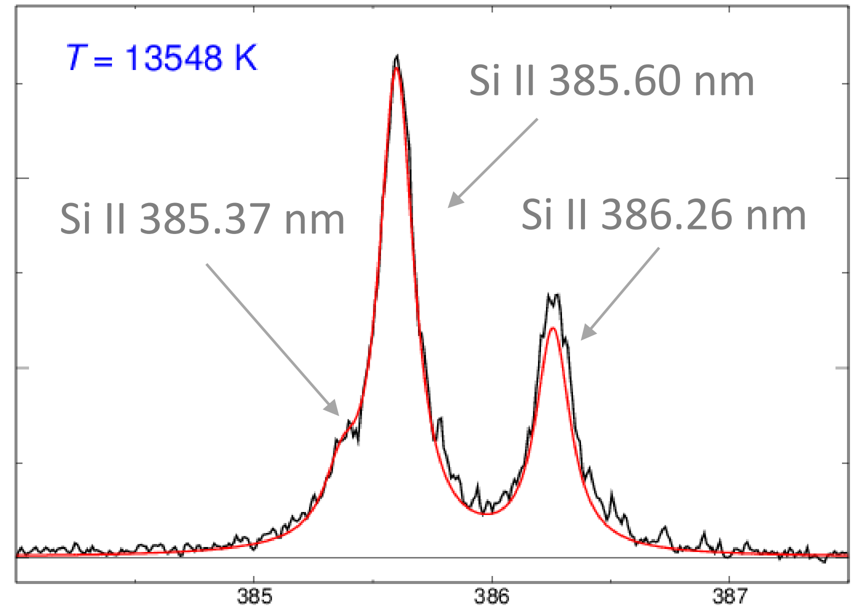


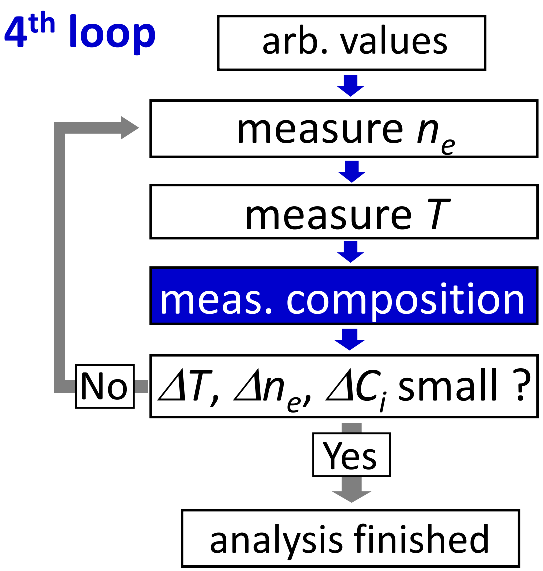


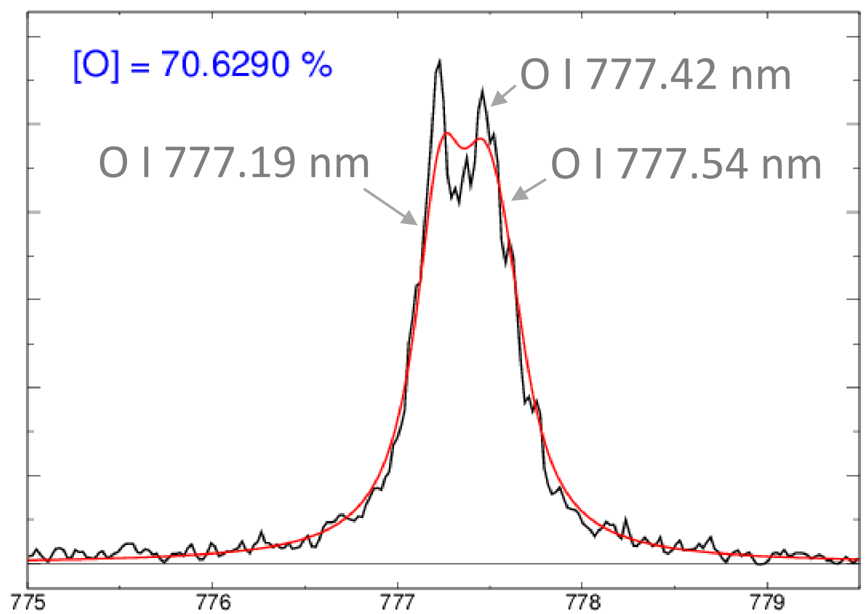


laser: 266 nm, 8 mJ
100 Jcm$^{-2}$

gas: argon, 5×10$^4$ Pa

gate: (500 ± 100) ns

NIST data

# analysis of fused silica

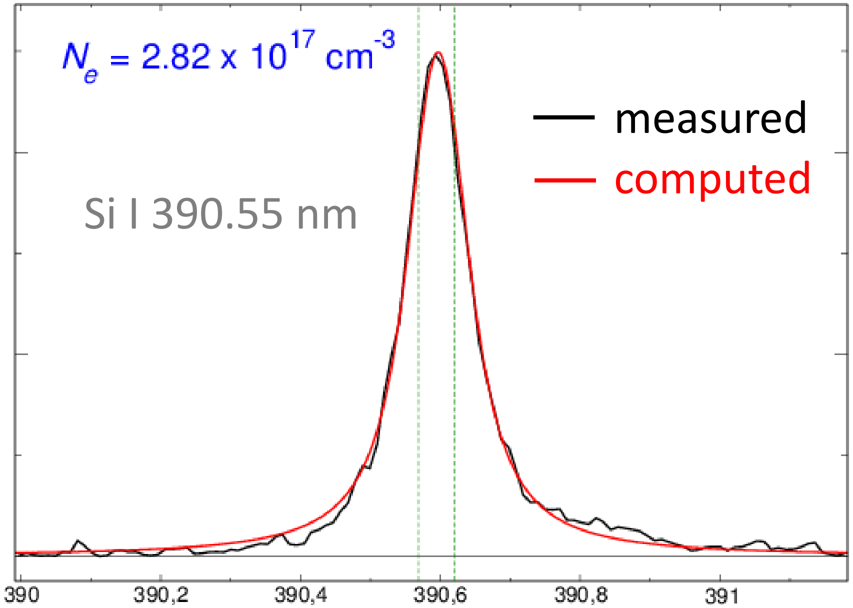


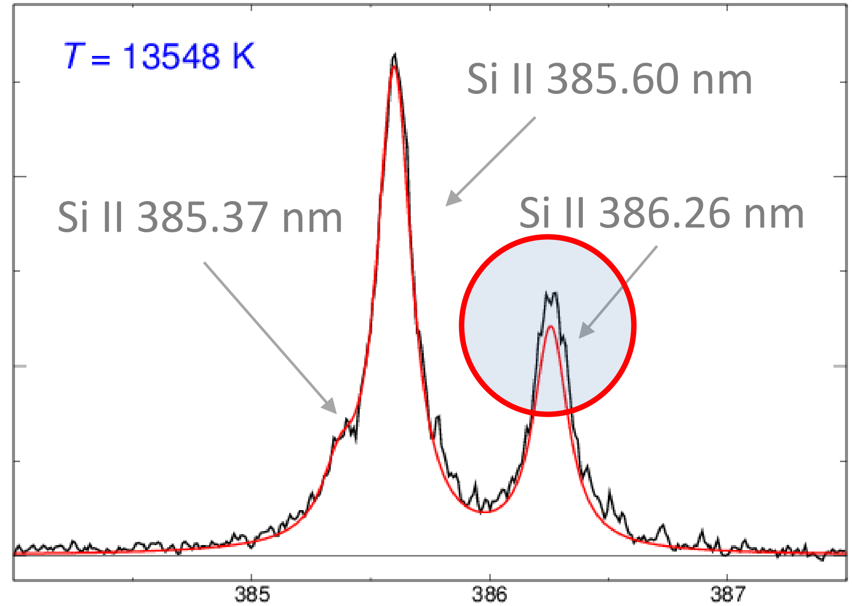


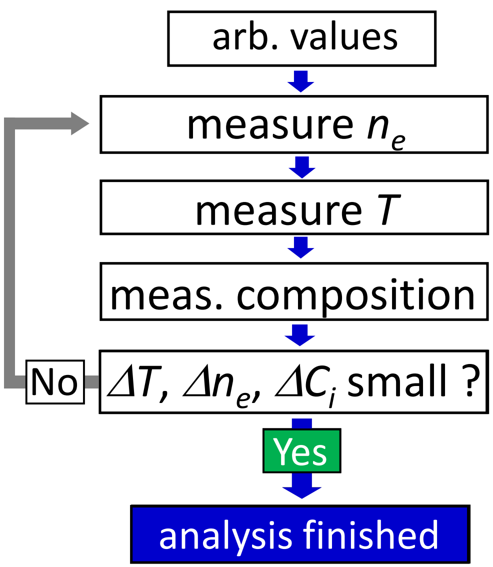


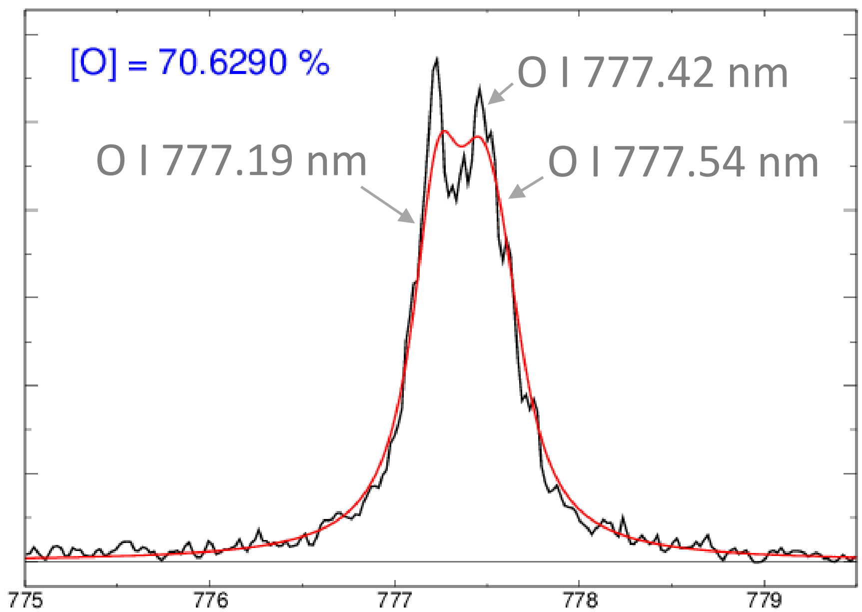


laser: 266 nm, 8 mJ
100 $Jcm^{-2}$
gas: argon, $5\times10^4$ Pa
gate: (500 ± 100) ns

NIST data

# NIST vs Kurucz databases

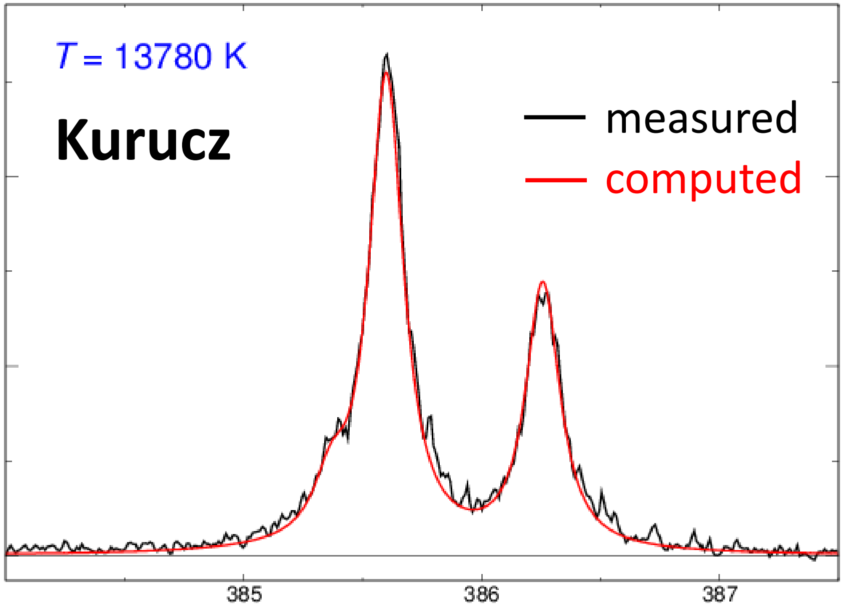


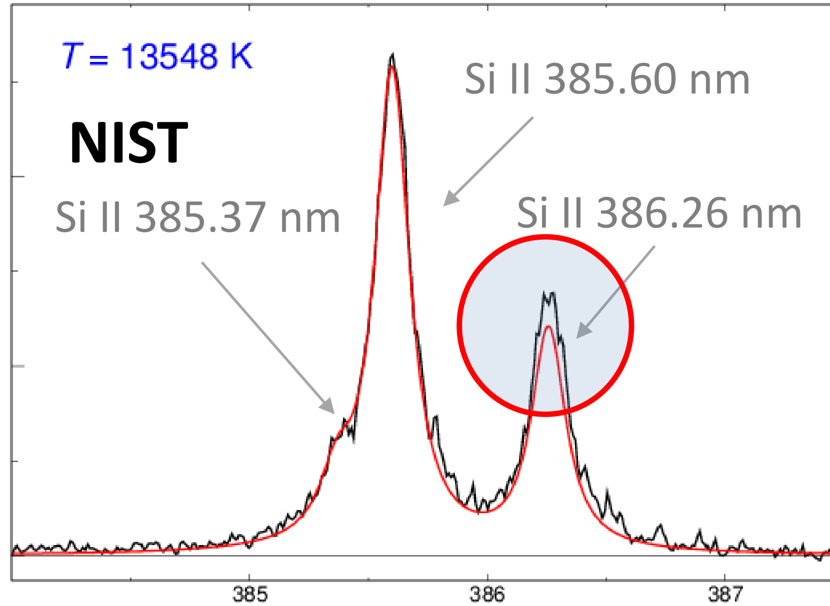


**NIST**

| Ion | Ritz Wavelength Air (nm) | Rel. Int. (?) | $A_{ki}$ ($s^{-1}$) | Acc. | $E_i$ ($cm^{-1}$) | $E_k$ ($cm^{-1}$) | Lower Level Conf., Term, J | Upper Level Conf., Term, J |
|---|---|---|---|---|---|---|---|---|
| Si II | 385.3665 | 100w | 5.11e+06 | C | | | | |
| Si II | 385.6018 | 500w | 4.40e+07 | C+ | | | | |
| Si II | 386.2595 | 200w | 3.91e+07 | C+ | | | | |
| Si I | 390.5523 | 300 | 1.33e+07 | B | | | | |

**Kurucz**

```
-------------------------------------------------------------------------------------
  Wl / nm      A-Value   Element E_
vac<200nm<air   / 1/s     (Name)
-------------------------------------------------------------------------------------
   385.3665  3.412e+06 Si II       55309.350   1.5 s3p2 2D       81251.320   1.5 4p   2P
   385.6018  3.108e+07 Si II       55325.180   2.5 s3p2 2D       81251.320   1.5 4p   2P
   386.2595  3.405e+07 Si II       55309.350   1.5 s3p2 2D       81191.340   0.5 4p   2P
   390.5523  1.184e+07 Si I        15394.370   0.0 3p2 1S        40991.884   1.0 p4s  1P
```

| | Kurucz | NIST | rel. error |
|---|---|---|---|
| $n_e$ ($cm^{-3}$) | $2.8\times10^{17}$ | $2.8\times10^{17}$ | 25% |
| $T$ (K) | 13,800 | 13,500 | 5% |
| Si (%) | 34.7 | 29.4 | 14% |
| O (%) | 65.2 | 70.6 | 6% |

cnrs Aix*Marseille université LP3

Introduction

- Principle and historical background

Validity conditions of physical model

Methods of calibration-free measurements

**Critical review of analytical performance**

Recommendations

Practical advice

# Critical review of analytical performance

many CF-LIBS studies ☞ low accuracy for minor and trace elements

**What is the origin of large measurements errors ?**

☞ **often attributed closure condition ( $\sum_A C_A = 1$ )** *Gornushkin et al., SAB 2018*

Small errors of major elements induce large errors on trace minor elements ?

mass fraction of element A : $C_A = \dfrac{n_A m_A}{\rho_{tot}}$ $\rho_{tot} = \sum_A n_A m_A$

fraction measurement error: $$\frac{\Delta C_A}{C_A} = \sqrt{(1 - C_A)^2 \left(\frac{\Delta n_A}{n_A}\right)^2 + \sum_{j \neq A}^{N} C_j^2 \left(\frac{\Delta n_j}{n_j}\right)^2}$$

**largest contribution of minor element errors**

⇨ **does not originate from uncertainties of major elements**

# Critical review of analytical performance

many CF-LIBS studies ☞ low accuracy for minor and trace elements

**What is the origin of large measurements errors ?**

☞ **low signal-to-noise ratio**

☞ CF-LIBS needs LTE validity

⇨ large electron density required

⇨ intense continuum (collisions between charged particles)

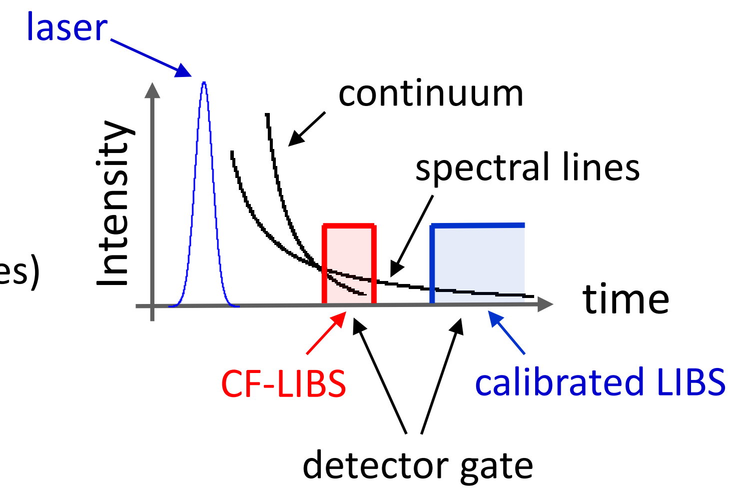


## situation worse with organic materials

☞ **C, H, N, O have large energy gaps**
⇨ **LTE establishment more difficult**
⇨ **higher $N_e$ required**
⇨ **continuum more intense**

# Critical review of analytical performance

many CF-LIBS studies ☞ low accuracy for minor and trace elements

**What is the origin of large measurements errors ?**

*Chen et al., SAB 2018*

☞ **low signal-to-noise ratio** **solution = two-step procedure**

**1. early measurement**
- ☞ large $N_e$
- ⇨ full LTE
- ⇨ low signal-to-noise
- ☞ measure major elements

**2. late measurement**
- ☞ reduced $N_e$
- ⇨ partial LTE
- ⇨ high signal-to-noise
- ☞ measure minor and trace elements

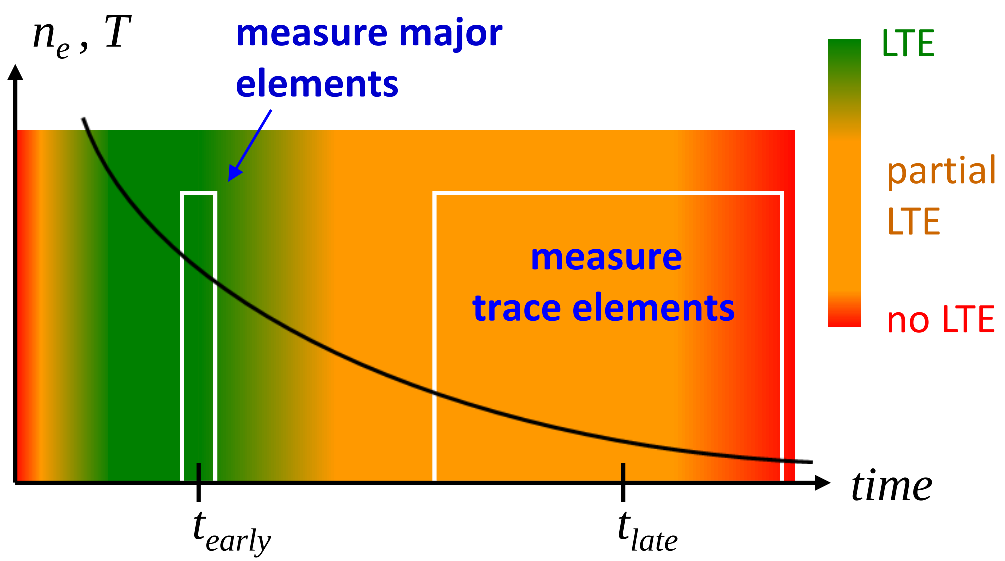


C, H, N and O out of equilibrium

☞ **enhanced CF-LIBS sensitivity**

# Critical review of analytical performance

many CF-LIBS studies ☞ low accuracy for minor and trace elements

**What is the origin of large measurements errors ?**

☞ **trace element fractions on surface differ from those of bulk**

**SF5 heavy flint glass**

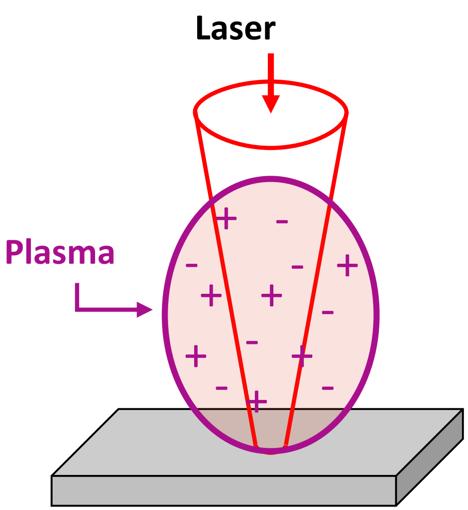


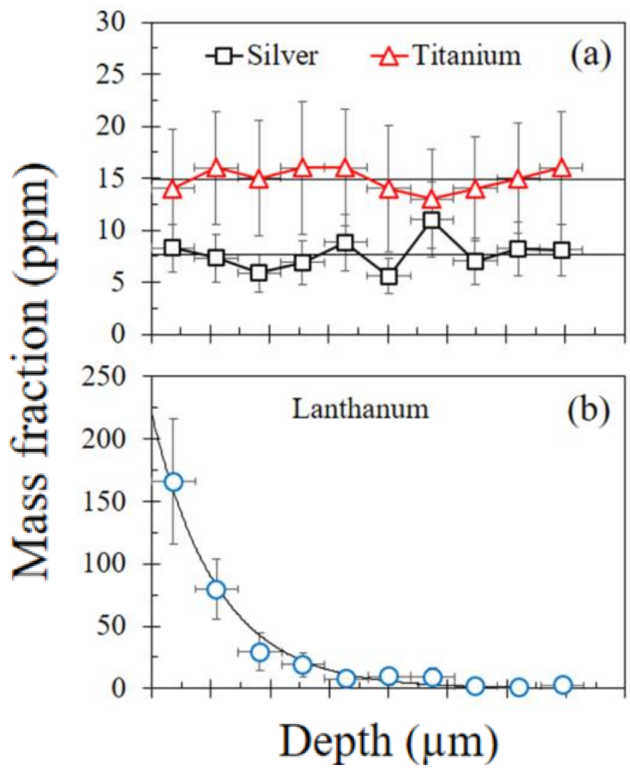


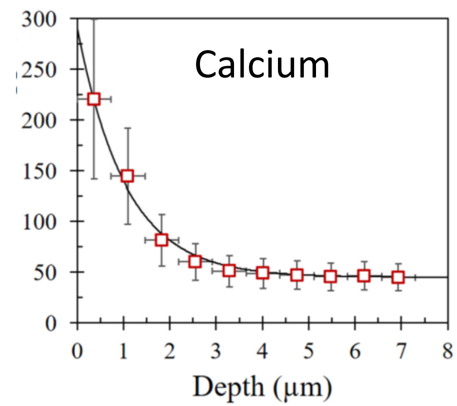


☞ La in surface polishing agent

☞ Ca in water of polishing solution

# Critical review of analytical performance

## What is the error due to self-absorption ?

$\Rightarrow$ Spectral radiance $B_\lambda = U_\lambda\left(1 - e^{-\tau}\right)$

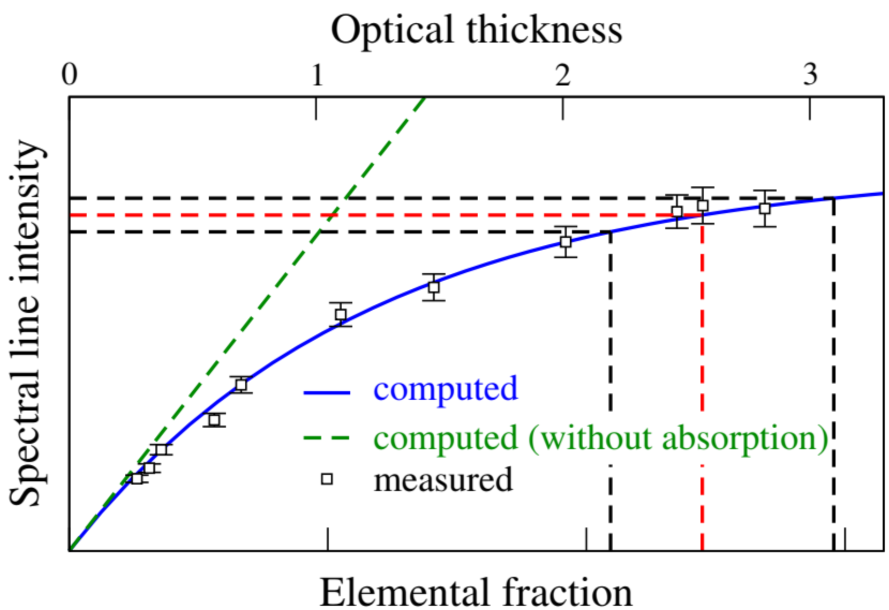


☞ **strong self-absorption** ($\tau >> 1$) $\Rightarrow$ $B_\lambda = U_\lambda$

⇨ **strong lines saturate at blackbody radiance**

# Critical review of analytical performance

## What is the error due to self-absorption ?

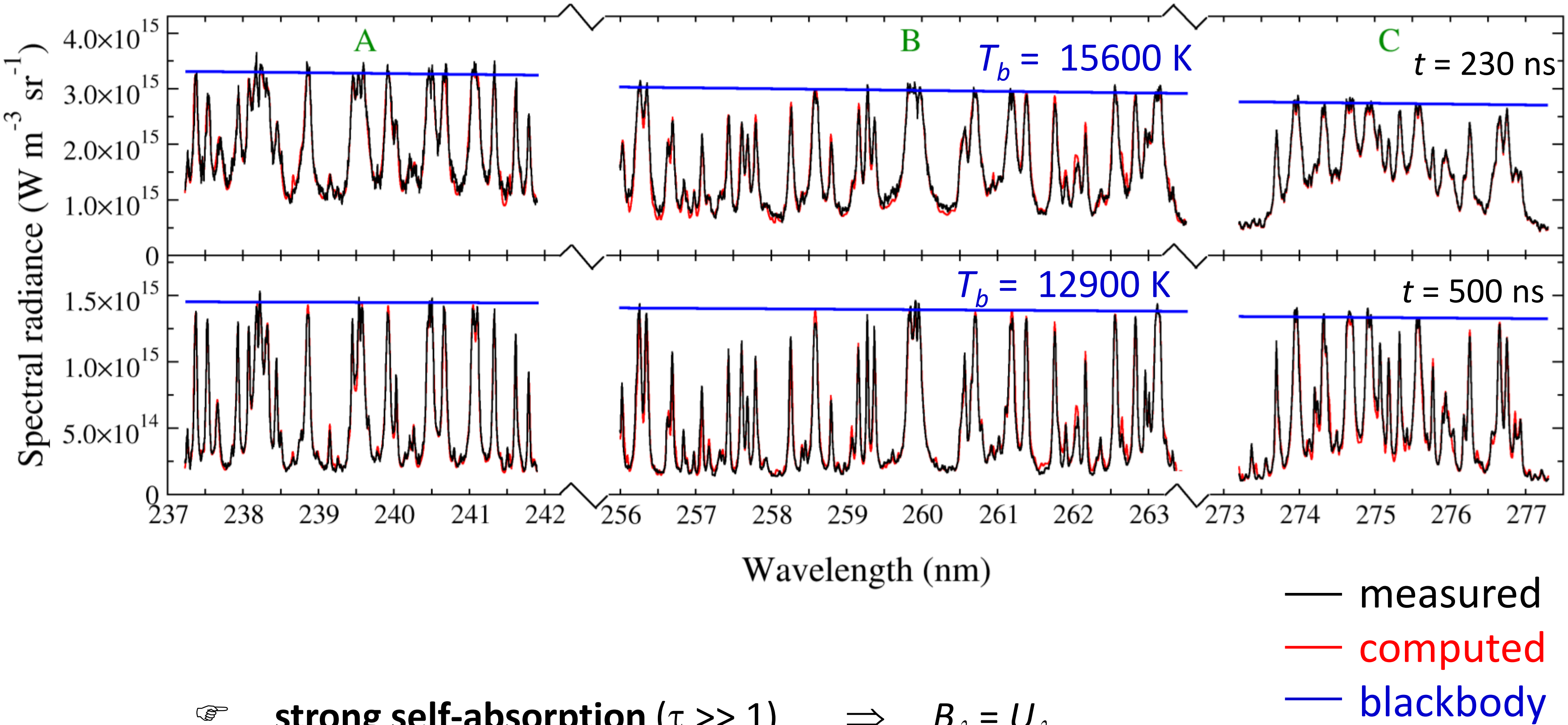


☞ **strong self-absorption** ($\tau >> 1$) ⇒ $B_\lambda = U_\lambda$

⇨ **strong lines saturate at blackbody radiance**

# Critical review of analytical performance

## What is the error due to self-absorption ?

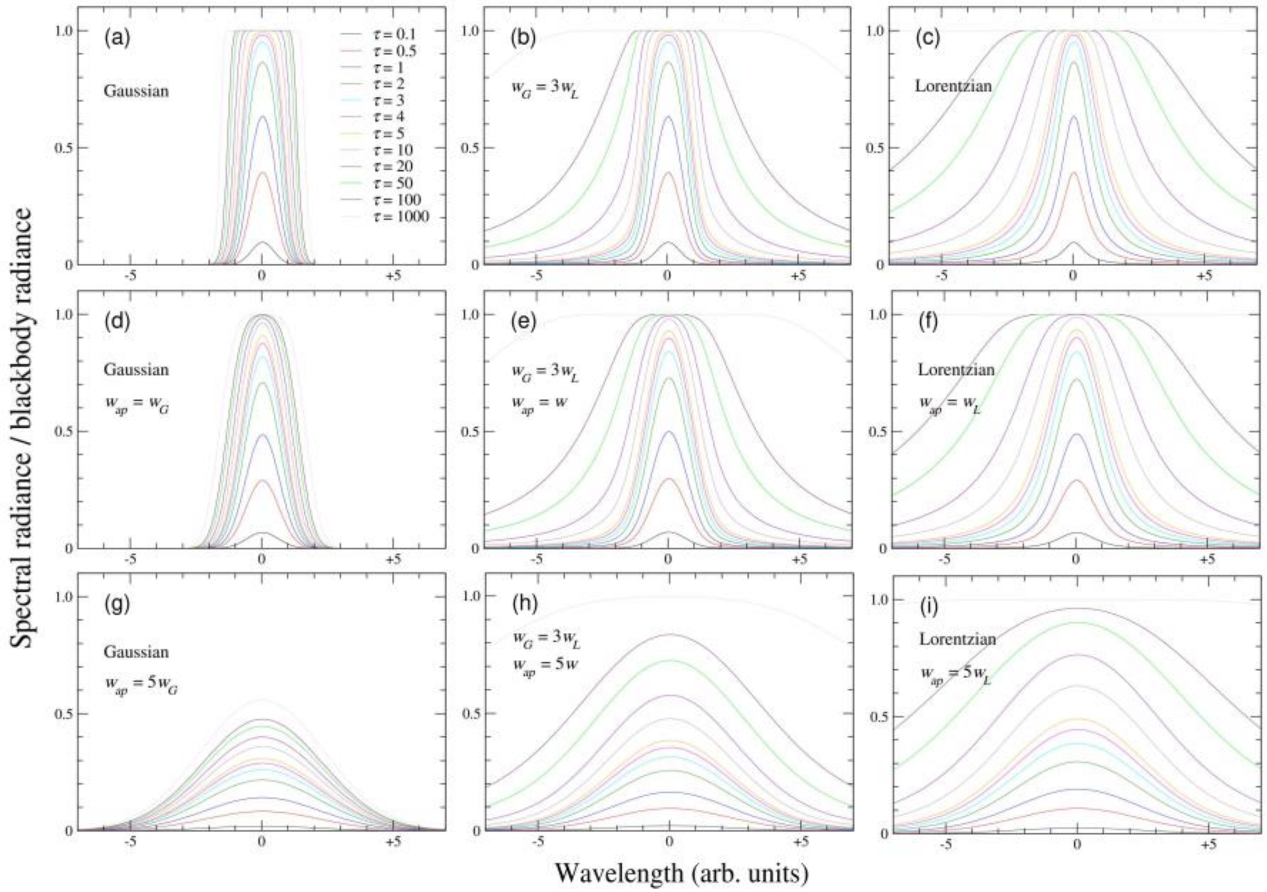


☞ **Intensity lowering due self-absorption to depends on line shape**

# Critical review of analytical performance

## What is the error due to self-absorption ?

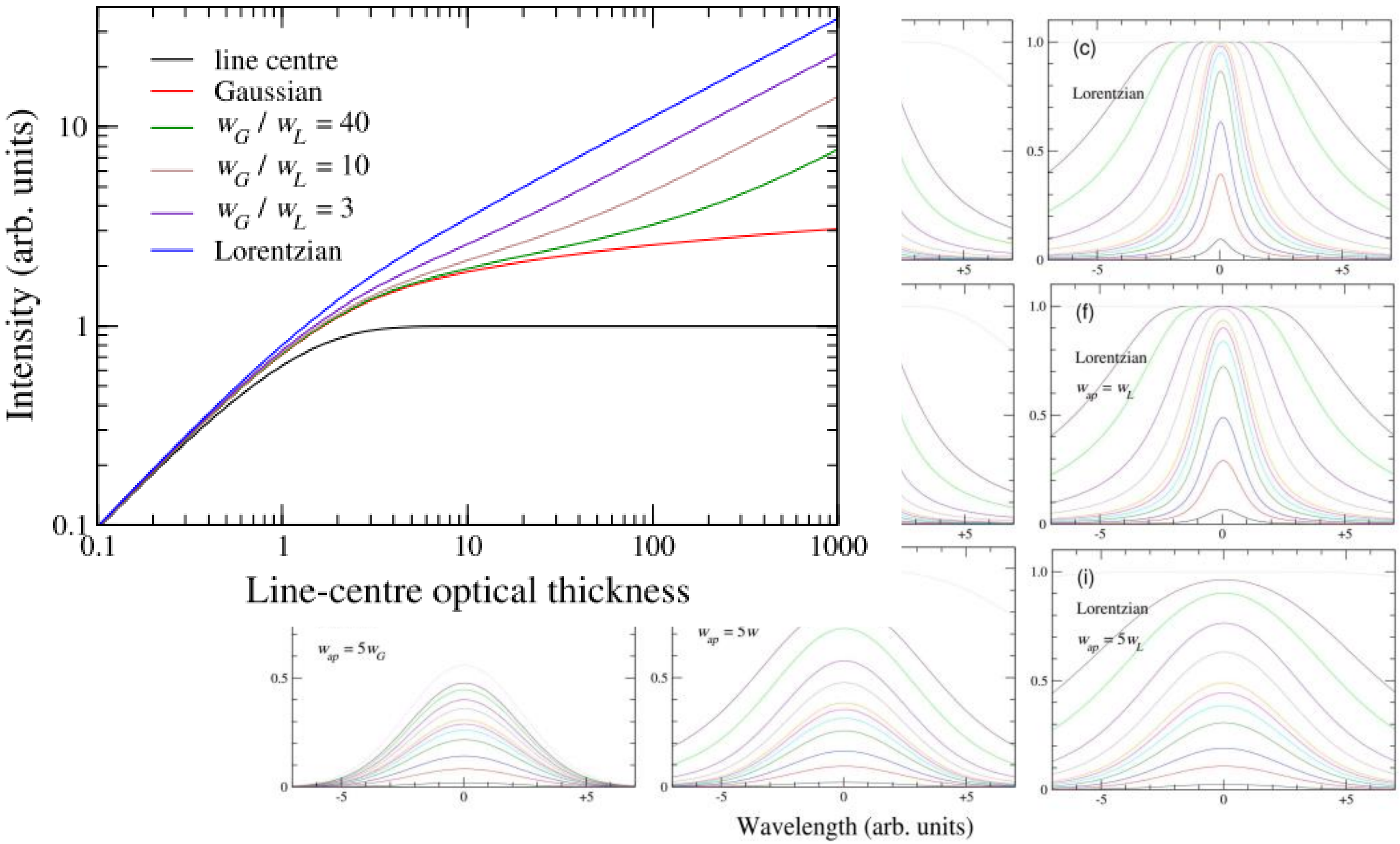


☞ **Intensity lowering due self-absorption to depends on line shape**

# Critical review of analytical performance

## What is the error due to self-absorption ?

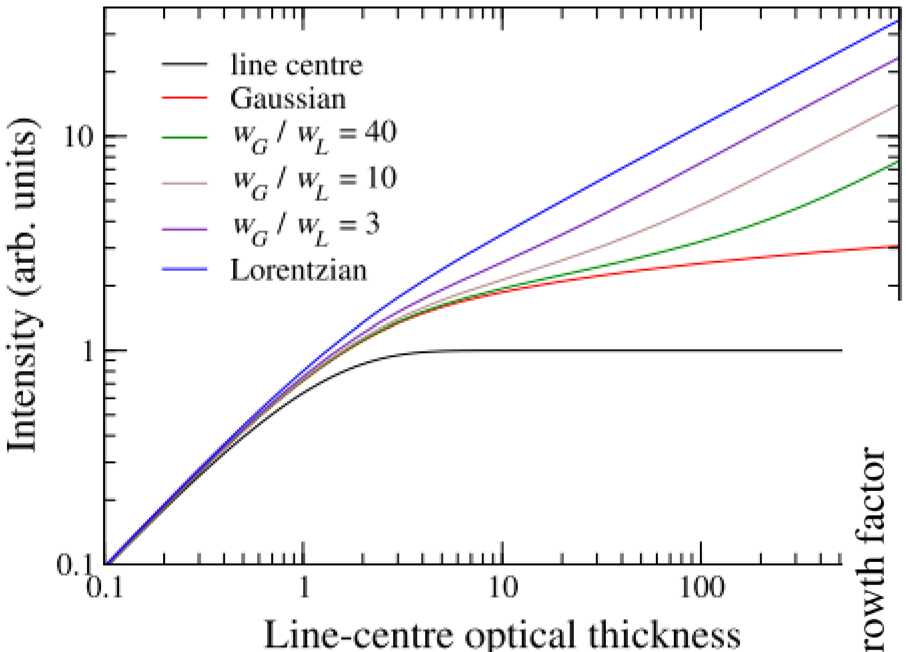


$$I = f(\tau_0)$$

derivative of inverse function

$$\frac{\Delta\tau_0}{\tau_0} = \frac{1}{\tau_0}\frac{f(\tau_0)}{f'(\tau_0)}\frac{\Delta I}{I} \equiv g(\tau_0)\frac{\Delta I}{I}$$

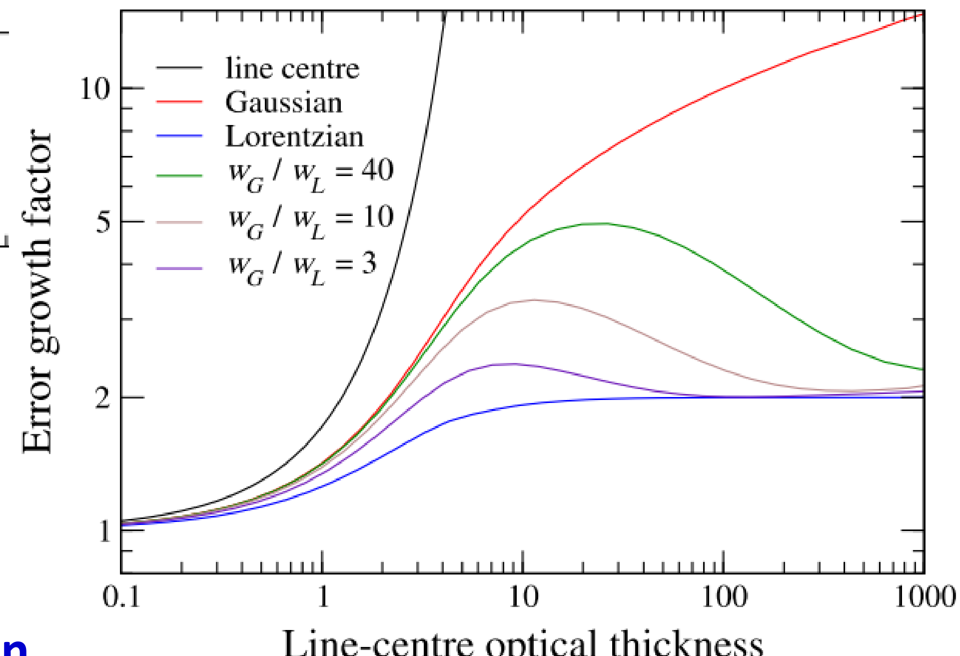


☞ **error growth due to self-absorption**

# Critical review of analytical performance

## What are the principal error sources ?

using rigorous error calculations we obtain *Taleb et al., SAB 2021*

**optically thin case** ($\tau << 1$) :

$$\frac{\Delta n_A}{n_A} = \sqrt{\left(\frac{\Delta I}{I}\right)^2 + \left(\frac{\Delta A_{ul}}{A_{ul}}\right)^2}$$

*ΔI* = intensity measurement error (signal-to-noise ratio, apparatus response, line interference, …)

$\Delta A_{ul}$ = uncertainty of transition probability

**general case :**

$$\frac{\Delta n_A}{n_A} = \sqrt{\left(\frac{\Delta \tau_0}{\tau_0}\right)^2 + \left(\frac{\Delta A_{ul}}{A_{ul}}\right)^2 + (1 - e^{-\tau_0})\left(\left(\frac{\Delta w_{sd}}{w_{sd}}\right)^2 + \left(\frac{\Delta L}{L}\right)^2\right)}$$

$$\frac{\Delta \tau_0}{\tau_0} = \frac{1}{\tau_0}\frac{f(\tau_0)}{f'(\tau_0)}\frac{\Delta I}{I} \equiv g(\tau_0)\frac{\Delta I}{I}$$

$\Delta w_{sd}$ = uncertainty of line width
*ΔL* = uncertainty of plasma diameter
} large errors, 10% in best case

**if $w_{sd}$ and *L* are precisely known**

**⇨ strongly self-absorbed lines can be used for CF-LIBS**

CNRS | Aix*Marseille université | LP3

Introduction

- Principle and historical background

Validity conditions of physical model

Methods of calibration-free measurements

Critical review of analytical performance

**Recommendations**

Practical advice

# Recommendations

## Apparatus requirements

**spectrometer:**

CF-LIBS ☞ all sample composing elements have to be measured

⇨ observation of broadband spectral range

$n_e$-measurement, evaluation of self-absorption ⇨ high resolving power

☞ **echelle spectrometer**

# Recommendations

## Apparatus requirements

**spectrometer:** ☞ **echelle type**

**sample holder:**

echelle spectrometers suffer low sensitivity

⇨ signal acquisition over large number of laser ablation events ( $\geq$ 100)

reproducible plasma generation ☞ avoid deep drilling

crater depth $\ll$ crater diameter

⇨ apply a few laser pulses per site (5, 10, 20)

☞ **motorized sample holder**

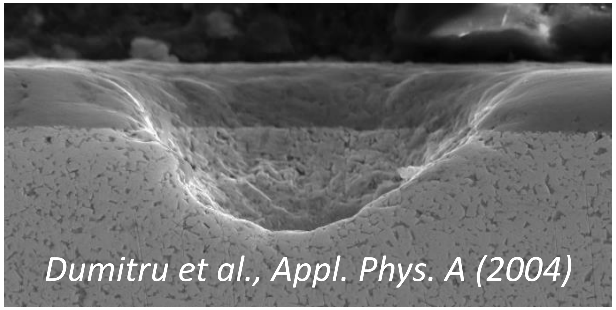

*Dumitru et al., Appl. Phys. A (2004)*

# Recommendations

## Apparatus requirements

**spectrometer:** ☞ **echelle type**

**sample holder:** ☞ **motorized**

**apparatus response correction:**

apparatus response typically measured with radiation standards

UV range (200 – 400 nm) ☞ deuterium arc

VIS/NIR range ( $\geq$ 400 nm) ☞ tungsten filament

☞ **calibration of echelle spectrometers challenging**

due to significant intensity variation on broad spectral range

# Recommendations

## Apparatus requirements

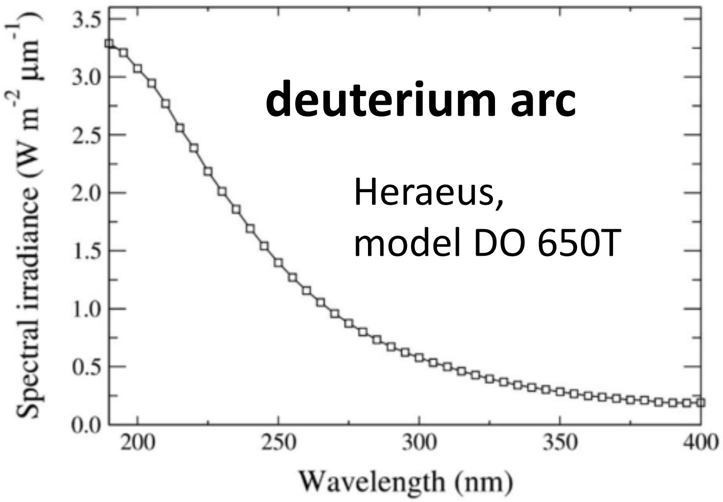


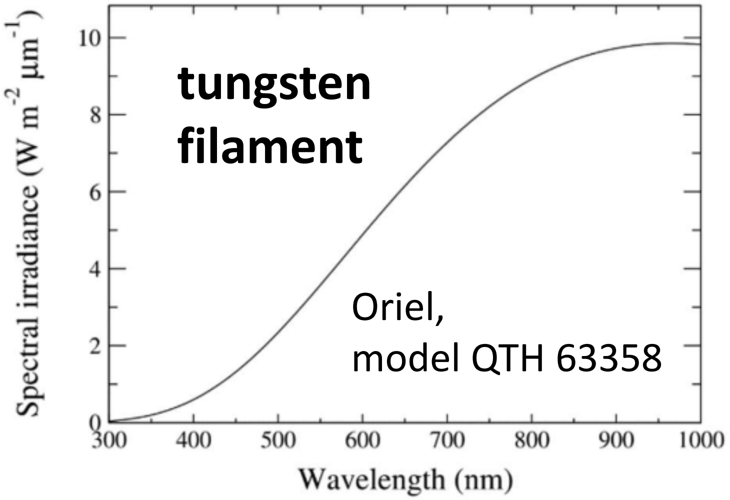


☞ **calibration of echelle spectrometers challenging**

due to significant intensity variation on broad spectral range

**situation is worse with compact radiation standards**

☞ **method for checking and correcting apparatus response**

# Etalonnage du spectromètre par plasma laser

plasma uniforme en ETL ☞ calcul précis du spectre

ablation de l'acier ☞ spectre riche, valeurs $A_{ul}$ précises sur NIST

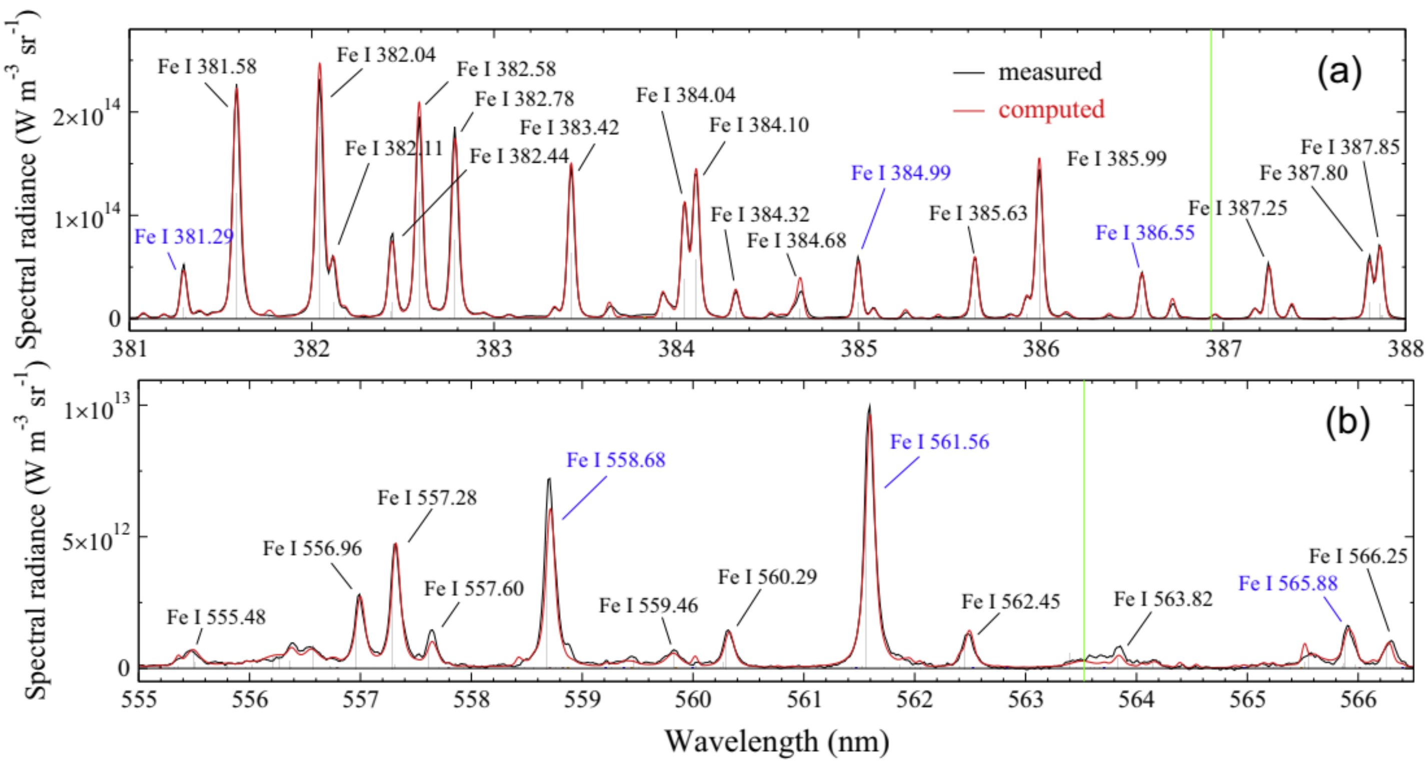


Réponse de l'appareil déduite du rapport $I_{mes}$ / $I_{comp}$

# Etalonnage du spectromètre par plasma laser

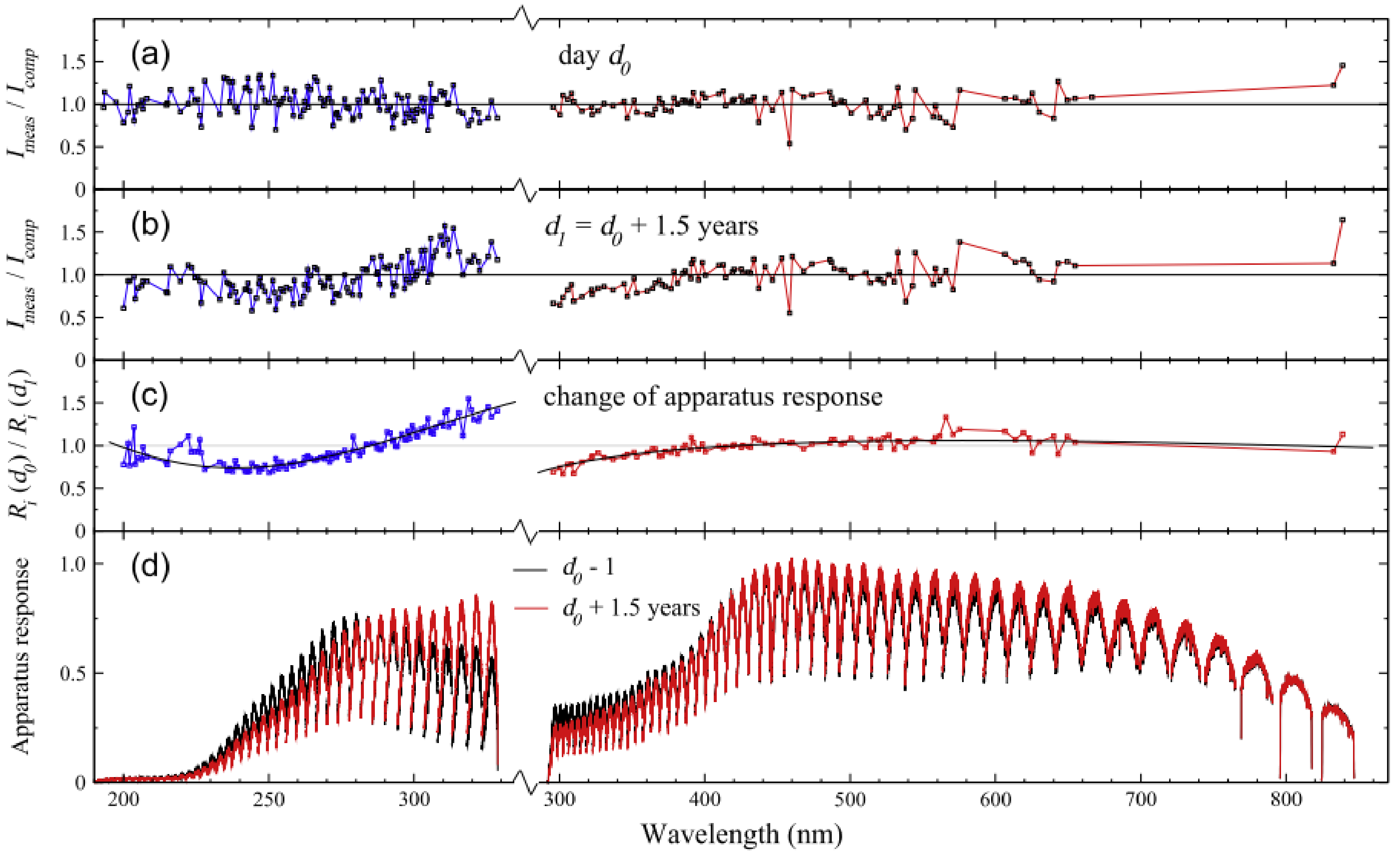


écart-type des fluctuations = intervalle de confiance moyenne des $A_{ul}$ = 15%

☞ **plasma laser = moyen pour mesurer $A_{ul}$**

# Recommendations

## Apparatus requirements

**spectrometer:** ☞ **echelle type**

**sample holder:** ☞ **motorized**

**apparatus response correction:** ☞ **radiation standards, checking with laser plasma on steel**

## Experimental conditions

**laser:** pulse energy ⇨ plasma lifetime ⇨ $E_{min}$ required for LTE
⇨ ablated mass ⇨ self-absorption

} a few mJ for UV laser

# Recommendations

## Apparatus requirements

**spectrometer:** ☞ **echelle type**

**sample holder:** ☞ **motorized**

**apparatus response correction:** ☞ **radiation standards, checking with laser plasma on steel**

## Experimental conditions

**laser:** pulse energy ☞ **a few mJ** (UV laser)

beam focusing ⇨ to spot of 100 µm ⇨ $F_{las} \approx 100\ \mathrm{Jcm^{-2}}$

⇨ stoichiometric ablation

# Recommendations

## Apparatus requirements

**spectrometer:** ☞ **echelle type**

**sample holder:** ☞ **motorized**

**apparatus response correction:** ☞ **radiation standards, checking with laser plasma on steel**

## Experimental conditions

**laser:** pulse energy ☞ **a few mJ** (UV laser)

beam focusing ☞ **to spot of 100 µm**

pulse duration ⇨ $\tau_{las} > \tau_{e\text{-}i}$ ⇨ laser heating of expanding vapor

⇨ nanosecond laser

# Recommendations

## Apparatus requirements

**spectrometer:** ☞ **echelle type**

**sample holder:** ☞ **motorized**

**apparatus response correction:** ☞ **radiation standards,**
**checking with laser plasma on steel**

## Experimental conditions

**laser:** pulse energy ☞ **a few mJ** (UV laser)

beam focusing ☞ **to spot of 100 µm**

pulse duration ☞ **nanosecond**

wavelength ⇨ UV radiation ⇨ energy deposition on sample surface
⇨ spatially uniform plasma

# Recommendations

## Apparatus requirements

**spectrometer:** ☞ **echelle type**

**sample holder:** ☞ **motorized**

**apparatus response correction:** ☞ **radiation standards, checking with laser plasma on steel**

## Experimental conditions

**laser:**
- pulse energy ☞ **a few mJ** (UV laser)
- beam focusing ☞ **to spot of 100 µm**
- pulse duration ☞ **nanosecond**
- wavelength ☞ **UV radiation**

**spectra recording:**
- gate delay ⇨ $n_e$ large enough to ensure LTE
- gate width ⇨ $\Delta T/T$, $\Delta n_e/n_e$ << 1 ⇨ $\Delta t_{gate}$ small
- ⇨ S/N ratio ⇨ $\Delta t_{gate}$ large

$$\Delta t_{gate} = t_{delay}/2$$

# Recommendations

## Apparatus requirements

**spectrometer:** ☞ **echelle type**

**sample holder:** ☞ **motorized**

**apparatus response correction:** ☞ **radiation standards, checking with laser plasma on steel**

## Experimental conditions

**laser:**
- pulse energy ☞ **a few mJ** (UV laser)
- beam focusing ☞ **to spot of 100 µm**
- pulse duration ☞ **nanosecond**
- wavelength ☞ **UV radiation**

**spectra recording:**
- gate delay ⇨ $n_e$ large enough to ensure LTE
- gate width ⇨ $\Delta t_{gate} = t_{delay}/2$
- signal treatment ⇨ noise subtraction before response correction

# Recommendations

## Experimental conditions

**laser:** pulse energy ☞ **a few mJ** (UV laser)

beam focusing ☞ **to spot of 100 µm**

pulse duration ☞ **nanosecond**

wavelength ☞ **UV radiation**

**spectra recording:** gate delay ⇨ $n_e$ large enough to ensure LTE

gate width ⇨ $\Delta t_{gate} = t_{delay}/2$

signal treatment ⇨ noise subtraction before response correction

**atmospheric conditions:** pressure ⇨ large enough to ensure LTE

⇨ low enough to minimize coll. quenching

⇨ atmospheric pressure

# Recommendations

## Experimental conditions

**laser:** pulse energy ☞ **a few mJ** (UV laser)

beam focusing ☞ **to spot of 100 µm**

pulse duration ☞ **nanosecond**

wavelength ☞ **UV radiation**

**spectra recording:** gate delay ⇨ $n_e$ large enough to ensure LTE

gate width ⇨ $\Delta t_{gate} = t_{delay}/2$

signal treatment ⇨ noise subtraction before response correction

**atmospheric conditions:** pressure ☞ **atmospheric**

gas nature ⇨ argon ⇨ higher brilliance

⇨ longer plasma lifetime

⇨ plasma spatially uniform

# Recommendations

## Experimental conditions

**laser:** pulse energy ☞ **a few mJ** (UV laser)

beam focusing ☞ **to spot of 100 µm**

pulse duration ☞ **nanosecond**

wavelength ☞ **UV radiation**

**spectra recording:** gate delay ⇨ $n_e$ large enough to ensure LTE

gate width ⇨ $\Delta t_{gate} = t_{delay}/2$

signal treatment ⇨ noise subtraction before response correction

**atmospheric conditions:** pressure ☞ **atmospheric**

gas nature ☞ **argon for improved accuracy**

**laboratory environment:** ☞ ***T*-stabilized**

# Recommendations

## Selection of spectral lines

transition probability $A_{ul}$ ☞ highest accuracy

upper level energy $E_u$ ☞ close values of analytical lines

⇨ reduce impact of *T*-measurement uncertainty

wavelength $\lambda$ ☞ close values of analytical lines

⇨ reduce impact of apparatus response error

optical thickness $\tau$ ☞ lowest

signal-to-noise ratio ☞ highest

automated choice ☞ minimize analytical error

$$\frac{\Delta n_A}{n_A} = \sqrt{\left(\frac{\Delta\tau_0}{\tau_0}\right)^2 + \left(\frac{\Delta A_{ul}}{A_{ul}}\right)^2 + \left(1 - e^{-\tau_0}\right)\left(\left(\frac{\Delta w_{sd}}{w_{sd}}\right)^2 + \left(\frac{\Delta L}{L}\right)^2\right)}$$

$$\frac{\Delta\tau_0}{\tau_0} = \frac{1}{\tau_0}\frac{f(\tau_0)}{f'(\tau_0)}\frac{\Delta I}{I} \equiv g(\tau_0)\frac{\Delta I}{I}$$

Introduction

- Principle and historical background

Validity conditions of physical model

Methods of calibration-free measurements

Critical review of analytical performance

Recommendations

**Practical advice**

# Practical advice

## How to perform CF-LIBS analysis ?

☞ record valid spectrum

☞ measure apparatus response function

☞ measure apparatus width as function of wavelength

☞ get user account on LP3 server

☞ deposit corrected spectrum on server

☞ proceed spectrum with semi-automated CF-LIBS software

**In the future**

☞ portable software will be available

# Practical advice

book chapter

**"Calibration-free laser-induced breakdown spectroscopy"**

in

**"Laser-Induced Breakdown Spectroscopy (LIBS):
Concepts, Instrumentation, Data Analysis and Applications"**

to be published by **John Wiley & Sons Ltd**

editors **Vivek K. Singh, Y. Deguchi, Zhenzhen Wang, Durgesh K. Tripathi**

get a pdf-copy

☞ jorg.hermann@univ-amu.fr